Document made available under the Patent Cooperation Treaty (PCT)

International application number: PCT/US05/007308

International filing date: 07 March 2005 (07.03.2005)

Document type: Certified copy of priority document

Document details: Country/Office: US
Number: 60/550,591
Filing date: 06 March 2004 (06.03.2004)

Date of receipt at the International Bureau: 18 April 2005 (18.04.2005)

Remark: Priority document submitted or transmitted to the International Bureau in compliance with Rule 17.1(a) or (b)

World Intellectual Property Organization (WIPO) - Geneva, Switzerland
Organisation Mondiale de la Propriété Intellectuelle (OMPI) - Genève, Suisse

130.1192

THE UNITED STATES OF AMERICA

TO ALL TO WHOM THESE PRESENTS SHALL COME:

UNITED STATES DEPARTMENT OF COMMERCE

United States Patent and Trademark Office

March 31, 2005

THIS IS TO CERTIFY THAT ANNEXED HERETO IS A TRUE COPY FROM THE RECORDS OF THE UNITED STATES PATENT AND TRADEMARK OFFICE OF THOSE PAPERS OF THE BELOW IDENTIFIED PATENT APPLICATION THAT MET THE REQUIREMENTS TO BE GRANTED A FILING DATE.

APPLICATION NUMBER: ***60/550,591***
FILING DATE: ***March 06, 2004***
RELATED PCT APPLICATION NUMBER: ***PCT/US05/07308***

Certified by

Jon W. Dudas

Under Secretary of Commerce
for Intellectual Property
and Director of the United States
Patent and Trademark Office

PTO/SB/16 (01-04)
Approved for use through 07/31/2006. OMB 0651-0032
U.S. Patent and Trademark Office; U.S. DEPARTMENT OF COMMERCE
Under the Paperwork Reduction Act of 1995, no persons are required to respond to a collection of information unless it displays a valid OMB control number.

PROVISIONAL APPLICATION FOR PATENT COVER SHEET

This is a request for filing under 37 CFR 1.53(c).

Express Mail Label No. ER493082116US

INVENTOR(S)		
Given Name (first and middle [if any])	Family Name or Surname	Residence (City and either State or Foreign Country)
Michael Norman	Trainer	186 Fretz Road, Telford, PA 18969

Additional inventors are being named on the zero *separately numbered sheets attached hereto*

TITLE OF THE INVENTION (500 characters max)

Methods and Apparatus for Determining the Size and Shape of Particles

Direct all correspondence to: **CORRESPONDENCE ADDRESS**

☐ Customer Number:

OR

☑ Firm or Individual Name	Michael Trainer				
Address	186 Fretz Road				
Address					
City	Telford	State	PA	Zip	18969
Country	USA	Telephone	2157238894	Fax	

ENCLOSED APPLICATION PARTS *(check all that apply)*

☑ Specification *Number of Pages* 72 ☐ CD(s), Number

☑ Drawing(s) *Number of Sheets* 60 ☐ Other (specify)

☐ Application Data Sheet. See 37 CFR 1.76

METHOD OF PAYMENT OF FILING FEES FOR THIS PROVISIONAL APPLICATION FOR PATENT

☑ Applicant claims small entity status. See 37 CFR 1.27.

☑ A check or money order is enclosed to cover the filing fees.

☐ The Director is herby authorized to charge filing fees or credit any overpayment to Deposit Account Number:

☐ Payment by credit card. Form PTO-2038 is attached.

FILING FEE Amount ($)

$80.00

The invention was made by an agency of the United States Government or under a contract with an agency of the United States Government.

☑ No.

☐ Yes, the name of the U.S. Government agency and the Government contract number are:

[Page 1 of 2]

Respectfully submitted,

SIGNATURE Michael Trainer

Date MARCH 6, 2004

REGISTRATION NO. *(if appropriate)*

Docket Number:

TYPED or PRINTED NAME Michael Trainer

TELEPHONE 215 723 8894

USE ONLY FOR FILING A PROVISIONAL APPLICATION FOR PATENT

This collection of information is required by 37 CFR 1.51. The information is required to obtain or retain a benefit by the public which is to file (and by the USPTO to process) an application. Confidentiality is governed by 35 U.S.C. 122 and 37 CFR 1.14. This collection is estimated to take 8 hours to complete, including gathering, preparing, and submitting the completed application form to the USPTO. Time will vary depending upon the individual case. Any comments on the amount of time you require to complete this form and/or suggestions for reducing this burden, should be sent to the Chief Information Officer, U.S. Patent and Trademark Office, U.S. Department of Commerce, P.O. Box 1450, Alexandria, VA 22313-1450. DO NOT SEND FEES OR COMPLETED FORMS TO THIS ADDRESS. SEND TO: **Mail Stop Provisional Application, Commissioner for Patents, P.O. Box 1450, Alexandria, VA 22313-1450.**

If you need assistance in completing the form, call 1-800-PTO-9199 and select option 2.

Methods and Apparatus for Determining the Size and Shape of Particles

Michael Trainer

This disclosure describes an instrument for measuring the size distribution of a particle sample by counting and classifying particles into selected size ranges. The particle concentration is reduced to the level where the probability of measuring scattering from multiple particles at one time is reduced to an acceptable level. A light beam is focused or collimated through a sample cell, through which the particles flow. As each particle passes through the beam, it scatters, absorbs, and transmits different amounts of the light, depending upon the particle size. So both the decrease in the beam intensity, due to light removal by the particle, and increase of light, scattered by the particle, may be used to determine the particle size, to classify the particle and count it in a certain size range. If all of the particles pass through a single beam, then many small particles must be counted for each large one because typical distributions are uniform on a particle volume basis, and the number distribution is related to the volume distribution by the particle diameter cubed. This large range of counts and the Poisson statistics of the counting process limit the size dynamic range for a single measurement. For example, a uniform particle volume vs. size distribution between 1 and 10 microns requires that one thousand 1 micron particles be measured for each 10 micron particle. The Poisson counting statistics require 10000 particles to be counted to obtain 1% reproducibility in the count. Hence one needs to measure more than 10 million particles. At the typical rate of 10,000 particles per second, this would require more than 1000 seconds for the measurement. In order to reduce the statistical count uncertainties, large counts of small particles must be measured for each large particle. This problem may be eliminated by flowing portions of the sample flow through light beams of various diameters, so that larger beams can count large count levels of large particles while small diameter beams count smaller particles without the small particle coincidence counts of the large beam. The best results are obtained by using multiple beams of ever decreasing spot size to improve the dynamic range of the count. The count vs. size distributions from each beam are scaled to each other using overlapping size ranges between different pairs of beams in the group, and the count distributions from all of the beams are then combined.

Light scattered from the large diameter beam should be measured at low scattering angles to sense large particles. The optical pathlength of this beam in the particle sample must be large enough to pass the largest particle of interest for that beam. For small particles, the interaction volume in the beam must be reduced along all three spatial directions. The beam crossection is reduced by an aperture or by focusing the beam into the interaction volume. However, for very small particles, reduction of the optical path along the beam propagation direction is limited by the gap thickness through which the sample must flow. This could be accomplished by using a cell with various pathlengths or a cell with a wedge shaped window spacing (see Figure 9b) to provide a range of optical pathlengths.

Smaller source beams would pass through the thinner portions of the cell, reducing the intersection of the incident beam and particle dispersant volume to avoid coincidence counts. The other alternative is to restrict the field of view of the scattering collection optics so as to only detect scatterers in a very small sample volume, which reduces the probability of multiple particles in the measurement volume. So particularly in the case of very small particles, a focused laser beam intersected with the limited field of view of collection optics must be used to insure single particle counting. However, this system would require correction of larger beams for coincidence counts based upon counts in smaller beams. To avoid these count errors, this disclosure proposes the use of a small interrogation volume for small particles, using multiple scattering angles, and a 2 dimensional detector array for counting large numbers of particles above approximately 1 micron at high speeds.

Three problems associated with measuring very small particles are scattering signal dynamic range, particle composition dependence, and Mie resonances. The low angle scattered intensity per particle changes by almost 6 orders of magnitude between 0.1 and 1 micron particle diameter. Below approximately 0.4 micron, photon multiplier tubes (PMT) are needed to measure the minute scattered light signals. Also the scattered intensity can change by a factor of 10 between particles of refractive index 1.5 to 1.7. However, the shape of the scattering function (as opposed to the amplitude) vs. scattering angle is a clear indicator of particle size, with very little refractive index sensitivity. This invention proposes measurement of multiple scattering angles to determine the size of each individual particle, with low sensitivity to particle composition and scattering intensity. Since multiple angle detection is difficult to accomplish with bulky PMT's, this invention also proposes the use of silicon photodiodes and heterodyne detection to measure low scattered signals from particles below 1 micron. However, the use of any type of detector and coherent or non-coherent detection are claimed.

Spherical particles with low absorption will produce a transmitted light component which interferes with light diffracted by the particle. This interference causes oscillations in the scattering intensity as a function of particle size. The best method of reducing these oscillations is to measure scattering from a white light or broad band source, such as an LED. The interference resonances at multiple wavelengths are out of phase with each other, washing out the resonance effects. But for small particles, one needs a high intensity source, eliminating broad band sources from consideration. The resonances primarily occur above 1.5 micron particle diameter, where the scattering crossection is sufficient for the lower intensity of broadband sources. So the overall concept uses laser sources and multiple scattering angles for particles below approximately 1 micron, and broad band sources with low angle scattering or total scattering for particle size from approximately 1 micron up to thousands of microns. We will start with the small particle detection system.

Figure 1 shows a configuration for measuring and counting smaller particles. A light source is projected into a sample cell, which consists of two optical windows for confining the flowing particle dispersion. The light source in Figure 1 could also be

replaced by an apertured light source as shown in Figure 1A. This aperture, which is in an image plane of the light source, blocks unwanted stray light which surrounds the source spot. In the case of laser sources, this aperture may be used to select a section of uniform intensity from the center of the laser crossectional intensity profile. In all figures in this disclosure, either source configuration is assumed. The choice is determined by source properties and intensity uniformity requirements in the sample cell. So either the light source, or the apertured image of the light source, is collimated by lens 1 and a portion of this collimated beam is split off by a beam splitter to provide the local oscillator for heterodyne detection. While collimation between lenses 1 and 2 is not required, it provides for easy transport to the heterodyne detectors 3 and 4. Lens 2 focuses the beam into a two-window cell as a scattering light source for particles passing through the cell. The scattered light is collected by two optical systems, a high angle heterodyne system for particles below approximately 0.5 microns and a low angle non-coherent detector for 0.4 to 1.2 micron diameter particles. Each system has multiple detectors to measure scattering at multiple angles. Figure 1 shows a representative system, where the representative approximate mean scattering angles for detectors 1, 2, 3, and 4 are 10, 20, 30, and 80 degrees, respectively. However, other angles and numbers of detectors could be used. All four scattering intensity measurements are used for each particle passing through the intersection of the field of view of each of the two systems with the focused source beam. Detectors 1 and 2 use non-coherent detection because the signal levels for the larger particles measured by these two detectors are sufficiently large to avoid the complexity of a heterodyne system. Also the Doppler frequency for particles passing through the cell at meter per second speeds are too low to accumulate many cycles within the single particle pulse envelope at these low scattering angles. The Doppler frequencies are much larger at larger scattering angles where the heterodyne detection is needed to measure the small scattering intensities from smaller particles.

Lens 4 collects scattered light from particles in the flowing dispersant. Slit 1 is imaged by lens 4 into the cell. The intersection of the rays passing through that image and the incident source beam define the interrogation volume 1 where the particle must reside to be detected by detectors 1 and 2. Detectors 1 and 2 each intercept a different angular range of scattered light. Likewise for lens 3, slit 2 and detectors 3 and 4. The intersection of the rays by back-projection image of slit 2 and the source beam define interrogation volume 2 for the heterodyne system. The positions of slit 1 and slit 2 are adjusted so that their interrogation volumes coincide on the source beam. A portion the source beam, which was split off by a beamsplitter (the source beamsplitter), is reflected by a mirror to be expanded by a negative lens 5. This expanded beam is focused by lens 6 to match the wavefront of the scattered beam through lens 3. This matching beam is folded through slit 2 by a second beamsplitter (the detector beamsplitter) to mix with the scattered light on detectors 3 and 4. The total of the optical pathlengths from the source beamsplitter to the particle in the sample cell and from the particle to detectors 3 and 4, must match the total optical pathlength of the local oscillator beam from the source beamslitter through the mirror, lenses 5 and 6, the detector beamsplitter, and slit 2 to detectors 3 and 4. The difference between these two total optical pathlengths must be less than the coherence length of the source to insure high interferometric visibility in the heterodyne signal. The

scattered light is Doppler shifted by the flow velocity of the particles in the cell. By mixing this Doppler frequency shifted scattered light with unshifted light from the source on a quadratic detector (square of the combined E fields), a Doppler beat frequency is generated in the currents of detectors 3 and 4. The current oscillation amplitude is proportional to the square-root of the product of the source intensity and the scattered intensity. Hence, by increasing the amount of source light in the mixing, the detection will reach the Shot noise limit, allowing detection of particles below 0.1 micron diameter. By vibrating the mirror with a vibrational component perpendicular to the mirror's surface, introducing optical phase modulation, the frequency of the heterodyne carrier can be increased to produce more signal oscillations per particle pulse. Then the mirror vibration signal could be used with a phase sensitive detection to improve signal to noise. For particles above approximately 0.4 microns, signals from all 4 detectors will have sufficient signal to noise to provide accurate particle size determination. The theoretical values for these 4 detectors vs. particle size may be placed in a lookup table. The 4 detector values from a measured unknown particle are compared against this table to find the two closest 4 detector signal groups, based upon the least squares minimization of the function:

(S1-S1T)^2 + (S2-S2T)^2 + (S3-S3T)^2 + (S4-S4T)^2

where S1,S2,S3,S4 are signals from the 4 detectors, S1T,S2T,S3T,S4T are the theoretical values of the four signals for a particular particle size, and ^2 is the power of 2 or square of the quantity preceding the ^.

The true size is then determined by interpolation between these two best data sets based upon interpolation in 4 dimensional space. For particles of size below some empirically determined size (possibly around 0.4 micron), detector 1 and 2 signals will be rejected for insufficient signal to noise, and only the ratio of the signals (or other function of two signals) from shot noise limited heterodyne detectors 3 and 4 are used to size each particle. If the low angle signals from detectors 1 and 2 are needed for small particles, they could be heterodyned with the source light using the same optical design as used for detectors 3 and 4. The look up table could also be replaced by an equation in all 4 detector signals, particle size equals a function of the 4 detector signals. These techniques, least squares or function, could be extended to more than 4 detectors. For example, 3 detectors could be used for each system, discarding the low angle non-coherent detection when the signal to noise reaches unacceptable levels. In this case, a 6-dimensional space could be searched, interpolated, or parameterized as described above for the 4 detector system. This disclosure claims the use of any number of detectors to determine the particle size, with the angles and parameterization functions chosen to minimize size sensitivity to particle composition.

By tracing rays back from slits 1 and 2, the field of view for systems 1 and 2 are determined, as shown in Figure 2. The traced rays and source beam converge into the interrogation volume, where they all intersect. Figure 2 shows these rays and beam in the vicinity of this intersection volume, without detailed description of the converging nature

of the beams. In this case, the beam from slit 1 may be wider than that from slit 2, so that the source beam and slit 2 field of view fall well within the field of view of slit 1. And the source beam falls well within the field of view of slit 2. By accepting only particle signal pulses which show coincidence with pulses from detector 4 (which has the smallest intersection with the source beam, shown by the crosshatched area) , the interrogation volume is matched for all 4 detectors. The source beam could also have a rectangular crossection, with major axis aligned with the long axis of the slits. This would reduce the edge effects for particles passing near to the edges of the beam. The slit images are designed to be much longer than the major axis of the source beam, so that both slits only need to be aligned in the direction perpendicular to the source major axis. This provides for very easy alignment to assure that the intersection of images from detectors 3 and 4 and the source beam fall within the intersection of images from detectors 1 and 2. The slit position could also be adjusted along the optical axis of the detection system to bring the crossover point of both detector fields of view to be coincident with the source beam. Another configuration is shown in Figure 2b, where slit 2 is wider than slit 1. Here detector 2 defines the smallest common volume as indicated by the cross hatched area. And so only particles which are counted by detector 2 can be counted by the other detectors. All other particles detected by the other detectors, but not detected by detector 2, are rejected because they do not produce signals in every detector. This process can be extended to more than 4 detectors. In some cases three or more detectors per optical system may be required to obtain accurate size measurement. In this case, the size would be determined by use of a look up table.

The data for each particle would be compared to a group of theoretical data sets. Using some selection routine, such as total RMS difference, the two nearest size successive theoretical sets which bracket either side of the measured set would be chosen. Then the measured set would be used to interpolate the particle size between the two chosen theoretical sets to determine the size. The size determination is made very quickly (unlike an iterative algorithm) so as to keep up with the large number of data sets produced by thousands of particles passing through the sample cell. In this way each particle could be individually sized and counted according to it's size to produce a number-vs.-size distribution which can be converted to any other distribution form. These theoretical data sets could be generated for various particle refractive indices and particle shapes.

In general, a set of design rules may be created for the intersection of fields of view from multiple scattering detectors at various angles. Let us define a coordinate system for the incident light beam with the z axis along the direction of propagation and the x axis and y axis are both perpendicular to the z axis, with the x axis in the scattering plane and the y axis perpendicular to the scattering plane. In all cases the detector slits are oriented parallel to the y direction. Three different configurations are considered:

1) The incident beam is smaller than the high scattering angle detector field crossection, which is smaller than the low scattering angle detector field crossection. Only particle pulses that are coincident with the high angle detector pulses are accepted. The incident beam may be spatially filtered in the y direction, with the filter aperture

imaged into the interaction volume. This aperture will cut off the Gaussian wings of the intensity profile in the y direction, providing a more abrupt drop in intensity. Then fewer small particles, which pass through the tail of the intensity distribution, will be lost in the detection noise and both large and small particles will see the same effective interaction volume.

2) The incident beam is larger than the low scattering angle detector field crossection, which is larger than the high scattering angle detector field crossection. Only particle pulses that are coincident with the high angle detector pulses are accepted. The correlation coefficient of the pulses or the delay (determined by crosscorrelation) between pulses is used to insure that only pulses from particles seen by every detector are counted.
3) The incident beam width and all fields from individual detectors progress from small to large size. Then particles counted by the smallest entity will be sensed by all of the rest of the detectors.

The two detector pairs, 1+2 and 3+4, could also be used independently to measure count vs. size distributions. The lower angle pair could only measure down to the size where the ratio of their angles is no longer sensitive to size and the scattering crossections are too small to maintain signal to noise. Likewise for the high angle detectors, they can only measure up to sizes where their ratio is no longer monotonic with particle size. However, absolute scattered signal levels could be used to determine the particle size outside of this size region. Since extremes of these operational ranges overlap on the size scale, the two pairs could be aligned and operated independently. The small angle detectors would miss some small particles and the high angle detectors would miss some large particles. But the two independently acquired particle size distributions could be combined using their particle size distributions in the size region where they overlap. Scale one distribution to match the other in the overlap region and then use the distribution below the overlap from the high angle detectors for below the overlap region and the distribution from the low angle detectors for the distribution above the overlap region. In the overlap region, the distribution starts with the high angle result and blends towards the low angle result as you increase particle size. Detector triplets could also be used, where the largest angle of the low angle set and the lowest angle of the high angle set overlap so as to scale the scattering measurements to each other.

The flat window surfaces could be replaced by spherical surfaces with center of curvature coincide with the interrogation volume. Then the focal positions of all of the beams would remain in the same location for dispersing liquids with various refractive indices. These systems can also be designed using fiber optics, by replacing beamsplitters with fiber optic couplers. Then the vibrating mirror could be replaced by a fiber optic phase modulator.

Figure 3 shows an alternate optical configuration for Figure 1, where the low angle scattering system is placed on the opposite side of the cell from the high angle system. In

some cases, this configuration will facilitate the mechanical design of the support structure for the cell and optical systems.

The detector currents from the low angle system and the high angle system must be processed differently. Every particle passing through the interaction volume will produce a pulse in the detector current. Detectors 1 and 2 will show simple pulses, but detectors 3 and 4 will produce modulated pulses. The heterodyne detection measures the Doppler beat frequency as the particle passes through the beam. So each heterodyne pulse will consist of a train of oscillations which are amplitude modulated by an envelope determined by the intensity profile of the incident beam. The heterodyne signal must pass through a high pass filter (to remove the large local oscillator offset) and then an envelope detector (see Figure 4) to remove the heterodyne oscillations before further processing. This preprocessing envelope detection is used in the process steps below.

For small particles the heterodyne signals will be buried in laser source noise. Figure 5 shows an additional detector 5 which measures the intensity of the local oscillator laser noise. If we define a heterodyne detector current as I1 and the detector 5 laser monitor detector current as I2 we obtain the following equations which hold for each of the heterodyne detectors.

$$I1 = \text{sqrt}(R*Io(t) * Is(t)) * COS(F*t + A) + R*Io$$

$$I1 = \text{sqrt}(R*Io(t) *S(1-R) Io) * COS(F*t + A) + R*Io$$

$$I2 = K*Io(t)$$

where:

COS(x) = cosine of x

K is a constant which includes reflectivity of the beamsplitter 1

R is the reflectivity of beamsplitter 2

sqrt(x) = square root of x

Io(t) is the source beam intensity as function of time t

F is the heterodyne beat frequency at a heterodyne detector due to the motion of the scatterer in the sample cell. And A is an arbitrary phase angle for the particular particle. Is(t) is the scattered light intensity from the particle:

$Is(t) = S*(1-R)*Io(t)$ where S is the scattering efficiency or scattering crossection for the particle

The light source intensity will consist of a constant portion Ioc and noise n(t):

$Io(t) = Ioc + n(t)$

We may then rewrite equations for I1 and I2:

$I1 = sqrt(S*(1-R)*R)*(Ioc +n(t))*COS(F*t + A) + R*(Ioc + n(t))$

$I2 = K*(Ioc + n(t))$

The heterodyne beat from a particle traveling with nearly constant velocity down the sample cell will cover a very narrow spectral range with high frequency F. For example, at 1 meter per second flow rate, the beat frequency would be in the megahertz range. If we use narrow band filters to only accept the narrow range of beat frequencies we obtain the narrow band components for I1 and I2:

$I1nb = sqrt(S*(1-R)*R)*Ioc*COS(F*t + A) + R*n(t)$

$I2nb = K*n(t)$

where we have assumed that n(t) is much smaller than Ioc. And also n(t) is the portion of the laser noise that is within the electronic narrowband filter bandwidth (see below).

The laser noise can be removed to produce the pure heterodyne signal, Idiff, through the following relationship:

$Idiff = I1nb - (R/K)*I2nb = Sqrt(R*(1-R)*S)*Ioc*COS(F*t + A)$

This relationship is realized by narrowband filtering of each of the I1 and I2 detector currents. One or both of these filtered signals are amplified by programmable amplifiers, whose gains and phase shifts are adjustable. The difference of the two outputs of these amplifiers is generated by a difference circuit or differential amplifier. With no particles in the beam, the gain and phase shift of at least one of the programmable amplifiers is adjusted, under computer or manual control, to minimize the output of the difference circuit. At this gain, the source intensity noise component in the detector 5 beat signal, with particles present, is corrected for in the difference signal, which is fed to an analog to digital converter (A/D), through a third narrowband filter, for analysis to sense the beat signal buried in noise. This filtered difference signal could also be detected by a phase locked loop, which would lock in on the beat frequency of current from the heterodyne detector.
The flow rate could also be adjusted to maximize the heterodyne signal, through the electronic narrowband filter, from flowing particle scattered light.

This entire correction could be accomplished in the computer by using a separate A/D for each filtered signal and doing the difference by digital computation inside the computer. If both signals were digitized separately, other correlation techniques could be used to reduce the effects of source intensity noise. Beamsplitter 2 reflection is adjusted to obtain shot noise limited heterodyne detection, with excess laser noise removed by the difference circuit.

The noise correction techniques described on the prior pages (and Figure 5) can be applied to any heterodyning system by simply adjusting the filtering of currents I1 and I2 to pass the signal of interest, while blocking the low frequency component (Ioc) of Io(t). Excess laser noise, shot noise, and any other noise component, which is present in both the heterodyne signal and the light source, can be removed from the signal of interest through this procedure. One application is dynamic light scattering, where the heterodyne signal is contaminated by laser source noise in the optical mixing process. The filters on I1 and I2 would be designed to pass the important portion of the Doppler broadened spectrum (using a lower frequency broad band filter or high pass filter instead of the high frequency narrow band filter) and to remove the large signal offset due to the local oscillator. Then by using the subtraction equation described on page 12 (where the narrow band filter is replaced by the above filter in all equations) the effects of laser noise can be removed from the Doppler spectrum, improving the particle size accuracy. In the case of fiber optic heterodyning systems, the laser monitor current, I2, could be obtained at the exit of the unused output port of the fiber optic coupler which is used to transport the light to and from the particle sample, because this port carries light only from the optical source, without any scattered light. This subtraction shown in the equation on page 12 could be accomplished by the analog difference circuit or by digital subtraction after digitization of both the filtered contaminated signal and the filtered source monitor as outlined on page 12. This procedure could also be accomplished using the unfiltered signals, but with much poorer accuracy due to the large signal offsets.

Figure 6 shows the system with some additional features. The sample cell windows contain spherical surfaces with center of curvature at the interaction volume. The light source beam and detector acceptance cones pass through these spherical surfaces in order to avoid focal shift of the source and detector beams when the refractive index of the dispersing fluid is changed. The heterodyne detector currents from detectors 3 and 4 are passed through a high pass filter to remove the large local oscillator current and then (after completing the noise removal described above) they are passed through an envelope detector to remove the heterodyne oscillation due to the Doppler shifted spectrum of the scattered light from the moving particles. As mentioned earlier, this Doppler frequency may be increased by vibrating the mirror so as to add phase modulation to the local oscillator. This will provide more signal oscillations per signal pulse. After the high pass filter, the signal will consist of a sinusoid which is amplitude modulated by the scattering pulse due to the particle's transit through the source beam. The envelope of this modulated sinusoid is measured by an envelope detector as shown in Figure 4. The

resulting single pulse is digitized by an analog to digital converter (A/D) before analysis by a computer. This process is similar for each of detectors 3 and 4. Since lower angle scattering produces lower Doppler frequency, the lower scattering angle signals are usually measured without heterodyne detection when the signals are large. So for large signal levels, Detectors 1 and 2 do not require heterodyne detection; but a heterodyne optical system, as used for detectors 3 and 4, could be used for detectors 1 and 2 if the signal levels were small. Then the vibrating mirror phase modulator, shown in figure below, could be used to increase the heterodyning frequency. If the signals are large, the scattered light current pulses from detectors 1 and 2 can be digitized directly before computer analysis, without envelope detection. The analysis of these signals is described below.

One other aspect of this invention is a means for auto-alignment of the optics. As shown in figure 2, the source beam and all four fields of view from the four detectors must intersect at the same point to all see scattering from the same particle. Images of slits 1 and 2 define the point where the view fields from each detector pair (1+2 or 3+4) intersect. The slit apertures usually only need alignment in one direction, perpendicular to the slit, but position adjustment may also be needed along the optical axis of the detector system to place the intersection between the fields of view from detectors 1 and 2 (or 3 and 4) on the source beam. Either one or both slits may be adjusted to obtain alignment. Figure 5 shows an example where both slit positions are optimized by a computer controlled micro-positioner. For example, the digitized signals from detector 2 and detector 3 could be digitally multiplied (after the envelope detector) and the resulting product integrated or low pass filtered to produce a correlation between the two detector signals. The position slit 1 is adjusted until this correlation signal is maximum with particles flowing through the interaction volume. If needed, both slits 1 and 2 may be moved to optimize this correlation signal. In general these should be small adjustments because the spherical window surfaces will prevent large beam refractions and focal shifts due to changing particle dispersant refractive index. In systems with large beam shifts, the slits may need to be moved perpendicular and parallel to the optical axis of each optical system to maximize the correlation between the detectors. This could be accomplished with dual axis micro-positioners.

Figure 2 shows larger fields of view for detectors 1 and 2 than for detectors 3 and 4. This is accomplished with slit 1 wider than slit 2 or by larger magnification for lens 4 than for lens 3 (image of the slit in the interaction volume). Hence the alignment of slit 1 is much less critical then slit 2 because image of slit 1 in the interaction volume is wider and has larger depth of focus than for slit 2. By placing computer controlled micro-positioners on slit 1 and slit 2, the system can be aligned by using the correlation between the signals. The micro-positioners move each slit perpendicular to the long axis of the slit opening and perpendicular to the optical axis of that lens. The alignment procedure is described below:

1) With low concentration of particles in the flow stream, adjust the position of slit 2 to maximize the correlation (using an analog multiplier and RMS circuit) between the signals from detectors 3 and 4. At this point the intersection of the fields of views of both detectors cross at the incident beam.
2) Then adjust the position of slit 1 until the correlation of detectors 1 and 2 with detectors 3 and 4 is a maximum. After this adjustment both detectors 3 and 4 view the intersection defined by step 1.

During particle counting and measurement, only particles seen by both detectors 3 and 4 are counted by all of the detectors, because they are a subset of the particles seen by detectors 1 and 2. By using different slit image sizes and using the smaller slit images to determine count acceptance, the system will accept only particles which are seen by all four detectors. If the slit images from detectors 3 and 4 are larger than the images from detectors 1 and 2, then detectors 1 and 2 would be adjusted before adjusting 3 and 4; and detectors 1 and 2 would select which particles are counted. The general rule is that the detector images which have the smallest intersection with the incident beam are adjusted first and they determine which particles will be counted. The slit widths are chosen to create one slit image with a small intersection volume and the other with a larger intersection volume so that when a particle is detected in the smaller volume, it is clearly within the larger volume. The smaller slit image only needs to cross the incident beam near to its image plane. Then the larger slit image only needs to cover the intersecting volume to insure that it sees all of the particles passing through the smaller slit image. Then by only counting particles detected by the smaller slit image, only particles which are seen by both detectors will be counted. If the slit images were comparable in size, very precise alignment of both slit images with each other would be required and the correlation between the detector signals would be needed to chose which particles to count. This comparable sized slit case is also claimed in this disclosure.

Figure 6b shows an example of scattered detection pulses from the four detectors. These signals are measured after a high pass filter for each of detectors 1 and 2, and after a high pass filter and envelope detector for each of detectors 3 and 4. This data describes the case where the particle passes through a corner of the volume which is common to the source beam and the field of view from detector 4 (see figure 2). Detectors 1, 2, and 3 shown similar profiles as a function of time as the particle passes through the interaction volume. However the signal from detector four is truncated at the leading edge due to the edge of the detector field of view. Over the region where the particle is well within the detector fields of view, each detector signal will maintain the same ratio with another detector signal as the detector signal amplitudes follow the particle passing through the source crossection intensity distribution. This region of stable signal ratio must be determined in order to eliminate the effects of the variation in source intensity by ratioing pairs of detector signals. Each of the four detector signals is digitized and the ratio of signal from the detector with the minimum interaction volume with one of the other detectors is calculated at each A/D (analog to digital conversion) sampling point. The A/D may be only turned on by a comparator during the period where all the detector

signals are above a noise threshold, between times T1 and T2 in Figure 6b. In this case the ratio between detectors 3 and 4 is used to determine the optimum portion the sampled data to use. The ratio of detector 4/detector 3 increases as the particle enters the field of view of detector 4. Once the particle is completely inside the field of view, the ratio between the two signals is nearly constant even though the individual signals are changing due to the source intensity distribution non-uniformity. Eventually, the signal levels drop and the signal ratio becomes very noisy. If we assume that there are 20 samples between T1 and T2, we could measure the variance of the ratio for samples 1 through 5 and then the variance of the ratio for samples 2 through 6, and so on up to samples 16 through 20. The 5 sample set with the lowest variance for the detector 3/ detector 4 ratio would be chosen to determine the detector to detector ratios for all detector combinations for that particle, either by choosing the sample in the middle (sample 3) of that set or by averaging all 5 ratios to obtain an averaged ratio for the 5 samples in the set.

The pulses shown in Figure 6b are the result of some prior electronic filtering and envelope detection. The signals from detectors 1 and 2 will be simple pulses which may be cleaned up by a high pass filter before the A/D conversion. The signals from the heterodyne detectors 3 and 4 are the product of a pulse and a sinusoid. The pulse may consist of a megahertz sine wave, amplitude modulated by the intensity profile of the source beam over a period of about 100 microseconds. This oscillatory signal sits on top of a large offset due to the local oscillator intensity. This offset and other source noise components may be removed from the heterodyne signal by high pass or narrow-band electronic filtering. The power spectrum of these pulses will reside in a 100 kilohertz band which is centered at 1 megahertz. Hence a narrow-band filter may provide optimal signal to noise for the heterodyne signals. After the filtering, the signals could be digitized directly for digital envelope detection or an analog envelope detector could be used to remove the 1 megahertz carrier, reducing the required sampling rate to only 10 to 20 samples per pulse instead of 400 samples per pulse. By using a dual phase lock-in amplifier with reference oscillator set to the heterodyne frequency (1 megahertz in this example), extremely high signal to noise could be obtained by measuring the filtered signal without the envelope detector. By using the zero degree and quadrature outputs, the phase sensitive signal would be recovered even though the reference and signal carriers are not in phase.

The particle counting rate can also be increased by digitizing the peak scattered signal (directly from detectors 1 and 2 and after the envelope detector from detectors 3 and 4) from each particle instead of digitizing many points across the scattering pulse and finding the peak digitally. This is accomplished by using an analog peak detector whose output is digitized in sync with the positive portion of the signal pulse derivative and reset by the negative portion of the derivative. Then only one digitization is needed for each particle, as shown in figure 7. The negative comparator switches on when the input signal drops below the reference setting and the positive comparator switches on when the signal is greater than the reference setting.

Another variation of this concept triggers on the actual signal instead of the derivative, as shown in Figure 8. When the signal rises above a preset threshold, the positive comparator takes the peak detector out of reset mode. As the signal rises the output of the peak detector (see Figure 9) follows the input signal until the signal reaches a peak. After this point, the peak detector holds the peak value with a time constant given by the RC of the peak detector circuit. The input signal drops below this as it falls down the backside of the peak. When the signal reaches some percentage of the peak value, the A/D is triggered to read and then reset the positive comparator. This percentage value is provided by a voltage divider (shown in the figure as 0.5X voltage divider, but other divider ratios would also be appropriate between approximately 0.2 to 0.8) which determines the reference level for the negative comparator. The A/D is only triggered once per signal pulse and measures the peak value of the pulse. Using this circuit, the detector with the smallest interaction volume generates the A/D trigger for all of the other detectors, so that only particles seen by all of the detectors are counted.

The detector signals are either digitized directly, peak detected with the circuit in Figure 7 or Figure 8, or integrated and sampled at a lower rate. The signal can be continuously integrated (up to the saturation limit of the integrator). Then the integrated signal needs to be sampled only at points of zero slope in the integrated signal, between each pulse. By subtracting the integrated values on either side of the pulse, the integral of each pulse is sampled separately without having to sample the pulse at a high sampling rate. Also each pulse could be sampled at a lower rate and then a function could be fit to these samples to determine the peak value of the pulse. This should work particularly well using Gaussian functions which model the intensity profile of the laser beam. The parameters of the best fit Gaussian solution directly provides the peak, half width, or integral of the pulse. In any case, the final signal from each pulse will be analyzed and counted. One problem associated with conventional particle counters is the incident beam intensity profile in the interaction volume. Identical particles passing through different portions of the beam will see different incident intensity and scatter light proportionally to that intensity. But the scattered intensity also depends upon the particle diameter, dropping as the sixth power of the diameter below 0.3 microns. So the effective interaction volume will depend upon particle diameter and detection noise, because particles will not be detected below this noise level. Therefore small particles will be lost in the noise when they pass through the tail of the intensity distribution. This means that larger particles have a larger effective interaction volume than smaller particles and therefore the number distribution is skewed in favor of large particles. This invention includes a method for creating a particle diameter-independent interaction volume, using signal analysis. The systems in Figures 1,

2, and 3 use at least 2 detectors per scatter collection system to remove the incident intensity dependence by using the ratio of two scattering angles to determine the particle size. Also for any number of detectors, ratios between any pair of detectors could be used to determine the size of particles in the size range covered by that pair`. Instead of detector pairs, detector triplets or quadruplets, etc. could also be used with appropriate equations or lookup tables to determine the size of each particle independent of the incident intensity on the particle. In the case of detector pairs, both scattered signals, S(A1) and S(A2), are proportional to the scattering function, at that angle, times the incident light intensity:

$$S(a1) = K*I0*F(D,a1)$$

$$S(a2) = K*I0*F(D,a2)$$

where I0 is the incident intensity, K is an instrumental constant, and F(D,A) is the scattering per particle per unit incident light intensity for a particle of diameter D, at scattering angle A. For more than two detectors, there is a similar equation for each detector signal for angles a1, a2, a3, a4, etc. The scattering signals S(a) may be the pulse peak value or pulse integral of the envelope of the heterodyne signal (detectors 3 and 4) or of the direct non-coherent signals (detectors 1 and 2). So The ratio of the scattering at two angles is equal to F(D,a1)/F(D,a2), which is independent of incident intensity and relatively independent of position in the Gaussian beam profile of a laser. Figure 10 shows a conceptual plot of number of particles vs. S(a1)/S(a2) and S(a2). A plot of number of particles vs. S(a1)/S(a2) and S(a1) could also be used. The scattering signal, for any diameter D, will show a very narrow range of S(a1)/S(a2) but a broad range of S(a2). Particles passing through the peak of the laser intensity profile will produce pulse peak amplitudes at the upper limit, maximum S(a2). The surface, describing this count distribution, is determined by fitting a surface function to, or by interpolation of, this count surface in figure 10. This surface function provides the parameters to determine an accurate particle count, because S(a1)/S(a2) is a strong function of particle size, but a very weak function of particle path through the beam. By setting an acceptance threshold for S(a2) at a certain percentage of this maximum value, separately at each value of S(a1)/S(a2), only particles passing through a certain volume (independent of particle size) of the beam will be accepted and counted. Because the particles, which are counted by these detectors, are all much smaller than the source beam crossection, they all have the same probability functions for describing the percentage of particles passing through each segment of the beam. Therefore, at any value of S(a1)/S(a2), the shape of the count vs. S(a2) function is nearly identical when you normalize the function to maximum S(a2). By setting a count-above threshold at a certain percentage of maximum S(a2) (but well above the noise level) at each value of S(a1)/S(a2), only particles passing through a certain portion of the interaction volume will be counted and sized, as shown in figure 10b.

This analysis is usually done for the detector with the smallest interaction volume, the heterodyne system in the case of Figure1. All four detectors are used to determine the particle diameter, but the acceptance criteria is determined by only detector 3 and 4 (S(a1)=detector 3 and S(a2)=detector 4). These counts are accumulated into a set of size ranges, each range defines a different size channel. In many cases, each size range has a very narrow width in size and S(a1)/S(a2). The optimum channel size width is the minimum width which still contains sufficient particle counts in that channel to avoid statistical errors. Hence, the distribution of S(a2) for the range of S(a1)/S(a2) within a certain channel can determine the S(a2) acceptance limit for counts in that channel. This is accomplished by only counting particles with S(a2) above a certain percentage of the maximum S(a2) for that channel. If the theoretical scattering efficiency changes substantially across any channel, the S(a) for each count is divided by the theoretical scattering efficiency indicated by the size corresponding to the S(a1)/S(a2) for that particle. This may be especially important below 0.4 microns where the scattering efficiency drops as the inverse of the sixth power of the particle diameter.

The shape and width of the S(a2) profile is determined by how sharply the source crossectional intensity distribution drops off at the edges of the beam. If the beam profile was a step function, the effective interaction volume would not be particle size dependent. This shape can be accomplished by spatially filtering the source, with the spatial filter aperture in a plane conjugate to the interaction volume. Then an image of the aperture, which is smeared by aberrations and diffraction limits, defines the sharpness of intensity drop at the edges of the beam. The intensity tails of the Gaussian beam are cut off by the aperture, which could be sized to cut off at any appropriate percentage of the peak intensity to limit the variation of scattering from a particle as it traverses the beam. The beam crossectional intensity distribution may also be shaped by use of appropriate apodization of the beam.

Figure 10b describes this concept for data collected in one size channel. The pulse signal is collected and stored for each pulse above the count noise threshold. But only pulses which are within the range of S(a1)/S(a2) for that channel are collected into that channel. The frequency distribution of counts at each pulse level is plotted for a beam with a Gaussian intensity profile. The problem is that some particle pulses fall below the noise threshold and are not counted. The amount of missed particles depends upon the scattering efficiency of the particles. For smaller particles with lower scattering efficiency, a higher percentage of particles will be lost below the noise threshold. So the count error will be particle size dependent. The source beam can be spatially filtered to cut off the low intensity wings of the source intensity distribution. Then the count distribution would be as shown in the "with aperture (ideal)" curve and no particles would be lost in the noise. This could be accomplished by using a rectangular spatial filter that cut the wings off in the Y direction, because the particle flows in the XZ plane

and the tails in this plane are actually measured in each pulse shape. However, the image of the spatial filter aperture in the interaction volume will be aberrated and diffraction limited as shown by the "with aperture (aberrated)" curve. In this case a few particles may still be lost in the noise and a count threshold must be set above this level to reject all questionable particle pulses. The maximum S(a2) value changes in each channel due to the change in scattering efficiency for the particles in that channel. As long as the count threshold is set to be the same percentage of that maximum S(a2) for each channel, all channels will lose the same percentage of particles and the distribution will be correct. Without this channel specific threshold, the smaller particle channels will lose a larger percentage of particles than the larger particle channels and the distribution will be skewed towards larger particles. This assumes that the sample is a homogeneous mixture of all the particle sizes and that the sufficient count exists in each channel to obtain an accurate estimate of the maximum S(a2).

The method described above handles the variations caused by the particle passing through various random paths in the interaction volume. This method can also correct for the variations due to random positions along the path where the digitization occurs. Therefore the peak detectors or integrators could be eliminated. The signal from the envelope detector (detectors 3+4) and direct signals from detectors 1+2 could be digitized directly at approximately 3 points per pulse. The maximum signal data point from each pulse would be added to the data list for input to the analysis described above. Any deviation from the peak value would not be a problem because the ratio of the signals determines the size and all four detectors will be low by the same percentage if they are not sampled at the peak intensity position in the interaction volume.

Also all the signals could be digitized directly after the high pass filter on the detectors (detectors 3 and 4 are high pass filtered to remove local oscillator current and detectors 1 and 2 could also be high pass filtered to remove low frequency noise). Then all of the analog and digital operations (phase sensitive detection, envelope detection, etc.) could be done digitally but at the cost of high data collection rates. Also the source could be modulated for detectors 1 and 2 to use phase sensitive detection (lock-in amplifier) when their signals are low.

All of the optical design and algorithm techniques described in this disclosure may leave some residual size response broadening which may be particle size dependent. This instrument response broadening is determined by measuring a nearly mono-sized particle sample (such as polystyrene spheres). For example, due to noise or position dependence in the beam, a certain size particle will produce a range of S(a1)/S(a2) values as it repeatedly passes through different portions of the interaction volume. In any event, the broadening may be removed by solving the set of equations which describe the broadening phenomena. If the broadening is relatively the same for all size particles, the response broadening can be described by a convolution of the broadened number distribution response and the actual number vs. size distribution. Iterative deconvolution algorithms may be used to deconvolve the measured number vs. measured parameter distribution to obtain size resolution enhancement. This resolution enhancement will

work for any ergodic stochastic process, where the broadening statistics are stable over time. This idea could be applied to (and is claimed for) any broadened counting phenomena with stable stochastic or deterministic broadening mechanisms. In particle counting measurements the amount of scatter from a particle may vary due to the random orientation and position of a particle as it passes through the exciting light beam, or by other structural and optical noise sources. The counting and classification of each of a group of identical particles will not produce a narrow peak when plotting count number vs. measured parameter. Here "measured parameter" refers to the parameter which is measured from each particle to determine its size. Examples of measured parameters are scattering optical flux amplitude, ratio of flux from two scattering angles, a function of fluxes from multiple scattering angles, or the decrease in intensity due to particle scattering and absorption, as will be described later in this disclosure. The peak of the number-vs.-measured parameter function from a group of monosized particles will be broadened in a predictable way. This broadening can be determined experimentally with a calibrated group of particles or it can be calculated theoretically based upon models for the random and deterministic broadening sources. Then the entire system can be modeled using a matrix equation, where each column in the matrix is the broadened measured parameter distribution from a certain sized particle. This broadening is reproducible as long as a large number of particles are counted for each trial. The matrix equation is described by the following relationship:

$$Nm = M*N$$

Where Nm is the vector of values of the measured (broadened) number-vs.-measured parameter distribution and N is the vector of values of the actual particle number-vs.-size distribution which would have been measured if the broadening mechanisms were not present. The number distribution is the number of particles counted with parameter amplitudes within certain ranges. It is a differential distribution which describes counts in different channels or bins, each bin with a different range of parameter, which may be size, scattering ratio, etc.. M is a matrix of column vectors with values of the broadened number-vs.-measured parameter function for each particle size in N. For example, the nth column of M is a vector of values of the entire measured number-.vs.-measured parameter distribution obtained from a large ensemble of particles of the size which is represented by the nth element of vector N. This matrix equation can be solved for the particle number-vs.-size distribution, N, by matrix inversion of M or by iterative inversion of the matrix equation. This particle number-vs.-size distribution can be determined by using this matrix equation in many different forms. The term "measured parameter" in this paragraph can refer to many size dependent parameters including: scattering signal amplitude (pulse peak or integral, etc.), the ratio (or other appropriate mathematical relationship) between scattered signals at two or more different angles, or even particle diameter (a broadened particle size distribution determined directly from a broadened process can also be "unbroadened" by using broadened particle size distributions for each monosized sample column in matrix M) .

If each column of M is simply a shifted version of the prior column, then the instrument response is shift invariant and the relationship is a convolution of N with the system impulse response IMP:

Nm = IMP **N

where ** is the convolution operator

For this case, deconvolution algorithms may be used to solve for N.

The generalized matrix equation above may also include the effects of coincidence counting. As discussed earlier, over one million particles should be counted for a uniform volume distribution to be accurately determined in the large particle region. In order to insure low coincidence counts, the source spot size in the interaction region must be reduced to approximately 20 microns in width so that the particle concentration can be raised to count 1 million particles at flow rates of 1 meter per second in a reasonable time. For example, the worst case is slit 1 being the largest slit, because then the largest interaction volume would be approximately 20 micron x 20 micron x 200 micron. If we require approximately 5 volumes per particle to avoid coincidence counts then the inter-particle spacing is 74 microns. 1 million particles spaced by 74 microns (on average) moving at 1 meter per second will take 74 seconds to measure. This spot size would provide good count reproducibility for the worst case of uniform volume distribution. However, a 20 micron spot and the corresponding detector fields of view may be difficult to align, requiring larger source spot size with a higher coincidence level. Even with a 20 micron spot, some coincidences will be seen at the 74 micron particle spacing. These coincidences can be corrected for by including their effects in the generalized matrix equation. A column in matrix M which corresponds to the large size end of vector N will have negative values in the region corresponding to the small size end of vector Nm, because the larger particles will block the scattered light from smaller particles which are ahead or behind that larger particle in the source beam. Also a column in matrix M which corresponds to the small size end of vector N will have a tail of positive values in the region corresponding to the large size end of vector Nm, because some smaller particles will be counted coincidently with the larger particles and increase their measured size relative to their actual size. The effects of coincident counts can be mitigated by using a wedge shaped cell as shown in Figure 9b. The cell consists of two windows at an angle so as to produce regions of different optical path along the cell. This cell could replace the cells in Figure 11 and 12. The red rays define the edges of the source beam. Then at any point along the wedge direction, only particles smaller than a certain size may pass through that portion of the cell. The size distributions gathered at different points along the wedge, from the 2 dimensional detector array in Figures 11 and 12, may be combined by correcting the count in the larger particle areas for coincidently counted smaller particles by using counts in the smaller particle regions of the wedge. This correction can be accomplished by solving a matrix equation of the form on page 24.

The correction for coincidences may also be accomplished by an iterative procedure, which solves for N, given Nm, and then corrects each scattered signal for coincidences. Each scattered signal, S1 and S2, consists of light scattered (or light lost due to absorption or scattering) from all the particles in the interaction volume. Ideally, the particle concentration is low and most of the time each scattering event is from a single particle. But for the general case, multiple coincident particles can be modeled by the following equation:

Ai= SUMj(G(Ni,Nj) Aj)

where SUMj means summation over the j index. Ai is the "particle signal" for a particle of the ith size bin in the particle size distribution. Particle signals can include S1, S2, or the log of attenuation or obscuration (described later in this disclosure) due scattering and absorption of a particle. G(Ni,Nj) is a function which describes the most probable total particle signal from a combination of particles of ith and jth sizes based upon their particle numbers (or concentrations), Ni (for the ith size) and Nj (for the jth size). Since the combination of particles in the interaction volume is a random process, G(Ni,Nj) represents the sum of all combinations (given Ni and Nj), weighted by their probability functions.

In the case of signals S(a1) and S(a2), the procedure for determining the number vs. size distribution is the following:

1) Use the surface plot of Figure 10 and 10b to determine the raw number distribution Nm.
2) Solve the matrix equation Nm = M*N for the true number distribution N.
3) Recalculate S(a1) and S(a2) using the equation above and the distribution N:
   S(a1)i= SUMj(G1(Ni,Nj) S(a1)j)
   S(a2)i= SUMj(G2(Ni,Nj) S(a2)j)
4) Do steps 1 through 3 again
5) repeat iteration loop of step 4 until the change in number distribution N between successive loops is below some threshold.

For particles between approximately 1 and 10 microns, the ratio of scattered intensities at two angles below approximately 3 degrees scattering angle is optimal to provide highest size sensitivity and accuracy. A white light source or broad band LED should be used to reduce the Mie resonances for spherical particles. Above 10 microns, the measurement of total scatter from a white light source provides the best size sensitivity and depth of focus for a spatially filtered imaging system as shown in Figure 11. A white light or broad band LED source is spatially filtered by lens 1 and pinhole 1 to provide a well collimated beam through lens 2. If a well collimated source beam is required to measure scattering at very low scattering angles (for large particles), a laser source might also be used. This collimated beam passes through a cell consisting of two windows, which confine the flowing particle dispersion. Lens 3 focuses this collimated beam through pinhole 2, which

removes most of the scattered light from the beam. This transmitted beam is transferred to a 2 dimensional detector array through lens 4, which images the center of the sample cell onto the array. This array will see dark images of each particle on a bright background due to the light lost through scattering or absorption by the particle. A beamsplitter after lens 3 diverts a portion of the light to an aperture and lens 5. The aperture defines a narrow pencil of light through the cell and a small scattering volume, lowering the probability of coincidence counts for detectors 1 and 2, which are near to the focal plane of lens 5. The aperture is optimally placed in the optical plane which is conjugate to the center of the sample cell, through lens 3. Detectors 1 and 2 are nominally placed in the optical plane which is conjugate to the optical source, through lenses 1, 2, 3 and 5. Detectors 1 and 2 measure scattered light at two angles, which are nominally below 3 degrees for larger particles but which can cover any angular range appropriate for the size range of the particle detector. Also more than two detectors could be used to increase the size range for this portion of the particle detection system. These detectors could also be annular ring detectors centered on the optical axis to reduce sensitivity to particle shape. For example, detector 1 could measure an scattering angular region around 1 degree and detector 2 could measure around 3 degrees. By combining the particle scattering pulse signals from these detectors, by ratio or polynomial, a relatively monotonic function of particle size is created without strong Mie resonances (due to the white light source and signal ratio). Detectors 1 and 2 count and size particles in much the same way as the system in Figure 1. The concept is to use two angles to remove the variations in scattering intensity due to particles passing through different portions of the incident beam and to reduce calculated size sensitivity to particle and dispersant composition. Particles of size between approximately 1 and 10 microns could be handled by detectors 1 and 2 of Figure 11; and particles above approximately 5 microns are handled by the 2-dimensional detector array. The two size distributions from these two measurements are combined with blending in the overlap region between 5 and 10 microns.

The 2-dimensional detector array is imaged into the center of the sample cell with magnification corresponding to approximately 10x10 micron per array pixel in the sample cell plane. A 10 micron particle will produce a single dark pixel if it is centered on one pixel or otherwise partially darkened adjacent pixels. By summing the total light lost in these adjacent pixels, the total light absorbed or scattered outside of pinhole 2 for each single particle in the view of the array is determined. The particle concentration is limited to prevent coincidence counting. At low concentrations, any group of contiguous pixels with reduced light levels will represent a single particle. And the total percentage light lost by these contiguous pixels determines the particle size. All pixels below a certain percentage of their non-obscured values are accepted as particle pixels. All contiguous particle pixels are then combined as representing one particle. This is accomplished by summing the pixel values of contiguous pixels and comparing that sum to the sum of those same pixels without the presence of a particle. This works well for smaller particles where the total scattered light is well outside of the pinhole 2 aperture, because then the total percentage drop represents the scattering and absorption extinction of the particle.

For larger particles, a portion of the scattered light will pass through pinhole 2 and cause a deviation which will not agree with the total theoretical scattering extinction. This can either be corrected for in the theoretical model by calculating the actual percentage loss for larger particles by integrating the actual scattered light outside of the pinhole, or the particle can be sized directly by counting contiguous pixels, because for large particles the pixel size may be less than 0.1 % of the total crossectional area of the particle. The accuracy of this calculation is improved by adding partial pixels at the edge of the particle image based upon their attenuation as a fraction of the attenuation of nearby interior pixels. Hence if a pixel in the interior of the image is attenuated by 10% and an edge pixel is attenuated by 4%, that edge pixel should count as 40% of its actual area when added to the sum of all contiguous attenuated pixels to determine the total crossectional area and size for that particle. Otherwise the theoretical loss per particle could be used.

This detector array system has an enormous particle size dynamic range. The particle will remove approximately the light captured by twice its crossectional area. So a 2 micron particle will reduce the total light flux on a 10x10 micron pixel by 8 percent. But the entire array of 1000x1000 pixels can cover a crossection of 10x10 millimeters. The size dynamic range is almost 4 orders of magnitude. The smallest particles are detected by their total light scattering and absorption. For very large particles, the angular extent of the scattering pattern may fall within the aperture of pinhole 2. Then the summed light from all the contiguous pixels may not indicate accurate size. For the larger particles, the actual imaged size is determined by counting contiguous pixels. Pixels at the outer boundary are counted as partial pixels based upon the amount of light lost as a fraction of the amount lost from pixels in the interior of the contiguous set. The light loss in each pixel is determined by storing the light value for each pixel without particles in the sample cell and subtracting the particle present values these stored values. The source intensity can also be monitored to normalize each pixel measurement for light source intensity fluctuations.

In order to avoid smeared images, the detector array must integrate the current from each pixel over a short time to reduce the distance traveled by the flow during the exposure. This may also be accomplished by pulsing the light source to reduce the exposure time. Smearing in the image can be corrected for using deconvolution techniques. But the scattering extinction measurements will be accurate as long as the contiguous pixel groups do not smear into each other. Simply add up all of contiguous pixel signals (from the smeared image of the particle) after presence of the particle to determine the particle scattering attenuation and size. If the particle image is smaller than one pixel, then the attenuation of that pixel is the scattering extinction for that particle. Essentially, you are measuring nearly the total amount of light scattered or absorbed by the particle during the exposure. Using this total lost optical flux divided by the incident intensity provides the scattering crossection for the particle, even if the particle is not resolved by the optical system or if that loss is distributed over more pixels than expected from perfect imaging of the particle. This is the power of this technique. A 10mm by 10mm detector array, with 10x10 micron pixels, can measure particle diameters from a few microns up to10 mm, with thousands of particles in the source beam at one time. The 10 mm particles will be

sized directly by adding up pixels and multiplying the interior pixels by 1 and the edge pixels by their fractional attenuation and adding all of the pixels up to get the total crossectional area and size. A 5 micron particle, centered on one 10x10 micron pixel, will attenuate that pixel by 50% (the total scattering extinction crossection is approximately twice the actual particle area, outside of the Mie resonance region). In both cases the particles are easily measured. You are simply adding up all of the signal differences (signal without particle – signal with particle) of contiguous changed pixels to get the total light lost due the particle. Pinhole 2 blocks all of the light scattered outside of the angular range of the pinhole 2, whose maximum scattering angle is equal to the inverse tangent of the pinhole 2 radius divided by the focal length of lens 3. So the signal difference (signal without particle – signal with particle) is the amount of light scattered by the particle at scattering angles above this maximum angle of the pinhole, including any light absorbed by the particle. The particle size is determined using scattering theory and the ratio of (signal without particle – signal with particle) to signal without particle.

Image smearing could also be reduced by using pulsed flow. The particle sample flow would stop during the period when the light source is pulsed or when the detector array is integrating. Then a flow pulse would push the next slug of sample into the detector array field of view before the next signal collection period. The sample would be approximately stationary during the signal collection on the detector array. This pulsing could be accomplished by pressurizing the particle dispersion chamber and using a pulsed valve to leave short segments of the sample dispersion through the source beam interaction volume.

The nearly parallel window cell could also be replaced by a wedge shaped cell which would control the particle count in different size regions, as discussed above.

Non-spherical particles present another problem for single particle sizing, non-symmetrical scattering patterns. Assume that the incident light beam is propagating along the Z direction and the XY plane is perpendicular to the Z direction, with origin at the particle. The XZ plane is the center scattering plane of the group of scattering planes which are intercepted by detectors 1,2,3, and 4. Each detector subtends a certain range of scattering angles, both parallel and perpendicular to the center scattering plane. For spherical particles, the scattering pattern is symmetrical about the Z axis and the scattering function could be described in cylindrical coordinates as a function of Z and of radius R from the Z axis, at some distance Z0 from the scattering particle. However, for non-spherical particles the scattering pattern is not symmetrical about the Z axis at Z0. The 2-dimensional array in Figure 11 measures approximately the total light lost to scattering or absorption at all scattering angles, in all scattering planes. Hence it will produce particle size estimates which are related to the total crossectional area of the particle, for both spherical and non-spherical particles, without sensitivity to particle orientation. But detectors 1, 2, 3, and 4 in Figures 1, 3, or 11 measure the scattering only over scattering planes close to the XZ plane (or a limited range of scattering planes). If the pattern is not symmetrical, the particle size estimate will depend upon the orientation of the particle. So a group of particles with identical crossectional areas, but random

orientations, would be reported over a wide range of particle crossectional area and size. This particle size distribution width could be corrected by deconvolution of the number vs. size distribution, as described by the matrix equation on page 24. But the theoretical model would change with the particle shape. Another way to reduce spread is to use two sets of detector systems, one centered on the scattering plane which is +45 degrees with respect to the XZ plane and the other at -45 degrees from that plane, to sample two perpendicular particle orientations and maintain the optimum orientation for heterodyne detection. The average of the size distributions from these two systems would reduce the spread of the distribution. Another more effective method is to collect all of the scattered planes at a certain scattering angle, using the system shown in Figure 12. A light source is focused into the sample dispersion. This focused spot is imaged onto a pinhole which removes unwanted background light. The light passed by the pinhole contains the incident light beam and the scattered light from the particles. This light is collected by lens 3 which projects the light onto two masks, using a beamsplitter. Each mask contains an annular aperture which defines the range of scattering angle accepted by the collection optics. Lens 4 collects high angle scattered light passing through mask 1 and focuses it onto detector 1. Likewise the low angle scatter is measured by mask 2, lens 5 and detector 2.

Figure 12 shows the annular aperture for mask 1, defining equal scattering collection in all the scattering planes. The ratio of signals from detector 1 and 2 would precisely determine the average radius of a non-spherical particle, without size broadening of the system response due to random particle orientation. The beam splitter and dual mask concept could also be applied to the system in Figure 11. Detectors 1 and 2 would be replaced by the beam splitter and dual mask system, with the masks in the same optical plane as detectors 1 and 2. Masks 1 and 2 act as angular filters which only pass scattered light in a certain range of scattering angles. The 2-dimensional array in Figure 11 is already insensitive to particle orientation and needs no modification.

The particle concentration must be optimized to provide largest count levels while still insuring single particle counting. The concentration may be optimized by computer control of particle injection into the flow loop which contains the sample cell, as shown in Figure 13. Concentrated sample is introduced into flow loop 2 through sample vessel 2. The sample vessel may also contain a stirring means for maintaining a homogenous dispersion in the vessel. Pump 2 pumps the dispersion around the loop to provide a homogenous dispersion in the loop and to prevent loss of larger particles through settling. A second flow system, flow loop 1, is attached to flow loop 2 through a computer controlled valve with minimal dead space. The computer opens the valve for a predetermined period to inject a small volume of concentrated dispersion into loop 1. The optical system counts the particles and determines the probability of coincidence counting based upon Poisson statistics of the counting process. The computer then calculates the amount of additional particles needed to optimize the concentration and meters out another injection of concentrated sample into loop 1. Actually, both the concentration and pump speed for loop 1 may be controlled by computer to optimize counting statistics. When the particle concentration is low, higher pump speed will maintain a sufficient

particle count for good count statistics. The optimum concentration may be different for different detectors and detection systems. Therefore the computer valve may adjust the concentration to various levels in succession. At each concentration level data is taken with the appropriate detector(s) or detector array for a sufficient period and flow rate to accumulate enough counts to reduce the count uncertainty (due to Poisson statistics) to an acceptable level.

Another consideration for Figure 6b is the determination of signal baseline. The baseline for the scattered signals must be determined for each detector. Digitized values, measured before and after the scattered signal pulse, determine the signal baseline to be subtracted from the pulse signal, by interpolation of those values through the pulse region. These regions before and after each detector pulse should be chosen to be before and after the widest pulse of the group (in some rare cases, the pulse with the largest amplitude should be used if the signals are lost in noise). Then the baseline will certainly be determined from values in a region where no particle scattering has occurred in each of the detectors.

The system shown in Figure 11 can also be modified to look at only scattered light over a certain angular region, instead of the total light removed from the beam by absorption and/or scattering. Figure 14 shows such an optical system where the light source is spatially filtered by lens 1 and pinhole 1. Lens 2 collimates and projects the source beam through the particle sample, which is imaged onto the 2 dimensional detector array by lens 3. A annular spatial filter is placed in the back focal plane of lens 3 to only pass scattered light over a certain range of scatter angle as defined by the inner and outer radii of the annular filter, which is similar to mask 1 shown in figure 12. The very low angle scattering and incident beam are blocked by central stop of the annular aperture in the back focal plane of lens 3. Hence the detector array 1 sees an image of the particles, and the sum of the contiguous pixels associated with each particle's image is equal to the scattered light from that particle over the angular range defined by the aperture (or spatial filter) in the back focal plane of lens 3. A beam splitter splits off a portion of the light to a second annular filter (in the back focal plane of lens 3) and detector array 2. The angular ranges of the two annular filters are chosen to produce scattered values which are combined by an algorithm which determines the size of each particle. The sum of signals from contiguous pixels which view the same particle are analyzed to produce the particle size. One such algorithm would be a simple ratio of the corresponding sums (the sum of contiguous pixels from the image of each particle) from both arrays. The key advantage is that when the particle size becomes too small to size accurately by dimensional measurements on the image (resolution is limited by pixel size) then the total scattered light from each particle may be used to determine the size. And if the total scattered light is sensitive to particle composition, then the ratio of the two scattering signals can be used to determine the particle size more accurately. In figure 14, scattered light is only present when a particle is present. In figure 11 the particle image creates a decrease in light, from a bright background level, on the 2-Dimensional array in the corresponding pixels, while in the system of figure 14 the particle image creates an increase from a dark background level. If the particle is smaller than a single pixel, then the amount of scattered light measured by that pixel will indicate the total light scattered from that particle in the

angular range defined by the focal plane aperture, providing that particle's size. If more than one pixel is associated with a particle, those pixel values are summed together to obtain the scattered signal from that particle in a similar fashion as described before for figure 11. The only difference is that the increase in pixel signals, relative to the signal without particles, are summed to produce the total light scattered from that particle in the angular range of the annular aperture in figure 14. In Figure 11, the decrease in pixel signals, relative to the signal without particles, are summed to produce the light lost due to scattering outside of pinhole 2 or absorption by that particle. Signal to background should be better for figure 14, but with higher sensitivity to particle composition and position in the sample cell. The depth of focus and signal to noise should be better for figure 11 than for figure 14, because the pixel values drop by the total light scattered and absorbed by the particle in figure 14 as opposed to the light increasing by only the amount scattered through a narrow range of scattering angles defined by the aperture. As with all other systems described in this disclosure, these ideas can be extended to more than two detector arrays or more than two scattering angles, simply by adding more annular spatial filter and detectors by using beamsplitters. In this way, each pixel in the detector array creates a small independent interaction volume with low coincidence probability. But yet contiguous pixels can be combined to measure particles of sizes approaching the dimensions of the entire array's image in the sample cell. The size dynamic range is enormous.

The optical source used with the detector arrays in Figures 11 and 14 could be a pulsed broad band source such as a xenon flash lamp which produces broadband light to wash out the Mie resonances, and a short light pulse to freeze the motion of particles flowing through the cell.

One problem with the techniques described above is coincidence counting. The cell path must be large to pass the largest anticipated particle (except for the wedge cell shown in figure 9b, where the pathlength changes across the cell). Hence for these collimated systems, many small particles may be in any sample volume seen by a single pixel. These coincidences could possibly be eliminated by measuring at various particle concentrations, but in order to count sufficient large particles to obtain reasonable count accuracy, the concentration must be raised to a level where more than one small particle is present in the sample cell volume, seen by each pixel. The scattered signals from these multiple particles can be separated, to be counted individually, by measuring their settling velocities. This is accomplished by the optical system shown in Figure 15. A light source is collimated and spatially filtered by lenses 1 and 2 and pinhole 1. A modulation transfer target or mask with a spatially periodic transmission function is placed in the collimated beam to create a sinusoidal (or other periodic function) intensity pattern in the collimated beam. Examples of the sinusoidal (or other periodic) patterns are shown in Figure 16. Each line in the patterns represents the peak of the sinusoidal transmission function which oscillates along the particle settling direction but is constant along the direction perpendicular to the settling. The mask consists of multiple regions with different spatial modulation frequencies. The projection of each region into the sample cell is imaged onto

a separate detector by lens 3. The light from lens 3 is split into one or more directions, each having a different annular spatial filter which defines a different range of scattering angles. Each image plane for each spatial filter has multiple detectors, each of which intercept light from only one of mask regions in the sample cell. As a particle settles through the sinusoidal intensity pattern, the scattered light on the detector is modulated because the scattered light is proportional to the light incident on the particle and the mask provides a spatially modulated illumination field. When a particle passes through a region where the spatial modulation wavelength is greater than the particle size, the scattered light from that particle will attain a large modulation visibility (the ratio of peak to trough values will be large). The scattered signal from the largest particles will have lowest modulation visibility in the high spatial frequency region because the particle will span over multiple cycles of the spatial modulation. Larger particles settle faster and produce higher frequency detector signals, because they have a higher terminal velocity. Therefore, a lower spatial modulation frequency can be used with larger particles to increase modulation visibility while still maintaining high signal oscillation frequency, because the scattering signal frequency is equal to the product of settling velocity and the mask spatial frequency. The size range is increased by using multiple regions with different spatial modulation frequencies, with higher frequencies for smaller slower settling particles. The area of the higher frequency portions of the mask are smaller to reduce the number of particles measured at one time by each detector, because typically there are much higher small particle counts per unit volume than for larger particles. Figure 15b shows a similar system with a single pinhole filter. Detector signals will show the same oscillation characteristics as Figure 15, but with a large offset due to the light transmitted by the pinhole. The power spectrum of the detector currents for the systems shown in both Figures 15 and 15b will be similar except that figure 15b will contain a large component at (and near to) zero frequency. Figure 17 shows the power spectra from the low and high angle detector signals in figure 15, for the two detector elements, B1 and B2, which view the same portion, B, of the mask, but pass through different annular filters. Since each particle settles at a different velocity, each particle will produce a separate narrow peak at the same frequency in both of the power spectra of detectors B1 and B2 (from signals for scattering angle 1 and scattering angle 2, respectively). This is due to the fact that the detector signal power at any certain frequency, measured by each of the corresponding low and high angle detectors, will originate from the same particle or group of particles. Since the smaller particles will create a continuum at lower frequencies, they can be removed from the spectrum of the larger particles. The corresponding single peak values from power spectrum of current from detector B1 at frequency f1 and the power spectrum from current of detector B2 at frequency f1 for example (from each scattering angle) can be ratioed (or analyzed by other algorithms) to determine the size of the particle which created that peak in each spectra. In this way, multiple particles in the sampling volume can be counted individually. When particle size is close to the line spacing of the modulation target, the modulation of the scattered light will decrease because the signal is the convolution of the particle with the modulation target. However, the amplitude of the scattered signals at both angles will both decrease by the same percentage so that their ratio will still accurately indicate the size. Any peaks with amplitudes that are higher than that which would be expected from

one particle are expected to originate from more than one particle. The expected amplitude for a single particle can be determined from the minimum value of other peaks in that frequency region for prior digitization sets. These multiple particle peaks can be either corrected for the second particle's contribution or eliminated from the particle count. If the particle density, liquid density and viscosity, are known, each individual particle size can also be determined by the frequency of the corresponding peak, by calculating the corresponding settling velocity and using the Stokes equation for settling to solve for the particle size.

The signal frequency for each particle signal pulse could also be determined individually by either the timing of zero crossings or by using a phase locked loop, avoiding the power spectrum calculation. Each particle pulse will consist of a train of oscillations which are modulated by the intensity profile through that particular mask region. The oscillation amplitude and frequency provide the scattering amplitude and settling velocity, respectively, for that particle. The size can be determined from the settling velocity, if the particle density and fluid viscosity are known, or the size can be determined from the ratio of amplitudes from two different scattering angles, or the amplitude of one scattering (but with possible higher sensitivity to particle composition).

The particle density or fluid viscosity can be determined by combination of the scattering amplitudes and the signal oscillation frequency.

Figure 18 shows another system for measuring the settling of particles, using crossed laser beams. An interference pattern is formed at the intersection of the beams. As the particles pass through this pattern, the scattered light is modulated, producing a power spectrum as described above.

This optical system could also be placed into a centrifuge to increase the terminal velocities of all of the particles, providing particle size measurement for smaller particles than simple gravitational acceleration. The detector signals would be transmitted from the rotating centrifuge to the stationary computer by either optical coupling, electromagetic radiation (radio) or stored into memory on the rotating centrifuge, to be transferred to the computer after the centrifuge has stopped rotating.

All slit apertures in this disclosure (for example, slit 1 and slit 2 in Figure 1) can be changed to pinholes or rectangular apertures, whose images at the source beam may be or may not be smaller than the source beam. Unlike slits, the pinholes or rectangular apertures may require alignment in the both of the mutually perpendicular X and Y directions, which are both approximately perpendicular to the optical axis of the detection system.

Figure 19 shows more detail of the actual beam shapes in Figure 1 for the angular ranges specified for detectors 1 through 4. The scattering angle range for each detector is controlled by the detector size or by an aperture on front of a larger detector. Figure 20 shows the detail of the intersection of the each detector field of view with source beam. If the signal to noise is sufficient for non-coherent detection with any detector in Figure 1, or in any other variation of Figure 1 shown in this document, the local oscillator optics for that detector can be removed and non-coherent detection can be used.
The progression of crossectional size from smallest to largest is: light source, fields of view from detectors 3 and 4, and the fields of view from detectors 1 and 2, as shown in Figure 20. The progression could also progress from the smallest to largest as light source, field of views of detector 4, detector 3, detector 2, and detector1, respectively. However, this would require different sized apertures for each detector. This would require a separate lens and aperture for each detector, but would insure that any particle passing through the intersection of the source beam and the detector 4 field of view, will be seen by all of the other detectors during the entire pulse period from detector 4. Then if all of the detector signal ratios are measured during a period near to the peak of the detector 4 signal (after the envelope detector), valid scattering ratios will be recorded for all of the detectors.

The particles being measured by system in Figure 19 are all much smaller than the crossection of the source beam. Therefore particles of different sizes produce the same count-vs.-parameter distribution for the following parameters:

1) scattered light amplitude normalized to the maximum scattered light amplitude measured over all the particles of the same size at that scattering angle.
2) Pulse width at certain fraction of pulse peak level
3) delay between pulses from two different detectors
4) correlation between pulses from two different detectors

Any of these parameters can be used to define a threshold for counting particles as shown in Figures 10 and 10b, by replacing the S(a2) axis with one of the parameters from above. If the particle count is large, the statistics of the above parameters will be stationary for all particle sizes. Then the strategy outlined for Figure 10 can be used to properly threshold particles of all sizes in an equivalent manner, by rejecting the same percentage of particles in each size bin in the count-vs.-size distribution. The 3 dimensional surface which corresponds to the one in Figure 10, can be interpolated or fit to a surface function in order to determine the rejection threshold. Based upon the function or interpolated values, a rejection criteria can be determined which eliminates the particles with poor signal to noise and also removes the same percentage of particles from each size range so as to maintain a true particle size distribution. The rejection threshold is chosen to maintain a sufficiently high signal-to-noise for any particles which are accepted into the total count distribution. In fact, this process will computationally define an interaction volume for the source beam and all detector fields of view, for all particle sizes being detected, where all scattering signals have sufficient signal-to-noise to produce accurate sizes based upon their amplitudes, ratios of amplitudes, or other multi-parameter

functions of scattering amplitudes. This selection process is required to reduce the effects of the tails in the intensity distribution of the source and the spatial response tails at the edges of the detector fields of view, where they intersect the source beam. If these tails are sharpened (or cut off) by spatial filtering the source or by using slits, pinholes, or other apertures with low aberration optics for the detectors, the errors due to these tails are further reduced. In any event, there is always some parameter which is statistically well described by the millions of particles which are detected. And by eliminating particles from the count based upon this parameter, you can define a group of particles which are sorted by the same criteria at all particle sizes, thereby creating an accurate size distribution.

In the sample cell with flat windows, many of the incident source beams and scattered light rays are at high angles of incidence on the sample cell windows. The interior surface of the window is in contact with a liquid which reduces the Fresnel reflection at that surface. However, the exterior surface is in air which can cause an enormous Fresnel reflection at these high incident angles. This reflection can be reduced by anti-reflection coating the exterior surface, but with high cost. A better solution is to attach prisms (see Figure 21) to the exterior surface with index matching optical adhesive. The prism surfaces present low angles of incidence for the source beams and the scattered light. Even simple antireflection coatings on the external prism surfaces will reduce the Fresnel reflections to negligible levels. A spherical plano-convex lens, with center of curvature near to the center of the cell could also be used instead of each prism, with plano side attached to the window.

Another configuration for the sample cell is a cylindrical tube. The particle dispersion would flow through the tube and the scattering plane would be nearly perpendicular to the tube axis and flow direction. In this case, the beam focus and detector fields of view would remain coincident in the scattering plane for various dispersant refractive indices and only inexpensive antireflection coatings are needed. However, since the flow is perpendicular to the scattering plane, the heterodyne oscillations cannot be produced by the particle motion. The optical phase modulation mirror in the local oscillator arm (called "mirror") in Figures 1 and 19 (and other figures) could be oscillated to provide a heterodyne signal on detectors 3 and 4 as described before.

Any of the measurement techniques described can be used individually or in combination to cover various particle size ranges. Examples of possible combinations are listed below:

For particle diameter 0.05-0.5 microns use Figure 19 with detectors 3 and 4 at 30 and 80 degrees, respectively.
Use heterodyne detection (if needed). Take ratio of the detector signals.
For particle diameter 0.4-1.2 microns use Figure 19 with detectors 1 and 2 at 10 and 20 degrees, respectively.
Use heterodyne detection (if needed). Take ratio of the detector signals.
All 4 signals can also be used together for the range 0.05 to 1.2 microns, using a 4 parameter function or lookup tables.

Use the detector with the smallest interaction volume to trigger data collection. These angles are only representative of general ranges. For example, instead of 10, 20, 30, 80 degree angles, any group of angles with one widely space pair below approximately 30 degrees and another widely spaced pair above approximately 30 degrees would work. Each detector sees an angular range centered about the average angle specified above. But each detector angular range should be somewhat less than the angular spacing between members of a detector pair. The particle size distribution, below 2 microns, from this system is combined with the size distribution above 1 micron as determined from various other systems described in this disclosure, including the following systems:

For particle diameter 1-10 microns use detectors 1 and 2, in Figures 11 or 14, at approximately 1 degree and 3 degrees , respectively. Use white light or LED source. Use ratio of detector signals to determine individual particle size.

For particle diameter greater than 1 microns, use the 2 dimensional array in Figure 11 with a pulsed white light source (such as a pulsed xenon source) to freeze the motion of the flowing particles. The two dimensional array could also be used alone to measure greater than 1 micron, without detectors 1 and 2. The system in Figure 14 could also measure particles greater than 1 micron in diameter, with one (absolute) or both (ratio) detector arrays.

Another configuration is to use the scattering flux ratio of scattering at 4 degrees and 1 degree, in white light, for 0.5 to 3.5 microns. And use absolute flux at 1 degree (white light, same system) for 3 to 15 microns. And use the 2 dimensional array in Figures 11 or 14 for particles above 10 microns. As noted above, each array in Figure 14 can separately be used to size particles by measuring the absolute scattered light from each particle, or light lost due to the particle, over one angular range. However, the system size response will be more composition dependent using data from a single array than the ratio of the corresponding measurements from both arrays.

In all of these systems, the white light source can be replaced by a laser. However, the particle size response will become more sensitive to particle and dispersant composition. And also the response vs. size may not be monotonic, producing large size errors. If lasers or LEDs are required for collimation or cost requirements, scattering measurements can be made at more than one wavelength, using multiple sources, to reduce the composition dependence. Particle size of each object would be determined from all of these multi-wavelength measurements by using a multi-parameter function (size = function of multiple parameters) or by interpolation in a lookup table as described above. And in all cases the angles are nominal. Many different combinations of average angles, and ranges of angles about those average angles, can be used. Each combination has a different useable particle size range based upon size sensitivity, composition sensitivity, and monotonicity. All of these different possible combinations are claimed in this disclosure. Also note that the ratio of S(a1)/S(a2) in Figure 10 can be replaced by any parameter or function of parameters which have nearly exclusive sensitivity to particle size, with low

sensitivity to incident intensity on the particle. This may include functions of scattering measurements at more than 2 angles.

One problem associated with measuring large particles is settling. The system flow should be maintained at a sufficiently high level such that the larger particles remain entrained in the dispersant. This is required so that the scattered light measurements represent the original size distribution of the sample. For dense large particles, impracticable flow speeds may be required. This problem may be avoided by measuring all of the particles in one single pass, so that the total sample is counted even though the larger particles may pass through the light beam as a group before the smaller particles.

A small open tank is placed above the sample cell region, connected to the cell through a tube. The tube contains a valve which can be shut during introduction of the particle sample into the tank to prevent the sample from passing through the cell until the appropriate time. The liquid in the tank is continuously stirred during the introduction of sample to maximize the homogeneity in the tank. A light beam is passed through the mixing vessel via two windows to measure scattered light or extinction to assist in determining the optimum amount of sample to add to obtain the largest counts without a high coincidence count level. The optical detectors are turned on and the valve is opened to allow the particle mixture to pass through the cell with gravitational force. This can also be accomplished by a valve below the sample cell or by tilting the tank up to allow the mixture to flow over a lip and down through the cell, as shown in Figure 22. The light beam could be wider than the width of the flow stream through the cell so that all of the particles passing through the cell are counted. Single particle counting is assured by only introducing a sufficiently small amount of sample into the tank. Since all of the larger particles are counted in one pass, the count distribution is independent of the sample inhomogeneity. After the entire sample has passed through the cell, the conventional flow system for ensemble scattering measurements is then turned on to circulate the sample through the cell. This flow rate must only be sufficient to suspend the particles which were too small to be counted during the single pass. Settling of the larger particles which have been counted does not matter because their count distribution (from the single pass) will be combined with the count-vs.-size distribution of the smaller particles (obtained during flow) to produce a single volume distribution over the entire size range.

The system in Figure 22 could also be used alone to provide significant cost savings by eliminating the pump and associated hardware. Figure 22 shows the concept for dispersing and measuring the particles in a single pass through the optical system. The particles and dispersant are mixed continuously in a mixing vessel which is connected to the optical system through a flexible tube. The mixing vessel is tilted while being filled, so that no sample enters the optical system. Then once the dispersion is well mixed, the mixing chamber is sealed with a gas tight cover and the mixing vessel is moved into an upright position to allow the dispersion to either fall through the sample cell under gravity (without gas tight cover) or to be pushed through the cell using gas pressure. If gas pressure is not used, the flexible tube could be eliminated and the mixing vessel could pour into a funnel on top of the sample cell.

The systems based upon Figure 19 and similar systems, where scattered light at multiple - angles are measured from a single particle, will have a lower particle size limit due to the lower scattering intensity of small particles and insensitivity of the scattering ratio to particle size. If the particle refractive index and dispersant refractive index are known, various scattering theories can be used to calculate the scattering signal ratios and absolute scattering signals vs. particle size to provide the look up table or function to calculate the size of each particle from these signals. Since these refractive index values are not always available, the scattering model (the effective refractive indices) may need to be determined empirically from scattering data measured in a region where the scattering ratio is independent of refractive index. This process assumes that the entire particle ensemble is homogeneous in composition. Any particle which shows a ratio in the size sensitive region of the response, can be used to determine the effective refractive index of the particle by using the ratio and the absolute values of the scattering signals, because these are unique for particle and medium refractive index. The optical model for this effective refractive index could then be used to extend the size response range of any set of detectors to a size range outside of the size region where the scattering signal ratio is sensitive to size. This process can extend the size to both smaller and larger particles by using the absolute scattering intensity in regions where the scattering signal ratio no longer works. Theoretically, very small particles are Rayleigh scatterers, where the shape of the angular scattering distribution is not size dependent. However for very small particles, the peak of the scattering intensity distribution scales as the 6^{th} power of the particle diameter and the heterodyne signal scales as the 3^{rd} power of the diameter. So as the particle size decreases, the ratio of the intensity at two angles becomes constant, but the actual intensities continue to drop as the particle size decreases. So when the intensity ratio approaches this constant, the particle size algorithm should use absolute scattering intensity to determine the size. The absolute scattered intensity is proportional to a constant (which is a function of scattering angle, particle and dispersant refractive indices, and light wavelength) divided by particle diameter to the 6^{th} power (3^{rd} power for the heterodyne signal). This constant is determined from the absolute scattered intensities of particles, in the distribution, whose intensity ratios still provide accurate particle size. Also the functional form for the absolute intensities can be calculated using various scattering theories. This process can also be used to extend the useful range to larger particles. As the particle becomes larger, the scattering signal ratio from the detector pair will become more dependent upon the refractive index of the particle. The absolute intensity data from particles, in the region where the ratio is independent of particle composition, can be used to determine the effective composition of the particles and determine which theoretical scattering model to use for absolute scattering intensity from particles outside of that size region. Then the larger particles are measured using this model and the absolute values from each scattering detector, instead of the ratio of scattering signals.

The only remaining problem with absolute scattering intensity measurements is the sensitivity of pulse intensity to the position where the particle passes through the beam. Measuring the distribution of pulse amplitudes from a nearly mono-sized calibration

particle dispersion (with a low coefficient of variation for the size distribution) provides the response of the counter for a group of particles of nearly identical size. This count distribution, which is the same for any particle whose size is much smaller than the light beam crossection, provides the impulse response for a deconvolution procedure like the one described previously. The scattering pulses can be selected based upon their pulse length by only choosing pulses with intensity normalized lengths above some threshold or by using the various pulse selection criteria listed below. This selection process will help to narrow the impulse response and improve the accuracy of the deconvolution.

The scattered signal from any particle is proportional to the intensity of the light incident on the particle. Hence as the particle passes through different portions of the incident light beam, each scattered signal will vary, but the ratio of any two signals (at two different scattering angles) will theoretically be constant as long as the field of view of each detector can see the particle at the same time. This can be insured by eliminating the signals from long intensity tails, of the gaussian intensity profile of the laser beam, which may not be seen by all detectors. This is accomplished by placing an aperture, which cuts off the tails (which may be gaussian) of the incident light intensity distribution, in an image plane which is conjugate to the interaction volume. This aperture will produce a tail-less illumination distribution in the interaction volume, providing a narrower size range response to mono-sized particle samples (the impulse response). In the case of an elliptical gaussian from a laser diode, the aperture size could be chosen to cut the distribution at approximately the 50% points in both the x and y directions (which are perpendicular to the propagation direction). Such an aperture would cause higher angle diffractive lobes in the far field of the interaction volume, which could cause large scatter background for low scattering angle detectors. Since this aperture should only be used for measurements at high scattering angles where the background scatter can be avoided, the low angle detector set and high angle detector set may need to view separate light beams. The apertured beam size should be much larger than the particles which are being measured in that beam. Hence, to cover a large size range, apertured beams of various sizes could be implemented. The particle size distributions from these independent systems (different source beams or different detector groups) could be combined to produce one continuous distribution.

The apertured beams will help to reduce the size width of the system response to a mono-sized particle ensemble. Other analysis methods are also effective to reduce the mono-sized response width for absolute scattering and scattering ratio measurements. Methods which accept only scattering signal pulses, or portion of pulses, which meet certain criteria can be very effective in narrowing the size width of the system response to mono-sized particles. Some examples of these acceptance criteria are listed below. Any of these criteria can be used to determine which peaks or which portion of the peaks to be used for either using the scattering signal ratios or absolute values to determine the particle size.

1. Choose only the time portion of both pulses where the pulse from the detector which sees the smaller interaction volume, or has the shorter duration, is above some threshold. The threshold could be chosen to be just above the noise level or at some

higher level to eliminate any possibility of measuring one signal while the second signal is not present. Then either take the ratio of the signals (or ratio the peaks of the signals with peak detector) over that time portion or the ratio of the integrals of the signals over that time portion. The absolute integrals or peak values during this time portion could also be used to determine size, as described before.

2. Only accept pulses where the separation (or time delay between peaks or rising edges) between pulses from the multiple detectors is below some limit
3. Only accept pulses where the width of a normalized pulse or width of a pulse at some threshold level is above some limit
4. Only accept the portion of the pulses where the running product S1.*S2 (a vector containing the products of S1 and S2 for every point during the pulses) of the two signals is above some limit. Then either take the ratio of the signals over that portion or the ratio of the integrals of the signals over that portion.
5. Only use the portion of pulses where sum(S1.*S2)/(sum(S1)*sum(S2)) is greater than some limit (sum(x) = summation of the data points in vector x)
6. Use only the portion of the pulses where (S1.*S2)/(S1+S2) is greater than some limit
7. integrate each pulse and normalize each integral to the pulse length or sample length
8. Use only the portion of the pulses where the value of S1*S2 is be greater than some fraction of the peak value of the running product S1.*S2
9. Integrate both signals S1 and S2 only while the signal from the smaller interaction volume is above a threshold or while any of the above criteria are met.
10. fit a function to the selected portion (based upon various criteria described above) of each pulse. The fitting function form can be measured from the signal of a particle passing through the center of the beam or can be based upon the beam intensity profile
11. When both S1 and S2 have risen above some threshold, start integrating (or sample the integrators from) both signals. These sampled integrals are IT10 and IT20 for S1 and S2 respectively. When the first signal to drop falls back down below the threshold, sample the integrator on each of S1 and S2 (integrals IT1a and IT2a). When the second signal (signal number *) to drop falls below the threshold, sample the integral IT*b for that signal. Use the ratio of the integral differences, (IT1a-IT10)/(IT2a-IT20), during the period when both signals are above the threshold to determine size. Accept and count only pulses where a second ratio (IT*a-IT*0)/(IT*b-IT*0) is above some limit. This second ratio indicates the fraction of the longer pulse which occurs during the shorter pulse. As the particle passes through the light beam further away from the center of the interaction volume, this ratio will decrease. Only particles which pass through the beam close to the center of the interaction volume will be chosen by only accepting pulses where the shorter pulse length is a large fraction of the longer pulse length. These pulse lengths could also be determined by measuring the difference in the length of time between the above trigger points for each pulse. Pulses with a shorter difference in time length are accepted into the count by ratioing their integrals during the period when both of them are above the threshold.

These criteria can be easily implemented by digitizing S1 and S2 and then doing the above comparisons digitally. However, full waveform digitization and digital analysis of 1 million particles may require too much time. Figures 23a and 23b show configurations for implementing some of these criteria using analog circuits. The signal digitization and computational load is greatly reduced by using analog equivalents to preprocess data before digitization. This concept is particularly effective when the thresholding or comparative functions, of the criteria described above, are replaced by analog equivalents; but the actual signal analysis used for size determination is done digitally to avoid the poorer linearity and accuracy of the analog equivalents. An example of this is shown in Figure 23b, where both integrator outputs (one integration per signal pulse) are separately digitized by the A/D convertors to do the amplitude or signal ratio calculations digitally instead of using analog ratio circuits; but the criteria related functions, analog multiply and comparator, are done analog to reduce the digitization load. This overall concept of using analog circuitry specifically for only the criteria related functions to reduce the digitization load is claimed by this disclosure, along with applications to other systems.

All of these variations will not be perfect. Many of them rely upon approximations which can lead to variation in calculated size for a particle that passes through different portions of the beam. The important advantage is that the broadening of the mono-sized particle response is the same for all size particles which are much smaller than the source beam. Therefore this broadened response, which is calculated by measuring the count distribution from a mono-sized distribution or by theoretical modeling, can be used to deconvolve the count distribution of any size distribution.

The intensity ratio is sensitive to size and mildly sensitive to particle and dispersant refractive index. Size accuracy is improved by using Mie theory, for the actual refractive index values, to calculate the scattering ratio vs. particle diameter function. However, sometimes these refractive indices are not easily determined. Three scattering angles could be measured to generate a function which has reduced sensitivity to refractive index.

D = A1*(S2/S1) + A2*(S2/S1)^2 + A3*(S2/S1)^3 +
B1*(S3/S1) + B2*(S3/S1)^2 + B3*(S3/S1)^3 + C1

D = particle diameter
A1, A2, A3, B1, B2, B3 are constants
S1 = scattering signal at the first scattering angle
S2 = scattering signal at the second scattering angle
S3 = scattering signal at the third scattering angle

Solve the set of equations:

Di = A1*(S2/S1)ij + A2*((S2/S1)ij)^2 + A3*((S2/S1)ij)^3 +
B1*(S3/S1)ij + B2*((S3/S1)ij)^2 + B3*((S3/S1)ij)^3 + C1

where i = diameter index
j = index of refraction index

and

S1ij = theoretical scattering signal over scattering angular range #1, for particle diameter D=Di and the jth index of refraction

S2ij = theoretical scattering signal over scattering angular range #2, for particle diameter D=Di and the jth index of refraction

(.....)ij indicates that all the variables inside the parentheses have index ij.

A set of simultaneous equations are created for various diameters Di using signal ratios calculated from the appropriate scattering theory (Mie theory or non-spherical scattering theory) for various particle and dispersant refractive indices. These equations are then solved for the constants A1, A2, A3, B1, B2, B3,C1. Of course this process can be extended to more than 3 angles and for polynomial order greater than 3.

Particles which are two small for single particle counting may be measured by stopping the flow and using the heterodyne signal of the scattered light to measure the size distribution from the Brownian motion of the particles. The particle size distribution is determined by inverting either the power spectrum or the auto-correlation function of the Doppler broadened scattered light from the moving particles. The particle size distribution from Brownian motion can also be used to determine the effective particle/dispersant refractive index model by measuring the hydrodynamic size of a particle along with the scattering signal amplitudes. The model can be determined from the scattering intensity at each angle, and the true size for a representative single particle or a group of particles. The true size can be determined by Brownian motion, from the ratio of intensities of light scattered at two angles in the size region where the ratio is an accurate indicator of size, or by other size measurement techniques.

Other methods of generating the heterodyne local oscillator are also claimed in this disclosure for systems like in Figure 19. For example a small reflecting sphere or scattering object could be placed in the interaction volume to scatter light into the heterodyne detectors along with the light scattered by the moving particle. Since this sphere or object is stationary, the optical phase difference between the scattered light from the moving particle and light scattered (or reflected) from the sphere or object would increase as the particle passed through the beam, creating an oscillating beat scatter signal on the detectors, at high frequencies. Then the local oscillator beam, which passes through lens 6, could be eliminated.

In Figure 19, the effective scattering angles seen by each detector can depend upon the position of the particle in the beam. The addition of lenses 7 and 8, as shown in Figure 24 (which only shows the detection portion of Figure 19) , will lower the scatter angle sensitivity to particle position. Each of these lenses place the detectors in a plane which is conjugate to the back focal plane of either lens 3 or lens 4. Essentially the back focal plane of lens 3 is imaged by lens 7 onto detectors 3 and 4; and the back focal plane of lens 4 is imaged by lens 8 onto detectors 1 and 2. This configuration nearly eliminates dependence of detector scattering angles on the position of particles in the beam.

By powering the source at various intensity levels, the scattered light from particles which span a large range of scattering intensities can be measured with one analog to digital converter. Even though the dynamic range of the scattered light may be larger than the range of the A/D, particles in different size ranges can be digitized at different source intensity levels. The resulting signals can be normalized to their corresponding source intensity and then used to determine the size of each particle.

In Figure 11, the 2-Dimensional detector array could also be moved farther away from lens 4 to the plane which is nearly optically conjugate to the center of the sample cell. This may provide better imaging resolution of the particles on the array.

Also it is recognized that many of the ideas in this disclosure have application outside of particle counting applications. Any other applications for these ideas are also claimed. In particular, the ideas put forth in Figures 21 and 22 would also have application in ensemble particle sizing systems.

. Many drawings of optical systems in this disclosure show small sources with high divergence which are spatially filtered by a lens and pinhole and then collimated by a second lens. In all cases, a low divergence laser beam could replace this collimated source, as long as the spectral properties of the laser are appropriate for smoothing of Mie resonances if needed.

Another issue is interferometric visibility in the heterodyne signals described before. Misalignment of beamsplitter or lenses 5 or 6 in Figure 24 can lower the visibility of the heterodyne signals. Since this loss may be different on different detectors, the ratio of two signals may not be preserved. However, the ratio of the visibilities for two detectors will be the same for all particles. Therefore a correction for the effects of low visibility, for both absolute signals and signal ratios, can be determined by measuring scattered signals from one or more nearly mono-sized particles of known size and comparing the results with theoretical values to determine the effective visibility for each channel or visibility ratio for pairs of channels. This is most easily accomplished by measuring larger particles with scattering signals of very high signal to noise and looking at the actual heterodyne signals to determine the interferometric visibility for each detector. This could be determined by blocking the local oscillator light and measuring the scattered signal pulse with and without the local oscillator to calculate the theoretical heterodyne signal from the measurement of the local oscillator power and the scattered pulse amplitude. Also

simply comparing the ratio of two scattering heterodyne signals to the theoretical value for that particle size would also provide a correction factor for the ratio, directly.

For particles which are much smaller than the size of the laser spot, the scattered signal for particles passing through various portions of the laser spot will be distributed over a range of peak amplitudes. For a group of monosized particles, the probability that a peak amplitude will be between value S-deltaS/2 and S+deltaS/2 is Pn(S)deltaS, where Pn(S) is the probability density function for scattering amplitude in linear S space. "deltaQ" means the difference in Q between the end points of the interval in Q, where Q may be S or Log(S) for example. For a group of monosized particles of another size, the scattering amplitudes, S, for particles that have passed through the same region of laser beam are changed by a multiplier R and the probability density amplitude is changed by a multiplier of 1/R, as shown in first graph of Figure 25 for two particle diameters, D1 and D2.

Pn(S)deltaS = Pn(RS)deltaS/R

If we switch to logarithmic space for S, we find that the probability density becomes shift invariant to a change in particle size (Pg(Log(S)) only shifts along the Log(s) axes as R or particle size changes.

Using deltaS = R*deltaLog(S)

Pg(Log(S))deltaLog(S) = Pg(Log(R) + Log(S))deltaLog(S)

Where Pg(Log(S)) is the probability density function in Log(S) space. This shift invariance means that the differential count-vs.-Log(S) distribution, Cg, in logarithmic space is a convolution of the probability function Pg shown in Figure 25, with the number-vs.-size Ng, where all are functions of Log(S).

Cg = Ng ⊙ Pg in convolution form where Pg is the response from a monosized particle ensemble

Cg = Ng * Pgm in matrix form, where each column in matrix Pgm is the probability function for the size corresponding to the element of Ng which multiplies it.

These equations can be inverted to solve for Ng, given Cg and Pg, by using deconvolution techniques or matrix equation solutions. Pg is determined theoretically from the laser beam intensity profile or empirically from the Cg measured for one or more monosized particle samples. If Pg has some sensitivity to particle size, the matrix equation is preferable.

These relationships also hold for the above functions, when they are functions of more than one variable. For example, consider the case where Cg is a function of scattering values S1 and S2 from two scattering detectors at different scattering angles. Then

Cg(Log(S1),Log(S2))deltaLog(S1)deltaLog(S2) is the number of events counted with log signals between Log(S1) – delta(Log(S1))/2 and Log(S1) + delta(Log(S1))/2, and between Log(S2) – delta(Log(S2))/2 and Log(S2) + delta(Log(S2))/2.Then Cg(Log(S1),Log(S2)) could be plotted as a surface on the (Log(S1),Log(S2)) plane as shown in Figure 26. This surface is determined from the event density of the "scatter plot" or "dot plot" of all of the particles on the Log(S1),Log(S2) plane (each particle is represented by its values of Log(S1) on the X axis and Log(S2) on the Y axis on the scatter plot). So an event is the dot or point in Log(S1),Log(S2) space (or S1,S2 space) which represents a counted object. The distribution functions Pg and Cg are calculated from the number of events for each small area in this space. A group of monosized particles will theoretically produce a group of points in S1,S2 space which follow the function Log(S2) = Log(S1) + Log(R). Hence the data points will line up along a line of slope =1 and with an offset of Log(R). The distribution of points along the length of the line for the particle group is determined by range of S1 and S2 for that group due to the intensity distribution of the source beam. If particles pass through the beam at random locations, the distribution of data points along the line will follow the intensity distribution along each of the S1 and S2 axes. R, which is the ratio between S2 and S1, changes with particle size. As the particle size decreases below the wavelength of the source, R becomes a constant for all sizes, as determined from Rayliegh scattering theory. However, real measurements do not follow theory exactly due to structural imperfections in the optical system. These imperfections will cause broadening of the line. This broadening is illustrated by an elliptical shape (however the actual shape may not be elliptical) in Figure 26. Each ellipse represents the perimeter around a group of counted data points on the S1,S2 plane from particles all of one size.
Notice, if the only cause of response broadening is due to the intensity distribution of the source spot, then the ellipses in Figure 26 will become nearly circles, because both signals will come from similar intensity distributions.

A group of monosized particles will produce a differential count distribution in S1,S2 or Log(S1),Log(S2) space. In each case, a differential count distribution from a polysized sample will be the sum of the monosized distributions, each weighted by the percentage of particles of that size in the total distribution. Hence the particle number-vs.-size distribution can be determined by inverting this total differential count distribution, as a function of S1 and S2, or Log(S1) and Log(S2), using algorithms which may include those already developed for image restoration. In Log(S1),Log(S2) space the monosized response functions will be similar in shape over a large size range, because the functions are approximately shift invariant to size over the Log(S1),Log(S2) space. In this logarithmic space, deconvolution can be used to invert the count distribution in either one or more dimensions. The signal pulse from each event may pass through an analysis or sorting as described before, to sharpen the monosized reponse for higher size resolution. These pre-processed pulses are counted vs. a parameter such as peak value, total area, total correlated signal, etc., using the methods outlined previously. Each counted event is placed into the S1,S2 or Log(S1),Log(S2) space, where S1 and S2 may be the pulse peak value, pulse area, or any of the other size related parameters which can be calculated from the scattering signals. Then this space is broken up into very small regions, and the events

in each region are summed to give sampled values of the differential count-vs.-parameter distribution in the space. The known monosized response, which may be size dependent, is used to invert this differential distribution to produce the particle number-vs. size distribribution. This monosized response may be calculated from scattering theory and the optical design parameters, or it may be measured empirically by recording the differential event count distribution in the space from particles of known sizes. The known monosized response defines a region in the space, where scattering from single particles can produce counts as shown in Figure 27. Events which are outside of this region, can be rejected as non-particle events (i.e. non-single particle events), which may be due to multiple particles in the interaction volume or noise. This is particularly important for small sized particles with low scattering signals, where detection noise can cause many non-particle counted events as shown in Figure 28. These noise events can also be included into the monosized response functions. For example, when a group of monosized particles are measured to produce an empirical monosized response function, many noise events will be measured. These noise events can be included in the monosized response function so that they are removed as part of the inversion process, when that function is used as one of response set in the inversion algorithm. The complete monosized response function set can be generated from scattering data from only a few well chosen monosized particle groups. The intervening response functions are interpolated from the trend of the theoretical scattering/optical system model. The empirical data from monosized samples may only be needed to locate the theoretical model in the space. The power of this process is that both the absolute signal data, which is needed to size particles in the Rayliegh scattering regime, and the scattering signal ratio information are combined into one space, where non-particle events are easily identified. This process can be applied to data taken in any number of dimensions, from one scattering angle to any number of scattering angles. Also any dimension of this process can be represented by a scattering signal related parameter (peak, integral, etc.) or combination of scattering signals (ratio of S2/S1, correlation between S2/S1, etc.). Higher number of dimensions provides better discrimination against non-particle events, but with added cost of more detectors and computer processing time. For example, more than two detectors could be placed behind each of slit 1 or slit 2 (aperture 1 or aperture 2), in the previous figures, to provide additional dimensions to the problem. For 3 detectors you could plot each event on the S3/S1, S2/S1 plane. Then the effects of source spot intensity variations would be reduced and the impulse responses (the ellipses shown previously) would become very small, perhaps eliminating the need for deconvolution. All four detectors from these figures (detectors 1, 2, 3, 4) could also be combined into one four dimensional space as described in this section or into two 2-dimensional spaces, which are first solved separately and then the results are combined into one final size distribution.

If all of the particles in a particular sample are in a size region where the signal ratio is not sensitive to particle size, such as the Rayliegh size regime, the scattering model could be determined empirically from dynamic scattering measurements. If the particle flow is stopped, the heterodyning detection system can measure the Doppler spectral broadening due to Brownian motion (dynamic light scattering). The particle size distribution from

this measurement may be used directly, or the optical scattering model may be determined from the dynamic scattering size distribution to invert the absolute scattering signal amplitudes from the count-vs.-scattering signal distribution. In this way, the low size resolution distribution from dynamic light scattering will provide scattering model selection for the higher size resolution counting method. This technique can be used over the entire size range of the dynamic light scattering to select the scattering model for counting particles inside or outside of the size range of dynamic light scattering. The scattering model may also be determined by inverting the count distribution in S1,S2 or Log(S1),Log(S2) space. This inversion will create a line function in the space. The shape of this line function in the transition from Rayliegh scattering (where the ratio between S1 and S2 is constant) and larger particles will indicate the scattering model and refractive index of the particles.

This multi-parameter analysis also provides for separation of mixtures of particles of different compositions such as polymer particles mixed with metal particles or polymer particles mixed with air bubbles. Hence, the count of air bubbles could be eliminated from the count distribution. Figure 27B shows the methodology. Particles of different composition will have different response profiles in the multi-dimensional space. So the data points (events) for particles of different composition will occupy different response profiles as shown in Figure 27B. Individual particle size distributions and particle concentrations, for each particle type, could be determined from analysis of this data using the techniques described in this disclosure. These techniques could also be extended to larger numbers of dimensions by measuring more signals.

This process could also be used by replacing signals, in these multiple parameter plots, with ratios of signals. Any of these multiple angle configurations may be extended to many more angles simply by adding more scatter detectors which view the same interaction volume. For example, lets consider 4 such detector signals, S1, S2, S3, S4. Each of these signals could be pulse peak, pulse area, or correlated peak, etc. The ratios S4/S1, S3/S1, and S2/S1 are plotted in 3-dimensional space, one point for each particle counted. These ratios could also be S4/S2, S3/S2, S2/S1, etc. The point here is that the Mie resonances cause the scattering signals at various angles to oscillate together vs. particle size. For any size range, there is always a region of scattering angles where the ratio of scatter from two different ranges of angle are nearly independent of Mie resonances and particle composition. The path of these ratios in 2-dimensional space (e.g. S3/S1,S2/S1) or 3-dimensional space (e.g. S4/S1,S3/S1,S2/S1), are only weakly dependent on particle composition. The strongest particle composition dependence is for spherical particles in the size region of the Mie resonances. When thousands of particles are measured, their points will follow a multi-dimensional curve or line, in this multi-dimensional space, which indicates the sphericity or composition of the particles. This multi-dimensional line is formed by the highest concentration of points in this multidimensional space. Only points which are within a certain distance of this line are accepted as true particles. The outliers represent particles which passed through the edge of the source beam or whose signals are contaminated by noise. Also non-single particle events, such as noise pulses or multiple particles, would also be rejected because their

combination of coordinates in this space would not agree with the possible coordinates of a particle. The signal ratios could also be replaced by the signal values to take advantage of absolute signal information, which is particularly advantageous in the Rayliegh region where signal ratios are weakly dependent on particle size, but absolute signal levels are strongly dependent on particle size. For particles of size above the Rayliegh region, the signal ratios may be preferred because the spread of particle events around the multi-dimensional line is very small for signal ratios which remove the dependence upon the particle position in the beam, removing a portion of the monosized response broadening shown in Figures 27 and 28. Both of the techniques, described here and in the description of Figures 27 and 28, will be needed to cover the entire size range, because the signal ratios are not strongly size dependent in the Rayliegh region (for particles below 0.1 micron in visible light). Another option would be to use a multi-dimensional space where some dimensions were signal ratios and other dimensions where absolute signals. Then the monosized response would only be strongly broadened in the absolute signal dimensions. For small particles, the absolute dimension would be used with deconvolution and noise event rejection as shown in figures 27 and 28; and for larger particles, signal ratio dimensions would be used to determine size with outlier rejection and minimal deconvolution. The entire path of the line constructed by the particle events determines the optical scattering model. This is particularly important for the Rayliegh region where the particle refractive index must be determined to calculate the dependence of absolute scattering amplitude on particle size. In any case, there will be a line or curve, in multi-dimensional space, which follows the path defined by the highest concentration of counted events. This line will define the optical scattering model and the particle shape or composition, if the user cannot provide that information. Size accuracy may be improved by using any apriori information about the particles to determine the scattering model from theoretical models. For example, the path of the multi-dimensional line could be calculated from scattering theory, given the particle refractive index and shape, but sometimes this information is not well known. If the particle composition or shape is unknown, then this empirically determined line in multidimensional space is compared to the theoretical lines for particles of various compositions and shapes. The theoretical line, which most closely matches the measured line from the unknown particle dispersion, is assumed to represent the composition and shape of the unknown particles.

The accuracy of the process described above improves as more scattering angles are measured. For example, the measured values of the scattered light for each of three scattering angles could be measured for each particle. These data points are then analyzed in a three dimensional scatter or dot plot. A line could be generated in 3 dimensional space by determining the path where the maximum concentration of particles (or dots in the plot) reside. In any one axis, this line may be mutli-valued vs. particle diameter, especially in the region of Mie resonances. However, the line will not be multi-valued in 3 dimensional space. The spread of points about this line will be determined by the intensity distribution of the source beam in the interaction region. This group of points could be deconvolved in 3 dimensional space to produce a more sharply defined set of points, with less spread from the line, providing better size resolution along the line. But a better solution is to measure 4 scattering values at 4 different scattering angles for each

particle. And then take ratio of each of any 3 values with the fourth value to remove the effect of intensity variation for particles which pass through different portions of the beam. Produce a scatter plot of these 3 ratios in three dimensions, where each point in 3 dimensional space is placed in Xm, Ym, and Zm values corresponding to the three ratios for each particle. Since the intensity distribution broadening is reduced, most of the points will tightly follow a line in three dimensional space. Outliers which are not close to the line passing through the highest concentration of data points may be eliminated as not being real single particles. The remaining data points (Xm,Ym,Zm) are then compared to different theoretical models to determine the composition and/or shape of the particles. The 3 dimensional function which describes the theoretical scattering is Zt where Zt is a function of Xt and Yt :

$$Zt = Zt(Xt,Yt)$$

Let (Xm,Ym,Zm) be the set of data points measured from the counted particles. Where the values in the X,Y,Z coordinates represent either absolute scattering signals S1, S2, S3 or signal ratios S4/S1, S3/S1, S2/S1 (or any other combination of ratios) . Then define an error function Et for a certain theoretical model as:

$$Et(Xm,Ym) = (Yt(Xm)-Ym)^2 \quad \text{for Xm in the region Xmy where Yt(Xm) is single-valued}$$

$$Et(Xm,Zm) = (Zt(Xm)-Zm)^2 \quad \text{for Xm in the region Zmy where Zt(Xm) is single-valued}$$

Where Yt(Xm) is the theoretical value of Yt at Xm and Zt(Xm) is the theoretical value of Zt at Xm. Then find the theoretical model which produces the minimum sum of Esum over all values of Xm in the data set.

$$Esum = SUM(Et(Xm,Ym))/Ny + SUM(Et(Xm,Zm))/Nz$$

Where Ny is the number of points in region Xmy and Nz is the number of points in Xmz. And SUM is the sum of Et over its valid region of Xmy or Zmy. Esum is calculated for various theoretical scattering models, for spherical and non-spherical particles, and the model with the lowest Esum is chosen as the model for the sample. The sum of Esum values from multiple particle samples can also be compared for different theoretical models. The model with the lowest sum of Esum values is used to analyze all of those samples of that type. This calculation may be computationally intensive, but it only needs to be done once for each type of sample. Once the optimal theoretical model is determined for each particle sample type, the appropriate stored model can be retrieved whenever that sample type is measured. The chosen theoretical model will provide the particle diameter as a function of Xm, Ym, and Zm for each detected object.

Signal ratios show reduced sensitivity to the position of the particle in the source beam because each scattering signal is proportional to the optical irradiance on the particle.

Usually to obtain optimal signal to noise, a laser source will be used to provide high irradiance but with lower irradiance uniformity due to the Gaussian intensity profile. The broadening in the monosized response, as shown in Figures 27 and 28 for example, may be reduced by insuring that only particles which pass near to the peak of the beam intensity profile are counted. Many methods have been described above to accomplish this selection process. Other methods could include the use of small capillaries or sheath flow to force all of the particles to go through the center of the source beam. But these methods are sometimes prone to particle clogging. In sheath flow, the particle dispersion is restricted to flow through a narrow jet, which is surrounded by a flow sheath of clean dispersant. If the particle concentration is low, the particles in this narrow stream will pass through the laser in single file and in locations close to the center of the beam. This method could be used with the ideas in this disclosure, but the wide range of particle sizes would require many different sized jets to handle the entire size range with the constant danger of clogging. The methods described in this disclosure can be used within a flow system of much larger dimensions, because the optical system only views and counts particles within a small interaction volume of that much larger volume. Particles which pass through that volume and which are outside of the size range for that measurement system will produce data points in the multidimensional space which are far from the multi-dimensional line of the optical model. They may be rejected based upon this criteria or simply based upon the length of the scattering pulse. Only the small particles are counted and sized by the higher angle system. The larger particles are sized by the 2-dimensional array or lower angle scattering systems. These independent particle size distributions are then combined to produce one size distribution over the full size range of the instrument.

The measurement of particle shape has become more important in many processes. Usually the shape can be described by length and width dimensions of the particle. If the length and width of each particle were measured, a scatter plot of the counted particles may be plotted on the length/width space to provide useful information to particle manufacturers and users. If the particles are oriented in a flow stream, the angular scattering could be measured in two nearly orthogonal scattering planes, one parallel and one perpendicular to the flow direction. Each of these scatter detection systems would measure the corresponding dimension of the particle in the scattering plane for that detection system. If the flow of particle dispersion flows through a restriction, so as to create an accelerating flow field, elongated particles will orient themselves in the flow direction. Figure 29 shows one of these scatter detection systems where the scattering plane is parallel to Ys and measures the projected particle dimension in the Ys direction, which is parallel to the projection of the flow direction of the particles in the Ys/Xs plane. A second scattering detection system could be placed in a scattering plane which includes the Z axis and Yp as shown in Figure 30. This detection system would measure the particle dimension in the plane perpendicular to the flow. Each particle is counted with two dimensions, one parallel to and the other perpendicular to the flow, as measured concurrently by these two detection systems. In some cases, the particles cannot be oriented in the flow and they pass through the beam in random orientations. The detection configuration in Figure 31 shows three scattering systems. Each system is in a scattering

plane which is approximately 120 degrees from the next one. If the particle shapes are assumed to be of a certain type: rectangular, ellipsoid, etc., three size measurements in various scattering planes can be used to solve for the length, width, (or major and minor axis, etc.) and orientation of each particle. These planes can be separated by any angles, but 120 degrees would be optimal to properly condition the 3 simultaneous equations formed from these three size measurements.

When measuring larger particles, which require smaller scattering angles, The scatter collection lens may be centered on the Z axis, with scattering detectors in the back focal plane of the collection lens, as shown in Figure 32. As shown before, lens 1, pinhole 1, and lens 2 are not needed if a spatially clean collimated beam, such as a clean laser beam, is incident on the particle dispersion in the sample cell. Lens 3 collects scattered light from the particles and focuses it onto a group of detectors in the back focal plane. As before, the length and width of each randomly oriented particle is determined by 3 independent size measurements or, in the case where the size measurements are not independent, you must solve a set of simultaneous equations as described below. If the particles are oriented in the flow, only the Ys direction (parallel to the flow) and a set of detectors in the direction perpendicular to Ys are needed. As before, these two directions can be at any angle, but parallel and perpendicular to the flow are optimal. In the random orientation case, each measurement is made by a separate arm of the detector set in the three directions Ys, Y1, and Y2. These directions can be separated by any angles, but 120 degrees (see Figure 33) would be optimal to properly condition the 3 simultaneous equations formed from these three size measurements. The scatter detector signals in each direction are combined by ratio of signals or other algorithms to determine the effective size in that direction. Then three simultaneous equations are formed from these size measurements to solve for the width, length, and orientation of each particle. Figure 34 shows how this detector configuration is used in the system from Figure 11.

The accuracy of the methods outlined above is improved by solving another type of problem. The sizes calculated from angular scattering data in each of two or more directions are not usually independent. In order to accurately determine the shape parameters of a particle, the simultaneous equations must be formed in all of the scattering signals. The form of the equations is shown below:

$$Si = Fi(W,L,O)$$

Where Si is the scattering signal from the ith detector. In the case of three directions (or scattering planes) and three detectors per direction, we have 9 total detectors and i = 1, 2, ..., 9)

W is the "width" parameter and L is the "length" parameter of the particle. In the case of a rectangular shape model, W is width and L is length. In the case of an ellipsoidal model, W is the minor axis and L is the major axis, etc. O is the orientation of the particle which could be the angle of the particle's major axis relative to Ys, for example. The functions

Fi are calculated from non-spherical scattering algorithms and the form of Fi changes for different particle shapes (rectangles, ellipsoids, etc.). These equations, Si = Fi, form a set of simultaneous equations which are solved for W, L and O for each particle. If the Fi functions do not have a closed form, iterative methods may be employed where the Jacobian or Hessian are determined by numerical, rather than symbolic, derivatives. Also the closed form functions for Fi could be provided by fitting functions to Fi(W,L,O) calculated from the non-spherical scattering algorithms.

If we had two detection angles per each of three scattering planes, we would have 6 equations with 3 unknowns. With three detectors per plane the size range may be extended and we will have 9 equations with 3 unknowns. For particles with more complicated shapes, such as polygonal, more scattering planes may be required to determine the particle shape parameters. In any case, a shape model is assumed for the particles and the set of equations Si = Fi are created for that model where Fi is a function of the unknown size parameters and Si is the scattered signal on detector i. This method can be applied to any of the shape measuring configurations shown before. This technique can also be applied to ensemble size measuring systems when the particles all have the same orientation as in accelerating flow.

Low scattering signals from small particles may be difficult to detect. Figure 35 shows another variation where the source beam is passed through a patterned target which is conjugate to the interaction volume. The image of the target occurs in the interaction volume which is defined by aperture 1 or aperture 2. This target could consist of a sinusoidal transmission pattern or a Barker code pattern. As the particles pass through the image of this pattern, the scattered light is modulated by the modulated source intensity distribution in the interaction volume and so the scattered signal-vs.-time distribution is equivalent to the spatial intensity distribution. For a sinusoidal pattern, a phase sensitive detector with zero degree and quadrature outputs could be used to detect the sinusoidal signal of arbitrary phase. For a given particle velocity, the scattered signal could be filtered by a bandpass filter which is centered on the frequency equal to the particle velocity divided by the spatial wavelength of the sinusoidal intensity distribution in the interaction volume. The phase sensitive detector reference signal would also match this frequency. Better signal to noise is achieved with other types of patterns. A Barker code target pattern will produce a single peak with very small side lobes when the scattering signal is correlated with a matching Barker code signal using a SAW or CCD correlator. When two scattering signals are multiplied and integrated, the zero delay (tau) value of the correlation function is obtained. This value will have the lowest fluctuation when the two signals have strong correlation as when both signals are from the same particle, instead of uncorrelated noise. The integrated product of the two signals will show less noise than the separated integrated signals. Figure 35 also illustrates an additional scattering detector on aperture 2 for detection of three scattering angles. This can also be extended to a larger number of detectors.

As shown before, ratios of scattering signals can be analyzed as a multi-dimensional function. Another method is to look at the individual signal ratios vs. particle diameter as shown in Figure 36 for the case of three signal ratios. Any real particle event should produce a point on each curve which align vertically at the same diameter. Each curve indicates the particle size, but the most accurate size is determined from the curve where its point is in a region of high slope and monotonicity. For any particle, the 3 measured ratios would determine the approximate particle size region and allow selection of the one ratio which is in the region of highest slope vs. particle size and is also not in a multi-valued region (caused by Mie resonances). This optimum ratio would then be used to determine the precise particle size for that particle.

The ratio of scattering signals from different scattering angles reduces the dependence of the particle size determination on the particle path through the light beam. Particles with signals below some threshold are eliminated from the count to prevent counting objects with low signal to noise. The accuracy of counts in each size bin will depend upon how uniform this elimination criteria is over the entire size range. Many methods have been described in this disclosure for reducing this problem. These methods are improved by having a source beam with a "flat top" intensity distribution and very sharply defined edges. This flat top intensity distribution can be provided by placing an aperture in an optical plane which is conjugate to the interaction volume. Another technique which will accurately define an interaction volume is shown in Figure 37. No selection criteria is required for the direction which is parallel to the particle flow direction, because in this direction each particle passes through a similar intensity distribution and digitized signal values may be analyzed to find maximum or the integral for each particle signal. The primary criteria for eliminating particles from the count is based upon the position of the particle along the axis which is perpendicular to particle flow direction. The position of the particle along the direction perpendicular to the particle flow and the scattering plane (y direction) can be determined by using a 3 element detector which is in an optical plane which is conjugate to the interaction volume as shown in Figure 37. This figure shows the position and orientation of the 3 element detector in the optical system and an enlarged view of the detector elements showing the path of various particles passing through the interaction volume as seen by the detector elements. The beamsplitter, following lens 3, splits off some scattered light to the 3 element detector. By measuring the signal ratio between elements 1 and 2 or elements 3 and 2, the y position of the each particle is determined and only particles within a certain y distance from the center of the light beam are accepted. This signal ratio criteria is extremely accurate and uniform among all particle sizes so that proper mass balance is maintained over the entire size range. The ratio is also insensitive to how well the particle is optically resolved because the fraction the particle image on each the two detectors spanning the image is not strongly dependent on the size or sharpness of the image, but is strongly dependent on the y position of the particle. Figure 37 shows the 3 element detector in a heterodyne arrangement, with a portion of the source light being mixed with the scattered light. However, this idea is also applicable to non-heterodyne configurations by just removing the beamsplitter between lens 3 and aperture 2.

Many figures (Figure 19 for example) show the heterodyne system with a negative and positive lens pair (lenses 5 and 6) which provide a local oscillator beam which matches the wavefront of scattered light from the particles. Figure 38 shows an alternative design where all beams are nearly collimated in the regions of the beamsplitters. This configuration may be easier to align and focus. Lens 1 collimates the source light which is sampled by beamsplitter 1 and directed to beamsplitter 2 by the mirror. Lens 3 collimates the light scattered by the particle and this light is combined with the source light by beamsplitter 2 and focused through aperture 2 by lens 7. As before, aperture 2 is conjugate to the particle interaction volume and defines the interaction volume, in the sample cell, which is viewed by the detectors 3, 4 and 5. Usually, the focal length of lens 2 is long to provide a source beam of low divergence and the focal length of lens 3 is short to span a large range of scattering angles. If the light source is a laser diode, without anamorphic optics, the major axis of the intensity distribution ellipse at the interaction volume should be in the plane of the particle flow and scattering plane to provide a long train of heterodyne oscillations for signal detection and to provide the lowest beam divergence in the scattering plane. A circular source beam may require anamorphic optics to create an elliptical beam in the interaction volume to provide the advantages mentioned above. However, the advantages of the ideas described in this disclosure can be applied to a source beam with any intensity distribution.

The matching of light wavefronts between the source beam and scattered light at the heterodyne detectors is important to maintain optimum interferometric visibility and maximum modulation of the heterodyne signal on each detector. Since perfect wavefront matching is not achievable, the interferometric visibility must be determined for each detector to correct the signals for deviation from theoretical heterodyne modulation amplitude. The visibility is determined by measuring particles of known size and comparing the heterodyne signals to the signals expected from theory. To first order, the interferometric visibility should be independent of particle size for particles much smaller than the source beam in the interaction volume. The visibility could be measured for particles of various sizes to measure any second order effects which would create visibility dependence on particle size. If only signal ratios are used for determining size determination, only the ratios of interferometric visibility need to be calibrated by measuring scattering from particles of known size.

The number of cycles in the heterodyne modulated pulse is determined by the length of the trajectory of the particle through the source beam. The frequency of the heterodyne modulation is determined by the velocity of the particle through the beam. In general the power spectrum of the signal will consist of the spectrum of the pulse (which may be 10 KHz wide) centered on the heterodyne frequency (which may be 1 MHz). Both of these frequencies are proportional to the particle velocity. Actually the best frequency region

for the signal will be determined by the power spectral density of the detector system noise and/or the gain-bandwidth product of the detector electronics. For this reason, in some cases the particle flow velocity should be lowered to shift the signal spectrum to lower frequencies. The particle concentration is then adjusted to minimize the time required to count a sufficient number of particles to reduce Poisson statistic errors. This is easily accomplished for small particles which usually have higher count per unit volume and require lower noise to maintain high signal to noise.

In cases where optical heterodyne detection is not used, the signal to noise may be improved by phase sensitive detection of the scattered light. Modulation of the optical source may provide for phase sensitive detection of the scattering signal. The source is modulated at a frequency which is much larger than the bandwidth of the signal. For example, consider a source modulated at 1 megahertz with a scattering pulse length of 0.1 millisecond. Then the Fourier spectrum of scattered signal pulse would cover a region of approximately 10 KHz width centered at 1 megahertz. If this signal is multiplied by the source drive signal at 1 megahertz, the product of these two signals will contain a high frequency component at approximately 2 megahertz and a difference frequency component which spans 0 to approximately 10 KHz. In order to eliminate the most noise but preserve the signal, this product signal could be filtered to transmit only the frequencies contained in the scattering pulse, without modulation (perhaps between 5000 and 15000 Hz). This filtered signal product will have higher signal to noise than the raw signal of scattered pulses. This signal product can be provided by an analog multiplier or by digital multiplication after both of these signals (the scattering signal and the source drive signal) are digitized. This product is more easily realized with a photon multiplier tube (PMT) whose gain can be modulated by modulating the anode voltage of the PMT. Since the PMT gain is a nonlinear function of the anode voltage, an arbitrary function generator may be used to create PMT gain modulation which follows the modulation of the source. The voltage amplitude will be a nonlinear function of the source modulation amplitude, such that the gain modulation amplitude is a linear function of the source modulation amplitude. An arbitrary function generator can generate such a nonlinear modulation which is phase locked to the source modulator.

As described at the beginning of this disclosure, multiple sized beams can also be used to control the effects of seeing more than one particle in the viewing volume at one time. The key is to choose the proper scattering configuration to provide a very strong decrease of scattering signal with decreasing particle size. Then the scattering signals from smaller particles do not effect the pulses from larger ones. For example, by measuring scattered light at very small scattering angles, the scattered light will drop off as the fourth power of the diameter in the Fraunhofer regiem and as the sixth power of diameter in the Rayleigh regiem. In addition, for typically uniform particle volume vs. size distributions, there are many more smaller particles than larger ones. The Poisson statistics of the counting process will reduce the signal fluctuations for the smaller particles because individual particles pulses will overlap each other producing a uniform baseline for the larger particles which pass through as individual pulses. This baseline can be subtracted

from the larger particle pulse signals to produce accurate large particle pulses. A typical optical configuration is shown in Figure 41.

Figure 41 shows such an optical system where the light source is spatially filtered by lens 1 and pinhole 1. Lens 2 collimates and projects the source beam through the particle sample and an aperture mask, which is imaged onto the detector array by lens 3. A annular spatial filter is placed in the back focal plane of lens 3 to only pass scattered light over a certain range of scatter angle as defined by the inner and outer radii of the annular filter, which is similar to mask 1 shown in figure 12. The very low angle scattering and incident beam are blocked by central stop of the annular aperture in the back focal plane of lens 3. Hence the detector array 1 sees an image of mask apertures and each detector element measures the scattered light from particles in it's corresponding mask aperture over the angular range defined by the aperture (or spatial filter) in the back focal plane of lens 3. Each detector element is equal to or slightly larger than the image of the corresponding mask aperture at the detector plane, as long as each detector only sees the light from only it's corresponding mask aperture. A beam splitter splits off a portion of the light to a second annular filter (in the back focal plane of lens 3) and detector array 2. The angular ranges of the two annular filters are chosen to produce scattered values which are combined by an algorithm which determines the size of each particle. One such algorithm would be a simple ratio of the corresponding pulses from both arrays. And if the total scattered light is sensitive to particle composition, then the ratio of the two scattering signals can be used to determine the particle size more accurately. As with all other systems described in this disclosure, these ideas can be extended to more than two detector arrays or more than two scattering angles, simply by adding more annular spatial filter and detectors by using beamsplitters.

This configuration allows each detector element to see scatter from only a certain aperture in the mask and over a certain scattering angle range determined by it's spatial filter. If the spatial filter defines a range of low scattering angles, the total scatter for the detectors viewing through that spatial filter will show a strong decrease with decreasing particle size. The signal will decrease at least at a rate of the fourth power of the particle diameter or up to greater than the sixth power of the diameter. Assuming the weakest case of fourth power, we can obtain a drop by a factor of 16 in signal for a factor of 2 change in diameter. This means that you need to control the particle concentration such that no multiple particles are measured for the smallest particle size measured in each aperture. The largest particle size which has significant probability of multiple particles in the aperture at one time should produce scattering signals which are small compared to the scattering from lower size measurement limit set for that aperture. However, this particle concentration constraint is relaxed if multiple pulses are deconvolved within a signal segment.

One annular filter aperture could also be replaced by a pinhole, which only passes the light from the source (the red rays). Then the signals on each detector element would decrease as a particle passes through it's corresponding aperture at the sample cell. This signal drop pulse amplitude would directly indicate the particle size, or it could be used in

conjunction with the other annular signals. No limits on the number of apertures in the sample cell mask or of annular filter/detector sets are assumed. More annular filter/detector sets can be added by using more beamsplitters.

Figure 42 shows another configuration for determining particle size and shape. The light source light is focused through by pinhole 1 by lens 1 and then focused into the sample cell by lens 2. The beam divergence and spot size in the sample cell are determined by the range of scattering angles to be measured and the size range of the particles. Essentially the spot size increases and the divergence decreases for larger particles. The scattered light is collected by lens 3, which focuses it onto many multi-element detector assemblies, which are in the back focal plane of lens 3. Each multi-element detector has multiple detector elements which measure a certain range of scattering angles along various scattering planes. Figure 42 shows an example with three scattering planes separated by approximately 120 degrees between adjacent planes. However, any number of scattering planes with any angular separation is claimed in this disclosure. Each multi-element detector contains a central region which either captures of passes the source light so that it does not contaminate the measurement of the scattered light. The beam divergence will determine the size of the source light capture region on the multi-element detectors.

Each detector element has a shape which determines how much of the scattered light at each scattering angle is collected by the detector element. For example detector 1 has wedge shaped detectors which weights all scattering angles equally. Detector 2 has a higher order weighting, the larger scattering angles are gradually weighted more in the total signal for each detector element. These detector element shapes can take on many forms: rectangular, wedged, and higher order. Any shape will work as long as the progression of collection width of the detector is different between the two multi-element assemblies so that when the particle pulse signals from the corresponding detector elements of the two multi-element detectors are ratioed, you obtain a ratio which is particle size dependent. The progression of the weighting function can also be defined by placing a variable absorbing plate, over each detector element, which varies absorption vs. radius r from the center of the detector assembly. This absorption plate can provide a weighting similar to that obtained by varying the width of the detector element vs. r. And since these size measurements are made in different scattering planes, multiple dimensions of each particle are determined separately. In general each detector element produces a signal Sab, where "a" is the multi-element detector assembly number and "b" is the element number within that assembly. Then we can define Sab as:

$$Sab = \int wa(r)\, f(r,d)\, \partial r \quad \text{for the bth element in the ath assembly}$$

Here d is the dimension of the particle in the direction of the corresponding scattering plane. The scattered intensity at radius r from the center of the detector assembly (corresponding to zero scattering angle) for dimension of d is f(r,d). And wa(r) is the angular width (or weighting function) of the detector element at radius r in assembly "a", in other words the angle which would be subtended by rotating the r vector from one side

of the element to the other side at radius r. For the simple 3 element assemblies shown in figure 42, we obtain 6 measured values:

S11, S12, S13 for assembly 1

S21, S22, S23 for assembly 2

The signal on each detector element will consist of pulses as each particle passes through the beam. The Sab values above can be the peak value of the pulse or the integral of the pulse or other signal values mentioned in this disclosure. For example, one possible case would be:

Angular width for assembly 1 $w1(r) = Ar$

Angular width for assembly 1 $w2(r) = Br*r$

For this case S11/S21, S12/S22, and S13/S are almost linear functions of the particle dimension in the direction of the corresponding scattering plane. These 3 dimensions can also be determined from an algorithm which uses all 6 S values by solving simultaneous equations which include the interdependencies of these values on each other. In any event, the actual dimensions of the particle can be determined by assumption of a certain particle form such as rectangular, ellipsoidal, hexagonal, etc. More detector elements in each assembly will produce more accurate dimensions for randomly oriented particles. The true power of this technique is that the shape of each particle can be determined over a large size range by measuring only a few signals. Each element of each detector assembly could be broken up into sub-segments along the "r" direction to provide better size information by measuring the angular scattering distribution in each of the scattering planes. However, this may reduce the particle count rate because more digitizations and data analysis may be required per particle.

The actual particle size system may consist of systems, each which is similar to the one shown in Figure 42. Each system would have a different source beam divergence and spot size in the sample cell to accommodate different size ranges. The count distributions from the systems are then concatenated into one total distribution over the entire size range of the product. For example, for rectangular or ellipsoidal particles, the width and length dimensions of each particle could be plotted on a "scatter" plot to display the information in a useful format.

For smaller particles, the source beam will be more focused (higher divergence and smaller spot size in the sample cell region) into the sample cell. This will help to define a smaller interaction volume for the smaller particles which usually have higher number concentration than the larger particles.

Figure 43 shows another version of this concept where the interaction volume for particle scattering is controlled by appropriately positioned apertures and by correlation

measurements between signals from different scattering angles. The system is similar to that shown in Figure 42. But in this case additional apertures and lenses are added in the detection system. Aperture 2 and aperture 3 are placed in optical planes which are conjugate to the source focused spot in the sample cell. These apertures are sized and oriented to only allow the image of the focused spot to pass on to the multi-element detector. The source beam in aperture 1 may have significant intensity variation so as to produce a large variation in scatter signals when particles pass through different portions of the source spot in the sample cell. In this case, the size of apertures 2 and 3 may be reduced such that their images, at the sample cell, only pass the uniform portion of the source beam intensity profile in the sample cell. These apertures and lens 3 limit the volume, in the sample cell, from which scattered light can be detected by the multi-element detectors. Lenses 4 and 5 image the back focal plane of lens 3 on to the multi-element detector so that the detector sees the angular scattering distribution from the particles. The multi-element detectors 1 and 2 can also measure scattered light in the back focal plane of lens 4 and lens 5, respectively. Detector 3 collects all of the light that is scattered in a range of scattering angles which are defined by the annular aperture 4. This detector provides a size based on particle area, without shape dependence. In some cases the size as determined by the total scatter thorough aperture 4 will be more accurate than the particle dimensions from the multi-element detectors. For example, detector 4 could be used to determine the particle area and the multi-element detectors could determine the aspect ratio of the particle using the ratio of the determined dimensions. Using the area and the aspect ratio, the actual dimensions could be determined. This may be more accurate than simply determining the dimensions separately using the multi-element detectors for particles whose major or minor axis may not line up with a scattering plane.

Another feature of this design is the ability to use correlation or pulse alignment to determine which particle pulses are accurately measured and which pulses may be vignetted in the optical system. Figure 45 shows a crossection of the source beam focus in the sample cell. The outline of the beam is shown in red and the outline of the optical limits for scattered rays is shown in black. These optical limits are defined by the angular size of the detector elements and the size of aperture 2 or aperture 3. Two extreme scattered rays are drawn in blue for scattered light at a particular scattering angle. The intersection (crosshatched area) of volume between those scattered rays and the source beam is the interaction volume in which a detector can detect scattered light at that scattering angle. For example, consider the highest angle detector elements, 1C and 4C which are both in a scattering plane which is parallel to flow direction of the particles. The bottom portion of Figure 45 shows an approximation to the interaction volumes for each of these detector elements. Notice that as particle A passes through these interaction volumes, both scattering signals from 1C and 4C will be highly correlated, they will rise and fall together with a large amount of overlap in time. However, particle B, which is farther from best focus, will show very poor correlation between these two detectors. In fact the pulses will be completely separated in time. This pulse separation between 1C and 4C can be used to determine where the particle has passed through the interaction volume; and particles that are too far from best focus can be eliminated from the particle count. This correlation or pulse separation can be measured between any two detector

elements, within a group (i.e. 1A and 1C) or between groups (i.e. 1C and 4C). Typically the scattering plane for detector groups 1 and 4 would be parallel to the particle flow to obtain maximum delay. The correlation or pulse separation can be determined from the digitized signals using algorithms. However, this may require very high speed analog to digital converters and enormous computational load to obtain a high particle count and size accuracy. Another solution is to use analog electronics to measure the correlation or the pulse separation as shown in Figure 46, where the P boxes are processing electronics which measure the pulse peak (peak detector) or pulse integral. The X box is an analog multiplier. And S1A, S1B, and S1C are the analog signals from detector elements 1A, 1B, and 1C, respectively. The following equations will provide an estimate to the correlation between the pulses:

$R12 = P12/(P1*P2)$

$R13 = P13/(P1*P3)$

When R12 or R13 are small, the pulses have poor correlation and they should be eliminated from the count.

The delay between any two pulses from separate detector elements can also be used to select valid pulses for counting. As the particle passes through the beam farther from best focus of the source beam, the delay between the pulses will increase. Some threshold can be defined for the delay. All pulse pairs with delays greater than the threshold are not included in the count. One example is shown in Figure 47, where the delay between pulses from detector elements 1C and 4C (see Figure 44) is measured to reject particles which pass through the beam too far from the source beam best focus.

Another criteria for pulse rejection is pulse width. As shown in Figure 45, particle B will produce a shorter pulse than particle A, because the detector element will only see scattered light from the particle while it is in the interaction volume (the crosshatched area) for that particular detector element. The pulses could be digitized and the pulse width would then be computed as the width at some percentage of the pulse peak height to avoid errors caused by measuring pulses of different heights. Any of these techniques discussed above can be implemented using digitization of the detector element signals and computation of parameters of interest from that digitized data or using analog modules which directly produce the parameter of interest (pulse delay, pulse width, correlation, etc.). While the analog modules may have poorer accuracy, they can be much faster than digitization and computation, allowing a larger particle count and better count accuracy.

The pulse rejection criteria described above is used to reduce the number of coincidence counts by using apertures to limit the volume which is seen by the detectors. The interaction volume can also be limited by providing a short path where the particles have access to the beam as shown in Figure 48. Two transparent cones are bonded to the inner walls of the sample cell windows using index matching adhesive. The tips of each cone is

cut off and polished to either a flat or a concave optical surface. The optical windows and transparent cones could also be replaced with solid cell walls with holes which are aligned to hollow truncated cones with optical windows on the truncated tip of each cone. This way the light travels through air, except for a thin layer of particle dispersion between the two windowed cone tips. The gap between the cone tip surfaces provides the only volume where the flowing particles can pass through the source beam and scatter light to the detectors. A dispersion with a large range of particle sizes will not clog this gap because the larger particles will flow around the gap and the particle concentration is very low. The cone tip surfaces can be tilted slightly so that the spacing between them is smaller on the side where the particles enter the gap and larger where they leave the gap. In this way, particles larger than the minimum width of gap, but smaller than the maximum gap width, are prevented from jamming inside the gap.

The beam focus may shift with different dispersant refractive indices due to refraction at the flat surface on the end of each cone. This shift in focus and angular refraction can be corrected for in software by calculating the actual refracted rays which intercept the ends of each detector element to define the scattering angular range of that element for the dispersant refractive. This correction is not needed for concave surfaces, on each cone tip, whose centers of curvature are coincident with the best focal plane of the source between the two tips. Then all of the beam rays and scattered rays pass through the concave surface nearly normal to the surface with very little refraction and low sensitivity to dispersant refractive index.

Another problem that can be solved by particle counting is the problem of background drift in ensemble scattering systems which measure large particles at low scattering angles. An ensemble scattering system measures the angular distribution of scattered light from a group of particles instead of a single particle at one time. The optical system measures scattered light in certain angular ranges which are defined by a set of detector elements. Each detector element is usually connected to it's own separate electronic integrator, which is connected to a multiplexing circuit which sequentially samples each of the integrators which may integrate while many particles pass through the beam. So particle pulses cannot be measured in the ensemble system.

The detector elements which measure the low angle scatter usually see a very large scattering background without particles in the sample cell. This background is due to debris on optical surfaces or poor laser beam quality. Mechanical drift of the optics can cause this background light to vary with time. Usually the detector array is scanned with only clean dispersant in the sample cell to produce background scatter readings which are then subtracted from the readings from the actual particle dispersion. So first the detector integrators are scanned without any particles in the sample cell and then particles are added to the dispersion and the detector integrators are scanned a second time. The background scan data is subtracted from this second scan for each detector element in the array. However, if the background drifts between the two scans, a true particle scattering distribution will not be produced by the difference between these two scans. A third scan could be made after the second scan to use for interpolation of the background during the

second scan, but this would require the sample cell to be flushed out with clean dispersant after the particles are present.

A much better solution is to connect each of the detector elements, for the lowest angle scatter, to individual analog to digital converters or peak detectors as shown before in this disclosure. Then these signals could be analyzed by many of the counting methods which are described in this disclosure. This would essentially produce an essemble/counting hybrid instrument which would produce counting distributions for the large particles at low scattering angles and deconvolved particle size distributions from the long time integrated detector elements at higher scattering angles for the smaller particles. These distributions can be converted to a common format (such as particle volume vs. size or particle count vs. size) and combined into one distribution. The advantage is that the frequency range for the particle pulses is so much higher than the frequencies of the background drift. And so these pulses can be measured accurately by subtracting the local signal baseline on either side of each pulse. At very low scattering angles, the scattering signal drops off by at least the fourth power of particle diameter. Therefore larger particle pulses will stand out from the signals from many smaller particles which may be in the beam at any instant of time. Also the number concentration of larger particle will be low and provide for true single particle counting.

As mentioned before in this disclosure, the particle shape can be determined by measuring the angular distribution of scattered light in multiple scattering planes, including any number of scattering planes. The particle shape and size is more accurately determined by measuring the angular scattering distribution in a large number of scattering planes, requiring many detector elements in the arrays shown figures 33 and 44. As the number of detector elements becomes large, the use of less expensive 2-dimensional detector arrays, such as CCD arrays, becomes more attractive to take advantage of the economies of scale for production of commercial CCD cameras. However, the use of these 2-dimensional detector arrays presents some problems, which are not associated with custom detector arrays with optimally designed elements as shown previously. These arrays usually have poor dynamic range, poor sensitivity, poor A/D resolution, slow digitization rates, and high levels of crosstalk between pixels (blooming for example). Methods for mitigation of these problems are described below.

The detector array could be scanned at a frame rate, where during the period between successive frame downloads (and digitizations) each pixel will integrate the scattered light flux on its surface during an entire passage of only one particle through the source beam. Each pixel current is electronically integrated for a certain period and then its accumulated charge is digitized and stored; and then this cycle is repeated many times. During each integration period the pixel detector current from scattered light from any particle which passes through the beam will be integrated during the particle's total passage through the light source beam. Therefore the angular scattering distribution for that particle will be recorded over a large number of scattering planes by all of the detector elements in the array. This 2-dimensional scattering distribution could be

analyzed as described previously, using a large number of simultaneous equations and more shape parameters, by assuming a certain model for the particle shape (ellipsoidal, rectangular, hexagonal, etc.). As shown before, the particle shape and random orientation can be determined from these equations. Also, conventional image processing algorithms for shape and orientation can be used on the digitized scattering pattern to find the orientation (major and minor axes, etc.) and dimensions of the scatter pattern. The particle size and shape can be determined from these dimensions. Also the particle size and shape can be determined from the inverse 2-dimensional Fourier transform of the scattering distribution for particles in the Fraunhofer size range, but with a large computation time for each particle. The inverse Fourier transform of the scattering distribution will produce an image, of the particle, from which various dimensions can be determined directly.

For example, consider an absorbing rectangular particle of width and length dimensions A and B, with both dimensions in the Fraunhofer size range and minor and major axes along the X and Y directions. The irradiance in the scattering pattern on the 2-dimensional detector array will be given by:

$I(a,b) = Io * (SINC(\pi a)*SINC(\pi b))^2$

Where $SINC(x) = SIN(x)/x$

Io is the irradiance in the forward direction at zero scattering angle relative to the incident light beam direction
$a = A*sin(anga)/wl$
$b = B*sin(angb)/wl$
where:
wl = wavelength of the optical source
anga = the scattering angle relative to the incident source beam direction in the scattering plane parallel to the A dimension of the particle
angb = the scattering angle relative to the incident source beam direction in the scattering plane parallel to the B dimension of the particle

The corresponding x and y coordinates on the 2 dimensional detector array will be:

$x = F*tan(anga)$ and $y = F*tan(angb)$

The scattering pattern crossections in the major and minor axes consist of two SINC functions with first zeros located at:

$xo = F*tan(arcsin(wl/A))$
$yo = F*tan(arcsin(wl/B))$

where F is the focal length of the lens 3 in Figure 32 or F = M*F3 in figure 49 where F3 is the focal length of lens 3 in figure 49 and M is the magnification of lens 4. By inspection of these equations, the dimension of the scattering distribution is inversely proportional to the particle dimension along the direction parallel to direction of the dimension measurement. So for a rectangular particle, use known image processing methods to determine the major and minor axes of the scattering pattern and then measure the width and length of the pattern at the first zeros (xo and yo) in the scattering distribution in the directions of the major and minor axes. Then the particle dimensions are given by:

A = wl/(sin(arctan(xo/F))
B = wl/(sin(arctan(yo/F))

These equations describe the process for determining particle shape for a randomly oriented rectangular particle where we have assumed that the particle is much smaller than the uniform intensity portion of the source beam. Other parameters (such as the point in the scatter distribution which is 50% down from the peak) which describe the width and length of the scattering pattern can be used instead of xo and yo, but with different equations for A and B. In general, the corresponding particle dimensions can be determined from these parameters, using appropriate scattering models which describe the scattering pattern based upon the effects of particle size, shape, particle composition and the fact that the scattering pattern was integrated while the particle passed through a light source spot of varying intensity and phase.

The hardware concept is shown in figure 49. This system is very similar to those shown previously in this disclosure in Figure 32. Pinhole 1 removes high angle background from the light source and lens 2 collimates the source for passage through the sample cell through which the particle dispersion flows. The light source, lenses 1 and 2, and pinhole 1 could be replaced by a nearly collimated light beam such as a laser beam. Two optical systems view the particles. The 2-dimensional array #1 measures the scattering distribution from each particle and 2-dimensional array #2 measures the image of each particle. Array #1 is used to measure the dimensions of a smaller particle and array #2 measures the larger particles where the array pixel size can provide sufficient size resolution as a percentage of particle dimension. The scattering pattern from the particle is formed in the back focal plane of lens 3 and this scatter pattern is imaged onto array #1 by lens 4. A small block is placed in the back focal plane of lens 3 to block the unscattered focused light from the light source so that it will not reach array #1. The source light would saturate some pixels on that array and these pixels may bloom or crosstalk into adjacent pixels where very low level scattered light is being measured. Aperture 1 (also see figure 50) is placed in an image plane of the sample cell to define a restricted region of the beam where particles will be counted. This region is confined to where the intensity profile of the source beam has sufficient uniformity. If this region confinement is not required and access to the surface of the CCD is available (windowless CCD array) then lens 4 and aperture 1 could be removed and the CCD array could be placed in the back focal plane of lens 3, behind the source block.

A second similar optical system (system B which contains lenses 1B, 2B, 3B, 4B etc.) is placed upstream of the particle flow from the system (the main system which contains lenses 1, 2, 3, 4, etc.) described above (see figure 49). This system B reduces many of the problems associated with CCD arrays which are mentioned above. System B measures the scattered light from each particle before it passes through the main system described above. This scattered light level determines the particle size and predicts the signal levels which will be seen from that particle when it passes though the main system. These predicted levels provide the ability for the system to either adjust the intensity of light source 1 or the gain of array #1 to fill the range of the analog to digital converter which digitizes the scattering pattern data from array #1. The analog to digital converter and array pixel dynamic signal range is not sufficient to measure scattered light levels from particles over a large range of sizes. For example, the lowest scatter angle signal will change over 8 orders of magnitude for particles between 1 and 100 microns. However, the dynamic range of most CCD arrays is between 200 and 1000. Therefore, by adjusting the source intensity so that the maximum pixel value on array #1 will be just below saturation for each particle, the optimum signal to noise will be obtained. The time of the pulse from the upper system B will predict when each particle will pass through the main system, using the flow velocity of the dispersion through the cell. So the array only needs to integrate during the particle's passage through the source beam. This minimizes the integration time and shot noise of array #1. This timing could also be used to pulse the laser when the particle is in the center of the source beam for imaging by array #2 to freeze the particle motion during the exposure. Also the predicted size from system B could be used to choose only particles in a selected size range for shape measurement. Or some smaller particles could be passed without dimensional measurement to increase the statistical count of larger particles relative to the smaller particles to improve the counting statistics for the larger particles which are usually at lower number concentration than the smaller particles. But the size distribution could then be corrected by the total count distribution from the upper system B, while the particle shape count distribution is determined from the fewer particles counted by the main system. The size of the scattering pattern could also be predicted by system B so that an appropriate sub-array of array #1 would be digitized and analyzed to save digitization time. The size prediction can also determine which array (#1 , #2 or both) will be digitized to determine the particle dimensions. The upstream system B particle counts could also be used to determine coincidence counting while the particle concentration is being adjusted. Many of these techniques are used to reduce the digitization load on the analog to digital converter, if required.

Lens 4B acts as a field lens to collect scattered light and place the scatter detector in the image plane of the sample cell. This detector could be a single element detector which simply measures the all of the scattered light over a large range of scattering angles. However, this single detector measurement could be complicated by the variation of light intensity across the source beam. The use of a three detector multi-element detector could be used in this image plane of the sample cell. Then only particles which produce signal primarily on the center detector (of the three detector set) would be accepted for counting.

This particle selection could be based upon the ratios between the signal from the center detector element with the corresponding signal from either of the outer elements. The particle will be counted only if these two ratios are both above some threshold. If a large single detector is used instead of the multi-element detector, lens 4B could be removed and the detector could be placed directly behind the source block if it is large enough to collect all of the scattered flux. Otherwise a lens should be used to collect the scattered light and focus it onto the detector.

If the upstream system B is not used, the CCD array scans of each scatter pattern should be made over multiple long periods (many particles counted per period with one array scan per particle) where the light source intensity or detector pixel gain is chosen to be different during each period. In this way particles in different size and scattering efficiency ranges will be counted at the appropriate source irradiance or detector pixel gain to provide optimal signal to noise. So during each period, some particles may saturate the detectors and other particles may not be measured due to low scattering signals. Only particles whose scattering efficiency can produce signals within the dynamic range of the array for that chosen light source level or gain will be measured during that period. So by using a different source level or gain during each period, different size ranges are measured separately. The counting distributions from each period are then combined to create the entire size and shape distribution. This method will require longer total measurement time to accumulate sufficient particle counts to obtain good accuracy because some particles will be passed without counting. The use of system B to predict the optimal light source level or pixel gain provides the optimum result and highest counts per second.

The main system counting capability, as shown in figure 49, could be added to any diffraction ensemble system by using the scatter collection lens in the ensemble system to act as lens 3 in the counting system in figure 49. The light path after the ensemble system scatter collection lens (the lens forming the scatter pattern) would be partially diverted, by a beamsplitter, to a detection system as shown in figure 49 after lens 3. This detection system could be any appropriate variation of the detection system (with or without array#2 and its beamslpitter as shown in figure 49 for example). Also if source region confinement (as discussed above) is not required and access to the surface of the CCD is available (windowless CCD array) then lens 4 and aperture 1 could be removed and the CCD array could be placed in the back focal plane of lens 3, behind the source block. System B could also be added to the ensemble scattering system, but with significant added expense.

Linear CCD arrays do not have sufficient dynamic spatial range to accurately measure scatter pattern profiles from particles over a large range of particle size. For example, for a million pixel array, the dimensions are 1000 by 1000 pixels. If at least 10 pixel values need to be measured across the scatter profile to determine the dimension in each direction, then 1000 pixels will only cover 2 orders of magnitude in size. This size range can be increased to 4 orders of magnitude by using two arrays with different angular scales. Figure 51 shows a system similar to that shown in figure 49, but with an additional

scatter detection array (2-dimensional array #2). Arrays #1 and #2 are in the back focal planes of lens 4 and lens 5, respectively. Lens 5 has a much longer focal length than lens 4, so that each pixel in array #1 covers a proportionately larger scattering angle interval. As each particle passes through system B, the particle size is estimated to determine which array (#1 of #2) should be scanned and digitized. Array #1 should be used for small particles which scatter over large angles and Array #2 should be used for larger particles. The use of two arrays with different angular scales provides much higher particle count rates. For example, for 2 orders of size magnitude with a single array, 1 million pixels must be digitized (1000 by 1000 with minimum of 10 pixels for the largest particle). However, if two smaller 100 by 100 pixel arrays were used for array #1 and array #2 and the focal length for lens #5 was 10 times longer than the focal length of lens #5. Then these two 10,000 pixel arrays could cover 2 orders of magnitude in size, equivalent to that of the single 1 million pixel array; but only a maximum of 10,000 pixels must be digitized for each particle by using the size estimate from system B to determine which array to digitize. This design provides a factor of 100 increase in the particle count rate. This rate could be further increased by only digitizing the minimum subarray needed to measure each particle, based upon the size prediction provided by system B. Also, figure 51 shows the use of separate apertures (aperture #1 and aperture #2) which have different size openings. A smaller opening is used for the smaller particle detector array to reduce the scatter volume and reduce the probability of coincidence counting.

Figure 49B shows an analog version of the laser power control by system B. The peak detector receives the total signal, through port E, from the detector elements of the multi-element detector behind lens B. This detector could also be a single element detector if particle position detection is not used to define a small interaction volume, as described previously. When the peak detector breaks a threshold, it starts (by port C) the integration of the detector arrays in the main system after an appropriate delay for the distance between the systems. When the integration is finished, the array (through port D) resets the peak detector to start to look for the next particle. The peak value held by the peak detector is input (input B) to an analog ratiometer with an adjustable reference voltage input A, which can be set to adjust the laser power, and hence the scatter signal, to nearly fill the analog to digital convertor of the detector array in the main system. In this way, the light source intensity is rapidly changed to always nearly fill the range of the A/D converter for particles over a large range of size and scattered light signal. The value A/B could also be used to set the gain on the detector arrays, but this will probably not have sufficient speed. This entire process could also be replaced by its digital equivalents, but with much slower response and lower count rate.

One note must be made about diagrams in this disclosure. The size of the scatter collection lens, (i.e. lens 3 in Figure 49 and 50) is not shown in proper size relationship to the source beam in order to show more detail of the source beam and different focal planes in the design. This is true for all scatter collection lenses shown in this disclosure. In all cases we assume that the scatter collection lens is of sufficient diameter to collect scattered light from the particles over all of the scattering angles being measured. In some

cases this may require the lens diameter to be much larger than the diameter of the source beam.

Hybrid Systems

This disclosure also describes concepts for combining three different particle size measurement modalities: particle counting, ensemble scattering measurements, and dynamic light scattering. Particle counting is used for the largest particles (>100 microns) which have the largest scattering signals and lowest particle concentration. The angular scatter distribution from a particle ensemble is used to determine particle size in the mid-sized range (0.5 to 100 microns). And dynamic light scattering is used to measure particles below 0.5 micron diameter. These defined size range break points, 0.5 and 100 microns, are approximate. These methods will work over a large range of particle size break points because the useful size ranges of these three techniques have substantial overlap:

Single beam particle counting (depends on the source beam size) 50 to 3000 microns
Particle ensemble 0.1 to 1000 microns
Dynamic light scattering 0.001 to 2 microns

One problem that can be solved by particle counting is the problem of background drift in ensemble scattering systems which measure large particles at low scattering angles. An ensemble scattering system measures the angular distribution of scattered light from a group of particles instead of a single particle at one time. Figure 53 shows an ensemble scattering system (except for detectors B1 and B2 which illustrate additional detectors) which illuminates the particles with a nearly collimated light beam and collects light scattered from many particles in the dispersion which flow through the sample cell. The light source is focused through pinhole 1, which removes high angle defects in the beam intensity profile. Lens 2 collimates the beam through the sample cell. Lens 3 collects scattered light from the particles in the sample cell and focuses that light onto a detector array in the back focal plane of lens 3. An example of the detector array design is shown in Figure 54. The optical system measures scattered light in certain angular ranges which are defined by the set of detector elements. The elements can have different shapes, but in general the scattering angle range for each element is determined by the radius from the optical axis in the back focal plane of lens 3. In some cases, the detector array will have a central detector, D0, which captures the light from the source beam. Detectors D1, D2, etc. collect various angular ranges of scattered light. Each detector element is connected to its own separate electronic integrator, which is connected to a multiplexing circuit and analog to digital converter (ADC) as shown in figure 54 for detectors D3, D4, D5, and D6. This multiplexer sequentially samples each of the integrators which may integrate while many particles pass through the beam. So particle pulses cannot be measured in the ensemble system.

The detector elements which measure the low angle scatter (for example D1 and D2) usually see a very large scattering background without particles in the sample cell. This

background is due to debris on optical surfaces or poor laser beam quality. Mechanical drift of the optics can cause this background light to vary with time. Usually the detector array is scanned with only clean dispersant in the sample cell to produce background scatter readings which are then subtracted from the subsequent readings of the actual particle dispersion. So first the detector integrators are scanned without any particles in the sample cell and then particles are added to the dispersion and the detector integrators are scanned a second time. The background scan data is subtracted from this second scan for each detector element in the array. However, if the background drifts between the two scans, a true particle scattering distribution will not be produced by the difference between these two scans. A third scan could be made after the second scan to use for interpolation of the background during the second scan, but this would require the sample cell to be flushed out with clean dispersant after the particles are present.

A much better solution is to connect each of the detector elements, for the lowest angle scatter, to individual analog to digital converters, or peak detectors as disclosed before by this inventor. Then these signals could be analyzed by many of the counting methods which were disclosed by this inventor. This would essentially produce an ensemble/counting hybrid instrument which would produce counting distributions for the large particles at low scattering angles and deconvolved particle size distributions from the long time integrated detector elements at higher scattering angles for the smaller particles. These distributions can be converted to a common format (such as particle volume vs. size or particle count vs. size) and combined into one distribution. The advantage is that the frequency range for the particle pulses is much higher than the frequencies of the background drift. And so these pulses can be measured accurately by subtracting the local signal baseline on either side of each pulse, using the digitized signal samples. At very low scattering angles, the scattering signal drops off by at least the fourth power of particle diameter. Therefore larger particle pulses will stand out from the signals from many smaller particles which may be in the beam at any instant of time. Also the number concentration of larger particle will be low and provide for true single particle counting.

The smallest particles are measured using dynamic light scattering as shown in Figure 55. A fiber optic dynamic light scattering system, as described previously by the inventor, is inserted into the tubing through which the particle dispersion flows. The counting and ensemble scattering measurements are made with dispersion flowing through the system. This flow would be turned off during the collection of dynamic light scattering signals to avoid Doppler shifts in the scattering spectrum due to particle motion.

The particle counting uses the lowest angle zones (D1, D2, etc.) and the beam measuring zone (D0) of the detector array (an example of a detector array is shown in figure 54). Each of these detector elements are connected to a separate ADC to measure the scattering pulse in D1, D2, etc. and the signal drop on detector D0 as each particle passes through the interaction volume where the beam illuminates and from which the scattering detectors can receive scattered light from the particles. One problem is that the amount of scattered light is nearly proportional to the illumination intensity of the source on the

particle. Therefore as particles pass through different regions in the beam they may produce different pulse heights. Figure 56 shows a Gaussian intensity distribution which might be characteristic of the cross-section of a laser beam. Since the probability of particle passing through this beam at any position is approximately the same, we can generate the count vs. pulse amplitude distribution in Figure 57, which shows the count distribution for large number of identical particles. Notice that many particles pass through the low intensity portions of the intensity distribution and many particles also pass through close to the peak of the intensity distribution, with a long lower count level in between. This broad count response to a group of mono-sized particles will prevent accurate determination of complicated particle size distributions, because the pulse heights may be ambiguous for various sized particles. For example, a large particle passing through the lower intensity region can produce a pulse which is very similar to that from a smaller particle passing through the higher intensity region. The region of the intensity distribution which can produce scattered light into the detectors must be truncated by apertures in the source optics (aperture 1 in figure 52) or in the detection optics (aperture 2 in Figure 52). Either of these apertures can create a "region passed by aperture" as indicated in Figure 56 and 57. By using either or both apertures, only the upper region of the count vs. pulse amplitude distribution will be seen for many particles of a single particle size.

Another method for eliminating this intensity distribution effect is to use ratios of detector signals. This works particularly well when many of the detectors have scatter signals. However, for very large particles, only scattering detector D1 will see a high scatter signal with high signal to noise. So for very large particles, the apertures described previously may be required to use the absolute scatter from D1. Another solution is to use the ratio of the drop in D0 (signal S0) and the increase in D1 (signal S1) due to scatter as shown in figure 58A. As a particle passes through the beam D0 will decrease by approximately the total scattered light and D1 will increase by only the amount of light scattered into the angular range defined by that detector. The drop in D0 can be determined by subtracting the minimum of drop in S0 from the baseline A0 to produce a positive pulse A0-S0 as shown in figure 58B. As shown in Figure 59, the ratio of either the integral or the peak value of the corresponding pulses from these two signals can be used to determine the size of the counted particle for the largest size particles which have insufficient scatter signal in D2 to produce a ratio between S1 and S2. As long as D2 has sufficient scatter signal and D2 captures a portion of the primary lobe of the angular scatter distribution, the ratio between S1 and S2 will produce more accurate indication of size, than a ratio between S0 and S1. The primary lobe of the scattering distribution is the portion of the distribution from zero scattering angle up to the scattering angle where the size information becomes more ambiguous and particle composition dependent. Usually this happens when the scatter function first drops below 20% of the zero angle (maximum) value of the function. For a certain range of smaller particles, the ratio between S1 and S3 may have higher sensitivity to particle size than the ratio of S1 to S2. For smaller particle diameters, ratios to larger angle scatter signals will provide better sensitivity.

The signal ratio technique is needed when the "region passed by aperture" in figures 56 and 57 is too large such that mono-sized particles produce pulse peaks over a large amplitude range. For example, if no aperture were used, then mono-sized particles will produce the entire count distribution shown in Figure 57, with ambiguity between small particles passing through the center of the Gaussian intensity distribution and large particles passing through the tail of the distribution. In cases where the "region passed by aperture" is too large, the use of signal ratios (as described previously) is required to reduce the effect of the intensity variation (because the intensity variation drops out of the ratio, approximately). If the source intensity distribution can be made more uniform by use of an aperture (aperture 1 of Figure 52) or by use of a non-coherent source, or if the viewing aperture (aperture 2 in Figure 52) of the detector only views a restricted region where the source intensity is more uniform, then scattering amplitude can be used directly to determine size as shown in figures 60 and 61. This may have some advantages when only one detector has sufficient signal so that two signals are not available to create a ratio. Also the absolute signal amplitude information, which is lost in the ratio calculation, can be useful in determining the particle composition and in eliminating pulses which are due to noise, as will be described in Figure 61. Figure 57 shows a count vs. pulse amplitude response with a "region passed by aperture". This count distribution in the "region passed by aperture" is plotted on a logarithmic scale of S (or pulse peak or integral) for two different particle sizes, in Figure 60. Each function has an upper and lower limit in log(S). Notice that, in logarithmic S space, the two functions are shift invariant to particle diameter. The upper limit is due to particles which pass through the peak of the source intensity distribution and the lower limit is from the edge of the intensity. So that the count vs. log(S), Ns(log(S)), distribution from particles of the count vs. particle diameter distribution Nd(d) is the convolution between the shift invariant function in Figure 60, H(log(S), and the count vs. particle size distribution, Nd(d):

$$Ns(\log(S)) = Nd(d) \ominus H(\log(S))$$

This equation is easily inverted by using iterative deconvolution to determine Nd(d) by using H(log(S)) to deconvolve Ns(log(S)). In some cases, for example when S=A0-S0, the form of this equation may not be a convolution and a more generalized matrix equation must be solved.

Figure 61 shows a scatter plot of the counted data points in the two dimensional space, where the two dimensions are the logarithm of pulse amplitude or pulse integral for two different signals A or B. For example SA and SB could be S1 and S2, or A0-S0 and S1. Two squares are shown which encompass the region where counts from particles could occur for each of two particle diameters. SAU and SAL refer to the upper and lower limits of the signal, respectively, as shown in Figure 60. The lower limit, SAL, is determined by the cutoff of the aperture on the source intensity profile. The upper limit, SAU, is the maximum signal value when the particle passes through the peak of the source intensity profile. In the two dimensional space, shown in Figure 61, points are shown where the particle passes through the intensity peak, [log(SBU),log(SAU)], and where the particle passes through the edge of the intensity profile, [log(SBL),log(SAL)],

where the intensity is lowest. As particle size changes, this square region will move along a curve which describes the scatter for particles of a certain composition, as shown in Figure 62. The moving square will define a region, between the two blue lines which pass through the edges of the square. Real particles can only produce points within this region. Points outside this region can be rejected as noise points or artifact signals. This two dimensional count profile can be deconvolved using image deconvolution techniques, because each square defines the outline of the two dimensional impulse response in Log(S) space. The two dimensional count profile is the concentration (counted points per unit area of log(SA) and log(SB) plot 2-dimensional space) of counted points at each coordinate in the log(SA) and log(SB) space. This count concentration could be plotted as the Z dimension of a 3-dimensional plot where the X and Y dimensions are log(SA) and log(SB), respectively. The two dimensional impulse function plotted in the Z dimension of this 3-dimensional space is determined from the product of functions as shown in Figure 60, one along each of the log(SA) and log(SB) axes of Figures 61 and 62.

The previous concept uses particle counting to eliminate the particle size errors caused by background drift in the angular scattering signals, because the frequency content of the counted pulses is much higher than the background drift, and so the pulses can be detected by methods described previously by this inventor, without being effected by background drift. The local baseline is easily subtracted from each pulse because the background drift is negligible during the period of the pulse. However, this advantage can also be used with the integrators as shown in Figure 63. The slowly varying baseline can be removed by high pass analog electronic filters with a cutoff frequency between the lowest frequency of the particle scatter pulse spectrum and the highest frequency of the background drift spectrum. The input to each of the integrators which follow each high pass filter are the particle scatter pulses, without background which is attenuated by the filter. These pulses can be integrated and multiplexed into the same analog to digital converter as the higher scattering angle signals, which do not need the highpass filtering to remove the baseline drift. These integrators integrate over an extended period where many particles pass through the beam. In the case of smaller particles, there may be many particles in the beam at any instant in time. However, since the scatter signal from larger particles is much larger than that for smaller particles and with many smaller particles in the beam, these smaller particle signals will have very low fluctuations relative to the discrete pulses from the larger particles. So this high pass filtering will only work for the larger particles where the scatter signal fluctuations are large. This measurement could also be made with an RMS (root mean squared) module which only detects the higher frequency portion of the scatter signal for the lower angle detectors. All of these integrated signals, from low and high angle scatter detectors, are then inverted by techniques such as deconvolution pass through The detector signals could also be digitized directly; and the filtering and integration steps could be done digitally. However, the model for the deconvolution must include the loss of the small particle contribution to these filtered signals, because as the number of particles in the beam increases, the higher frequency components will be attenuated due to overlap of pulses. Given this attenuation process and the fact that signals at the lowest scattering angles scale as the fourth power of particle diameter, the smaller particle signals should not be significant in these filtered

low angle signals. The correction to the model is very minor; essentially the small particle contribution to these filtered detector signals can be assumed to be near to zero in the scattering model.

These methods do not assume any particular number of lower angle zones. For example, D0, D1, D2, and D3 could be handled with the techniques above. Essentially, any detectors with background drift problems should be handled with these methods.

Normally all of the ADC scans of the multiplexer output are summed together and this sum is then inverted to produce the particle size distribution. But due to the large difference in scattering efficiency between large and small particles, smaller particles can be lost in the scatter signal of larger ones in this sum. This problem can be mitigated by shortening the integration time for each multiplexer scan and ADC cycle to be shorter than the period between pulses from the large particles. Then each multiplexer scan and subsequent digitization can be stored in memory and compared to each other for scattering angle distribution. ADC scans of similar angular distribution shape are summed together and inverted separately to produce multiple particle size distributions. Then these resulting particle size distributions are summed together, each weighted by the amount of total integration time of its summed ADC scans. In this way, scans which contain larger particles will be summed together and inverted to produce the large particle size portion of the size distribution and scans which contain only smaller particles will be summed together and inverted to produce the small particle size portion of the size distribution, without errors caused by the presence of higher angle scatter from larger particles.

Another method to measure larger particles is to place a sinusoidal target in an image plane of the sample cell on front of a scatter detector as described previously by this inventor. The dispersant flow could be turned off and particle settling velocity measured by the modulation frequency of the scatter signal from individual particles settling through the source beam. The hydrodynamic diameter of each particle can then be determined from the particle density, and dispersant density and viscosity.

Finally the three size distributions from dynamic light scattering, ensemble scattering and counting are combined to produce one single distribution over entire size range of the instrument by scaling each size distribution to the adjacent distribution, using overlapping portions of the distribution. Then segments of each distribution can be concatenated together to produce the complete size distribution, with blending between adjacent distributions in a portion of each overlap region. This method works well but it does not make most effective use of the information contained in the data from the three sizing methods. Each inversion process for each of the three techniques would benefit from size information produced by other techniques which produce size information in its size range. This problem may be better solved by inverting all three data sets together so that each of the three methods can benefit from information generated by the others at each step during the iterative inversion process. For example, the logarithmic power spectrum, logarithmic angular scattering distribution and logarithmic count distribution could be concatenated into a single data vector and deconvolved using an impulse response of

likewise concatenated theoretical data. However, in order to produce a single shift invariant function, the scale of the counting data must be changed to produce a scale which is linear with particle size. For example, the pulse heights on an angular detector array will scale nearly as a power function of particle size, but the power spectrum and ensemble angular scattering distributions shift along the log frequency and log angle axes linearly with particle size. So a function of the pulse heights must be used from the count data to provide a count function which shifts by the same amount (linear with particle size) as the dynamic light scattering and ensemble distributions. This function may vary depending upon the particle size range, but for low scattering angles the pulse height would scale as the fourth power of the particle diameter, so that the log of the quarter power of the pulse heights should be concatenated into the data vector. This technique will work even though the concatenated vectors are measured verses different parameters (logarithm of frequency for dynamic light scattering, logarithm of scattering angle for ensemble scattering, and logarithm of pulse height or integral for counting), simply because each function will shift by the same amount, in its own space, with change in particle diameter. And so the concatenation of the three vectors will produce a single shift invariant function which can be inverted by powerful deconvolution techniques to determine the particle size distribution. This technique can also be used with any two of the measurement methods (for example: ensemble scattering and dynamic light scattering) to provide particle size over smaller size ranges than the three measurement process.

Another way to accomplish this is to constrain the inversion process for each technique (dynamic light scattering, ensemble scattering and counting), to agree with size distribution results from the other two techniques in size regions where those other techniques are more accurate. This can be accomplished by concatenating the constrained portion of the distribution, Vc, onto the portion (Vk) which is being solved for by the inversion process during each iteration of the inversion. The concatenated portion is scaled relative to the solved portion (AVc), at each iteration, by a parameter A which is also solved for in the inversion process during the previous iteration. This can be done with different types of inversion methods (Newton's method, Levenburg-Marquart, etc.) where the scaling parameter A is solved for as one additional unknown along with the unknown values of the particle size distribution. This technique will work for any processes where data is inverted and multiple techniques are combined to produce a single result.

$Fn = Hnm * Vn$ (matrix equation describing the scattering model)

$Vn = Vk \mid AVc$ (concatenation of vectors Vk and AVc, n number of total values in Vn)

Solve for k values of Vk and constant A

$Vn = Fn/Hnm$ (solution of the matrix equation by iterative techniques)

$k \leq n+1$

Another hybrid combination is particle settling, ensemble scattering, and dynamic light scattering as shown in figure 64. As before, dynamic light scattering probes a portion of the particle dispersion flow stream, with the flow turned off. The ensemble scattering system uses a detector array to measure the angular scattering distribution from groups of particles in the sample cell as the dispersion flows through the cell. A particle settling measurement is used for the largest particles which have the highest settling velocities. The settling is measured by sensing the power spectrum of the scattered light as viewed through a set of sinusoidal or periodic masks, which are also referred to as multi-frequency modulation transfer target. Some examples of these masks are shown in figures 65 and 66. This type of system has also been disclosed elsewhere by the inventor. The mask can be placed between lens 2 and lens 3 or on front of a group of detectors as shown in figure 64. The detector is placed in the back focal plane of lens 3, as shown previously by the inventor, to collect scattered light in separate ranges of scattering angle. A portion of the scattered light is split off by a beam splitter to an aperture in the focal plane of lens 3. This aperture can be an annular opening, which passes a certain range of scattering angles, or a pinhole centered to pass only the focused spot of the source in the back focal plane of lens 3. The light passing through the aperture, also passes through a periodic mask, as described previously, which is in a plane conjugate to the sample cell. This mask contains multiple regions, each with a different spatial frequency for the periodic absorption or reflection pattern. Behind each region in the mask is a separate detector which collects the light which only passes through that region. As particles pass through a region, the scattered light (for the annular aperture) or the attenuation (for the pinhole passing the source) of the beam are modulated by the motion of the particle's image across the absorption cycles of the mask. The particle dispersion flow pump is turned off and the particles are allowed to settle through the sample cell. The frequency of signal modulation for any particle is proportional to its settling velocity, which indicates the hydrodynamic size of the particle, given the particle and dispersant densities and the dispersant viscosity. The signal can be digitized and analyzed on an individual particle basis to count and size individual particles by measuring the settling velocity of each particle. In this case zero crossing measurement or Fourier transform of the signal segments for each particle could be used. In the case where many particles are in the beam at each instant, the power spectrum of the signal could be measured over an extended time. This power spectrum would then be inverted to produce the particle size distribution. As identical particles pass though different focal planes (planes perpendicular to the optic axis) in the sample cell, the power spectrum will change because the sharpness of the image of the mask will be reduced as the particle moves farther from the image plane. Also if the source beam is focused into the sample cell, as shown previously, then the source intensity and the scatter signal will drop as the particle passes farther from the best focus plane of the source. These effects can be included in the counting system model which is inverted to produce the particle size. The H function (or H matrix) described previously will contain columns which describe the count vs. signal frequency from a group of identical particles, of the size corresponding to that matrix column, passing through every point in the sample cell. For the ensemble scattering system model, the H function (or H matrix) will contain columns which describe the

integrated scatter signal vs. angle from a group of identical particles, of the size corresponding to that matrix column, passing through every point in the sample cell.

The following list describes the various options for using scattered light to measure size. In each case, the following matrix equation must be solved to determine V from measurement of F:

$F = H*V$

This equation can be solved by many different methods. However, because this equation is usually ill-conditioned, the use of constraints on the values of V is recommended, using apriori knowledge. For example, constraining the particle count or particle volume vs. size distributions to be positive is very effective. In some cases, as shown previously by this inventor, changing the abscissa scale (for example from linear to logarithmic) of F can produce a convolution relationship between F and V, which can be inverted by very powerful deconvolution techniques.

$F = H \Theta V$

Particle Counting

1) Angular scatter or attenuation due to scatter:

V = particle count per size interval vs. size

F = count per signal amplitude interval vs. signal amplitude where signal amplitude is either pulse peak value or integral of the pulse

H = matrix where each column is the F function for the particle size corresponding to that column

Response broadening mechanisms in the H matrix:

source intensity variation in x and y directions where particles can pass

(mitigated by aperturing of intensity distribution at an image plane of the sample cell)

source intensity variation in z direction

(mitigated by double pulse sensing and detector aperture at image plane of sample cell)

Advantages: high resolution and aerosol capability

Disadvantages: counting statistic errors for low count

2) Centrifuge or settling (hydrodynamic size)

V = particle count per size interval vs. size

F = count per signal frequency interval vs. signal frequency where signal frequency is the frequency of the scatter signal segment for the counted particle

H = matrix where each column is the F function for the particle size corresponding to that column

Response broadening mechanisms in the H matrix:

Finite length of modulated signal segment from each particle

Brownian motion

Variation of signal frequency along z direction

Advantages: high size resolution, excellent detection of small particles mixed with large particles, excellent measurement of low tails in the size distribution

Disadvantages: counting statistic errors for low count; and difficulty measuring large particles in aerosols due to very high settling velocities

Ensemble scattering

1) Angular scatter or attenuation due to scatter

V = particle volume per size interval vs. size

F = scattered light flux per scattering angle interval vs. scattering angle

H = matrix where each column is the F function for the particle size corresponding to that column

Response broadening mechanisms in the H matrix:

The broad angular range of scatter from a single particle

Advantages: excellent size reproducibility

Disadvantages: low size resolution, poor detection of small particles mixed with large particles, poor measurement of low tails in the size distribution.

2) Centrifuge or settling (hydrodynamic particle size)

V = particle volume per size interval vs. size

F = scattered light detector current power per frequency interval vs. frequency

H = matrix where each column is the F function for the particle size corresponding to that column

Response broadening mechanisms in the H matrix:

Finite length of modulated signal segment from each particle

Brownian motion

Variation of signal frequency along z direction

Advantages: high size resolution, excellent detection of small particles mixed with large particles, excellent measurement of low tails in the size distribution

Disadvantages: difficulty measuring large particles in aerosols due to very high settling velocities

Figure 1

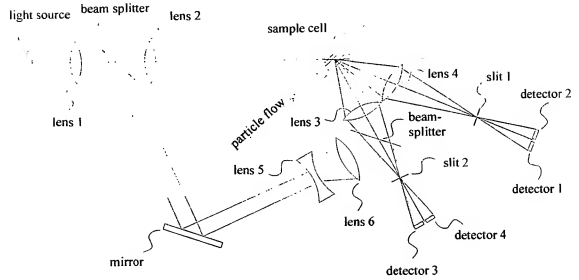

Figure 1A

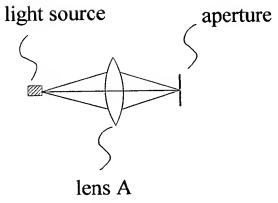

Figure 2

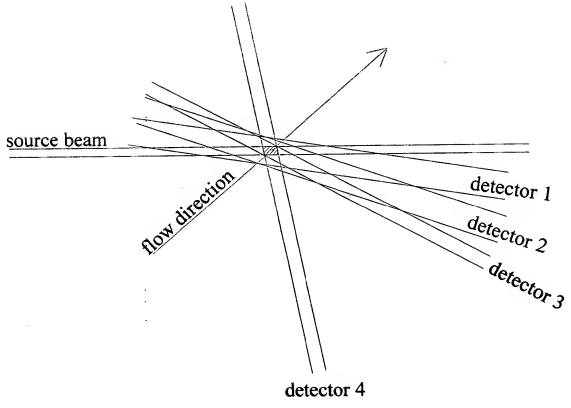
source beam
flow direction
detector 1
detector 2
detector 3
detector 4

Figure 2b

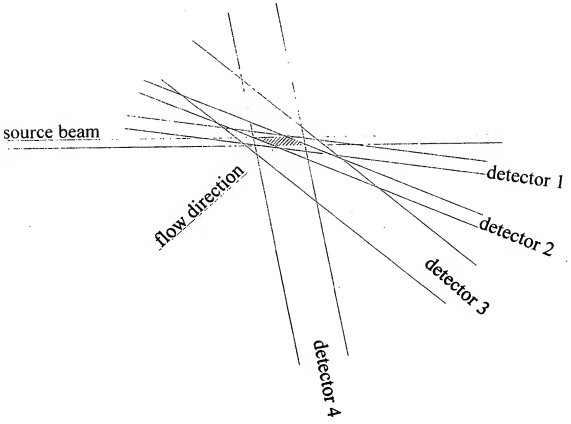
source beam
flow direction
detector 1
detector 2
detector 3
detector 4

Figure 3

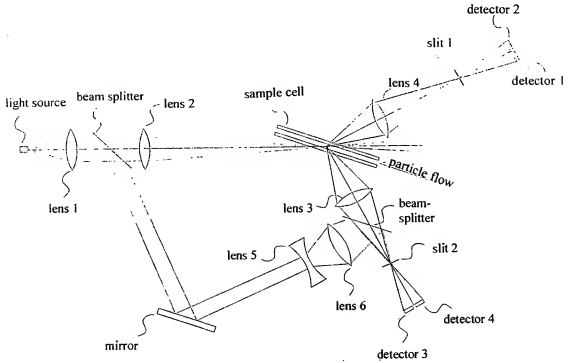

Figure 4

envelope detector

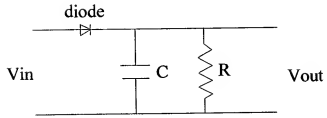

Figure 5

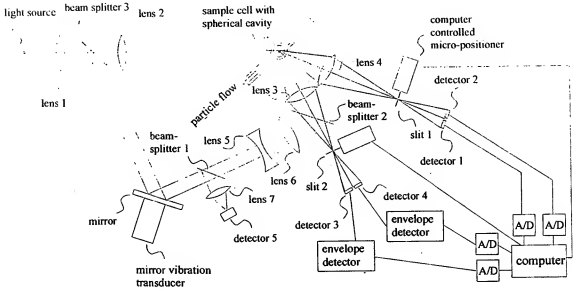

Figure 6

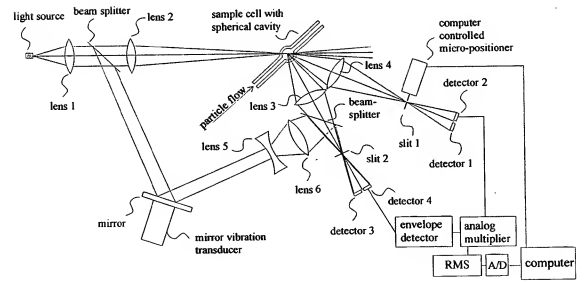

Figure 6b

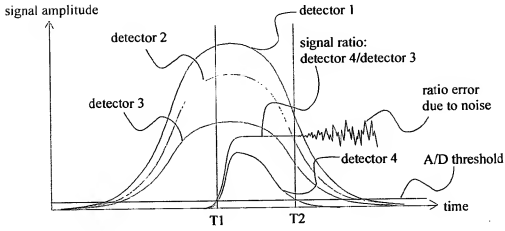

Figure 7

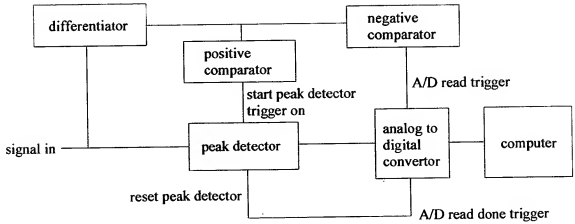

Figure 8

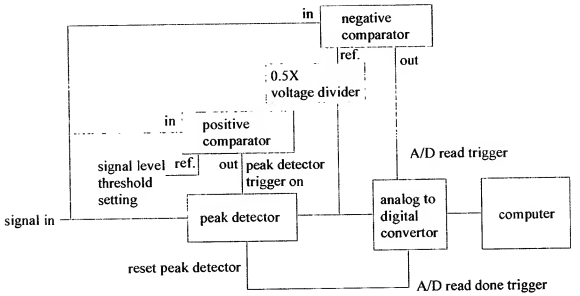

Figure 9

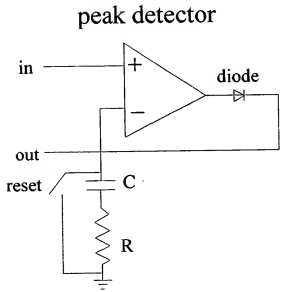

Figure 9b

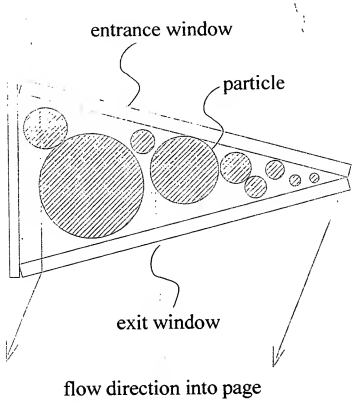

Figure 10

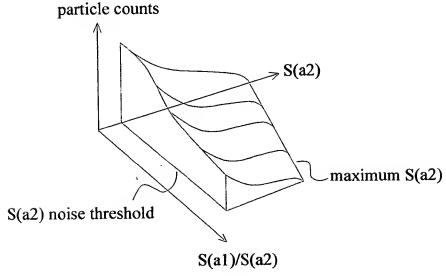

Figure 10b

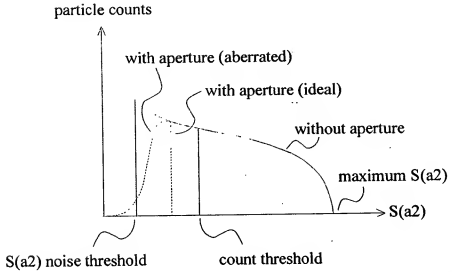

Figure 11

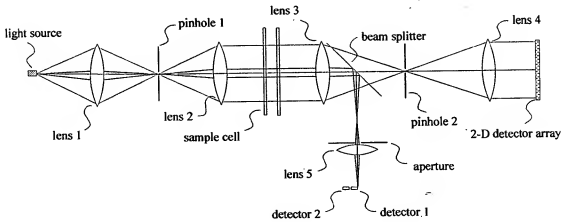

Figure 12

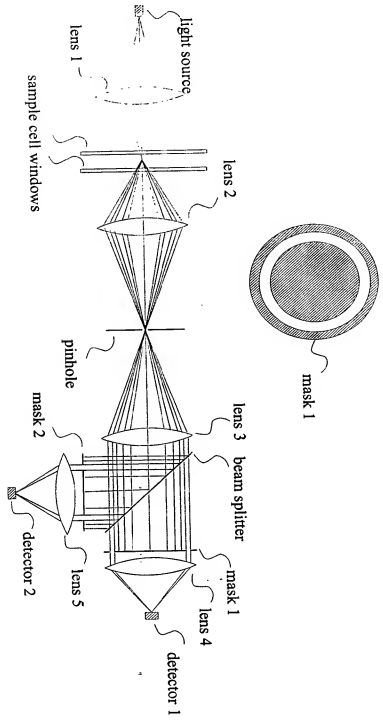
light source
lens 1
sample cell windows
lens 2
mask 1
pinhole
mask 2
lens 3
beam splitter
detector 2
lens 5
mask 1
lens 4
detector 1

Figure 13

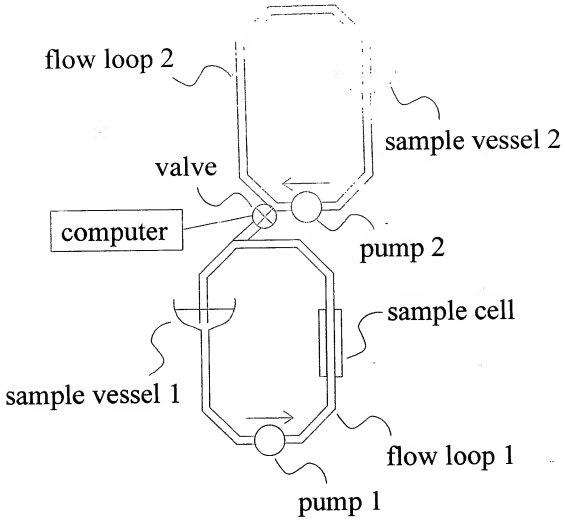
flow loop 2
sample vessel 2
valve
computer
pump 2
sample cell
sample vessel 1
flow loop 1
pump 1

Figure 14

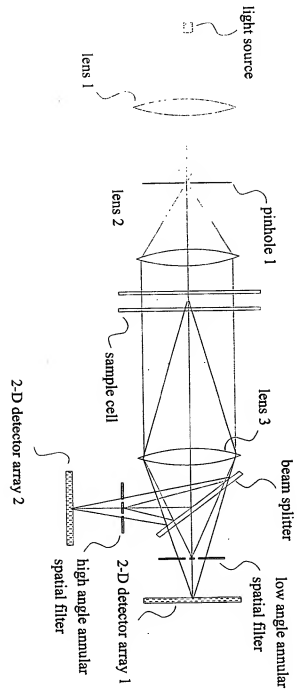
light source
lens 1
pinhole 1
lens 2
sample cell
lens 3
beam splitter
low angle annular spatial filter
2-D detector array 1
high angle annular spatial filter
2-D detector array 2

Figure 15

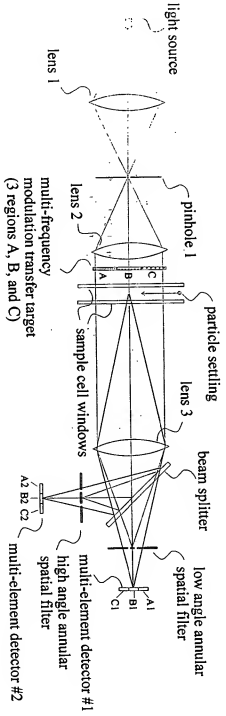
light source
lens 1
pinhole 1
lens 2
multi-frequency
modulation transfer target
(3 regions A, B, and C)
A
B
C
particle settling
sample cell windows
lens 3
beam splitter
low angle annular
spatial filter
multi-element detector #1
high angle annular
spatial filter
multi-element detector #2
A2 B2 C2
A1
B1
C1

Figure 15b

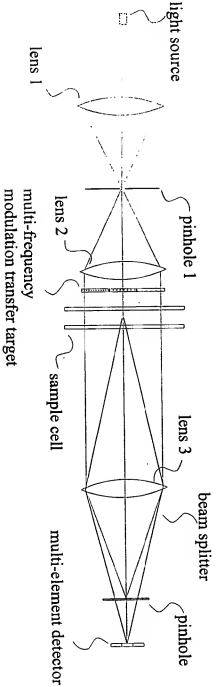
light source
lens 1
pinhole 1
lens 2
multi-frequency
modulation transfer target
sample cell
lens 3
beam splitter
pinhole
multi-element detector

Figure 16

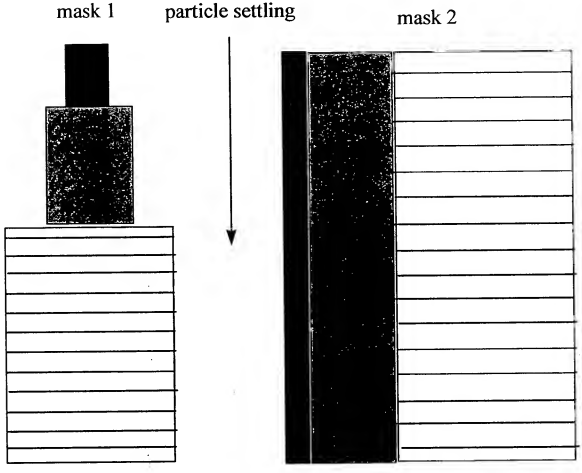

Figure 17

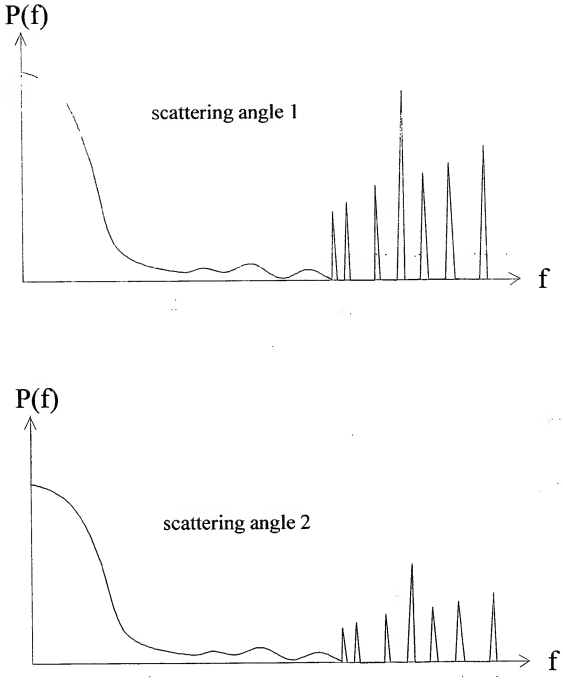

Figure 18

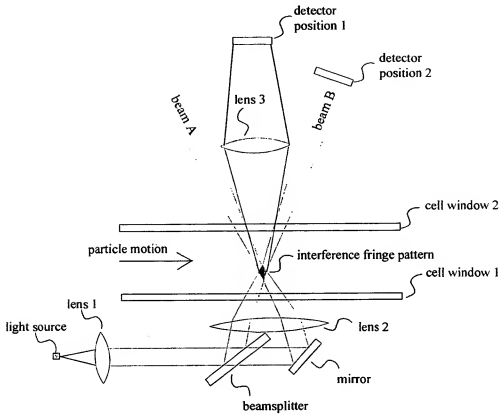

Figure 19

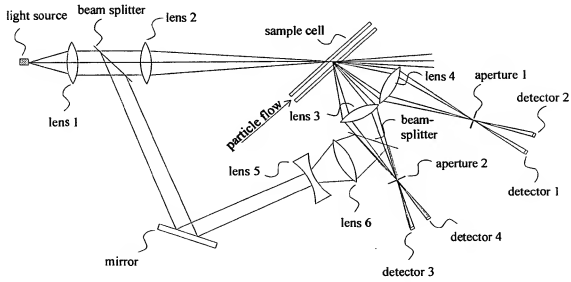

Figure 20

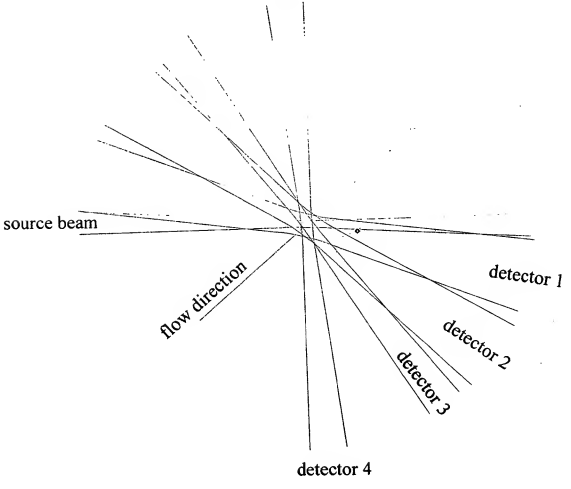
source beam
flow direction
detector 1
detector 2
detector 3
detector 4

Figure 21

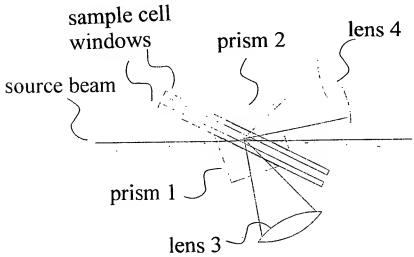

Figure 22

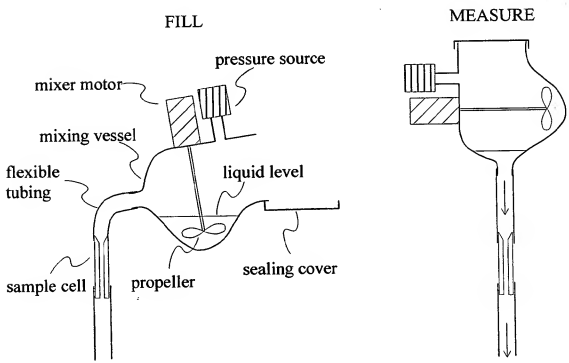

Figure 23a

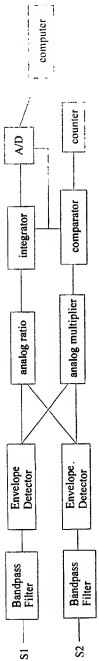

Figure 23B

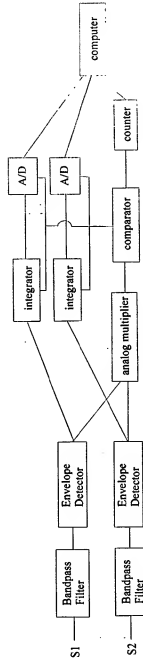

Figure 24

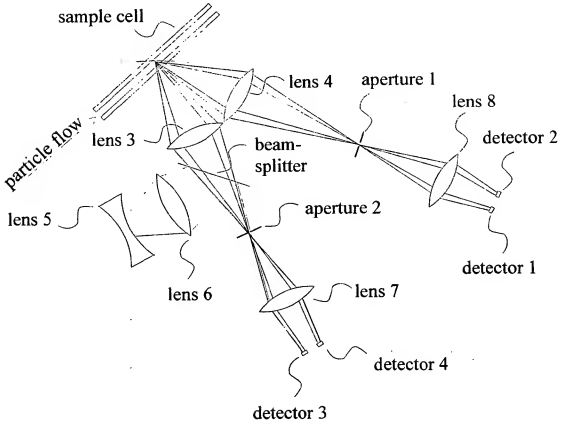
sample cell
lens 4
aperture 1
lens 8
particle flow
lens 3
beam-
splitter
detector 2
lens 5
aperture 2
detector 1
lens 6
lens 7
detector 4
detector 3

Figure 25

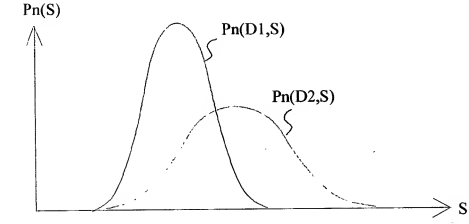

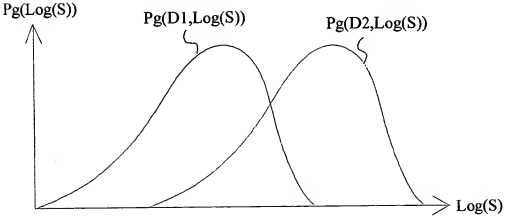

Figure 26

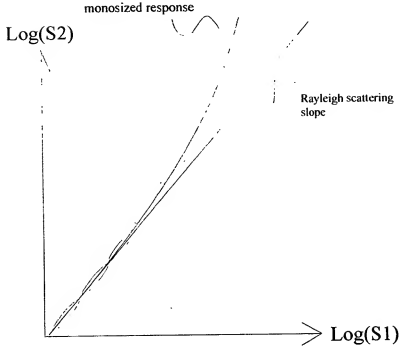

Figure 27

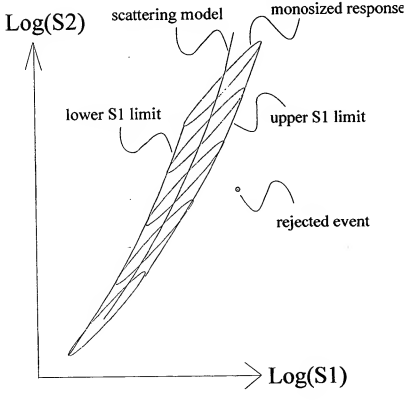

Figure 27B

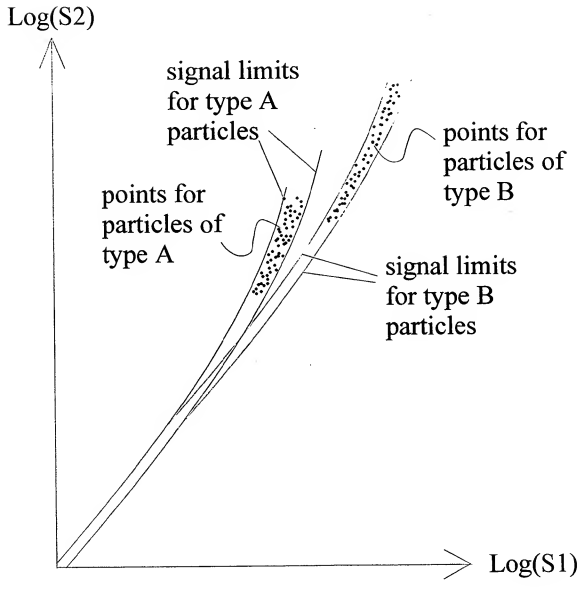
Log(S2)
signal limits for type A particles
points for particles of type B
points for particles of type A
signal limits for type B particles
Log(S1)

Figure 28

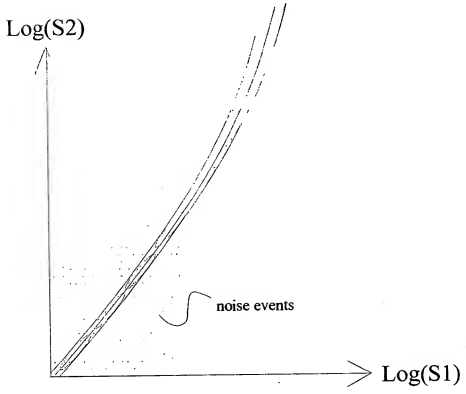

Figure 29

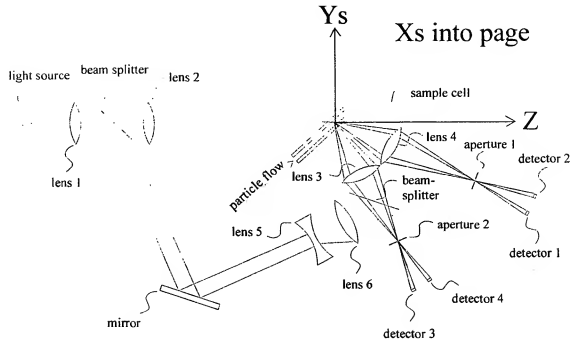

Figure 30

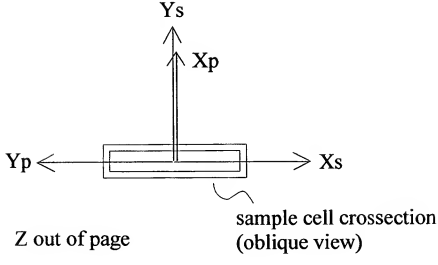

Figure 31

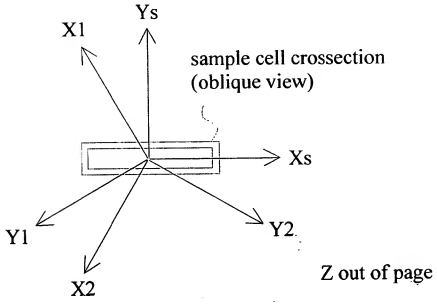
Ys
X1
sample cell crossection
(oblique view)
Xs
Y1
Y2
X2
Z out of page

Figure 32

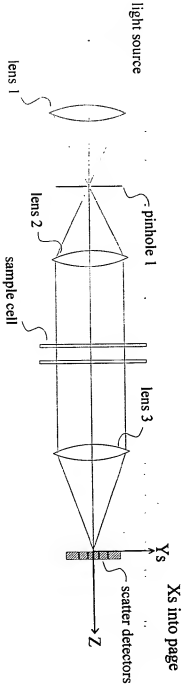
light source
lens 1
pinhole 1
lens 2
sample cell
lens 3
Ys
Xs into page
scatter detectors
Z

Figure 33

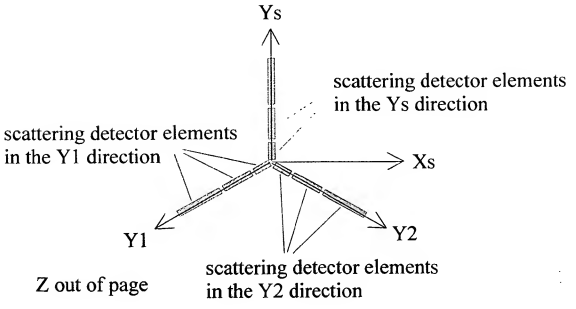
Ys
scattering detector elements
in the Ys direction
scattering detector elements
in the Y1 direction
Xs
Y1
Y2
Z out of page
scattering detector elements
in the Y2 direction

Figure 34

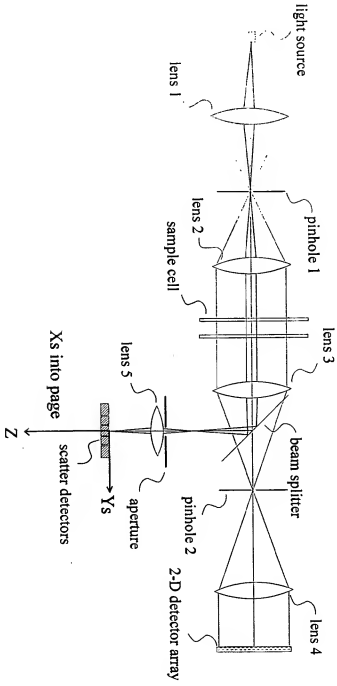
light source
lens 1
pinhole 1
lens 2
sample cell
lens 3
beam splitter
lens 5
Xs into page
Z
Ys
scatter detectors
aperture
pinhole 2
2-D detector array
lens 4

Figure 35

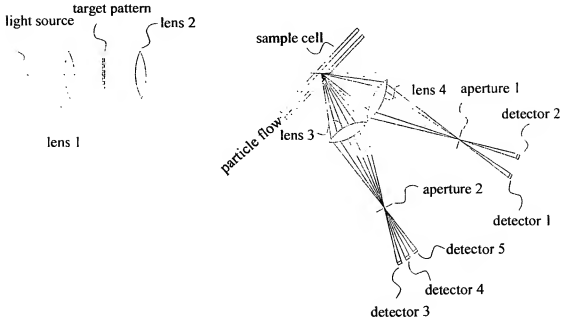

Figure 36

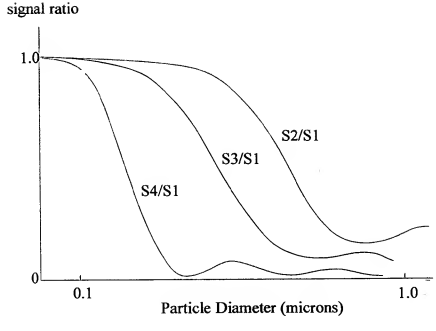

Figure 37

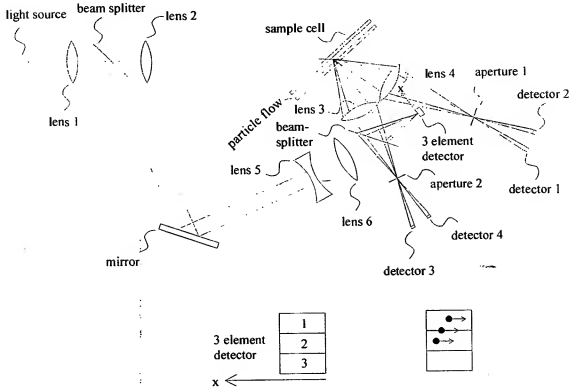
light source
beam splitter
lens 2
lens 1
sample cell
lens 4
aperture 1
detector 2
x
particle flow
lens 3
beam-
splitter
3 element
detector
lens 5
aperture 2
detector 1
lens 6
detector 4
mirror
detector 3
3 element
detector
1
2
3
x

Figure 38

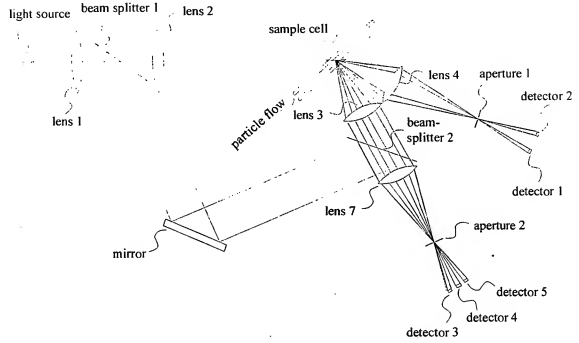
light source
beam splitter 1
lens 2
sample cell
lens 4
aperture 1
detector 2
lens 1
particle flow
lens 3
beam-
splitter 2
detector 1
lens 7
aperture 2
mirror
detector 5
detector 4
detector 3

Figure 39

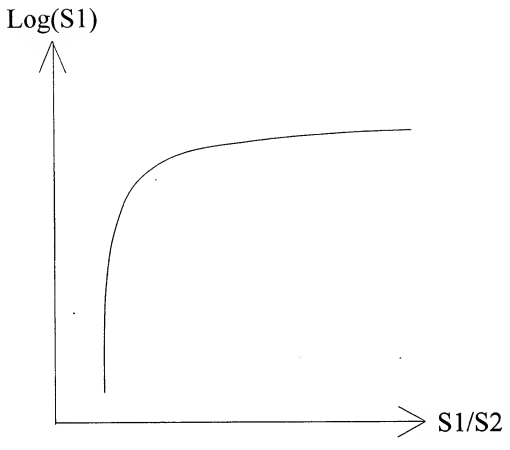

Figure 40

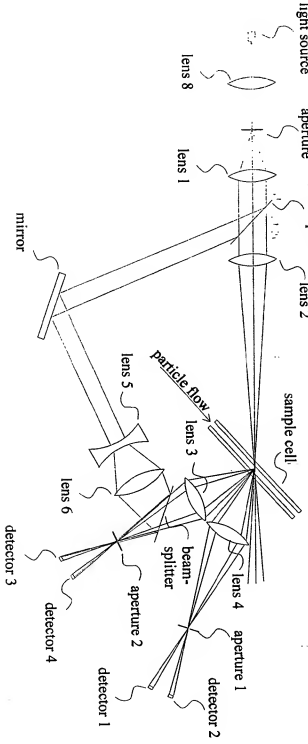
light source
lens 8
source aperture
lens 1
beam splitter
lens 2
mirror
particle flow
lens 5
lens 3
sample cell
lens 6
beam-splitter
lens 4
aperture 1
detector 3
aperture 2
detector 2
detector 4
detector 1

Figure 41

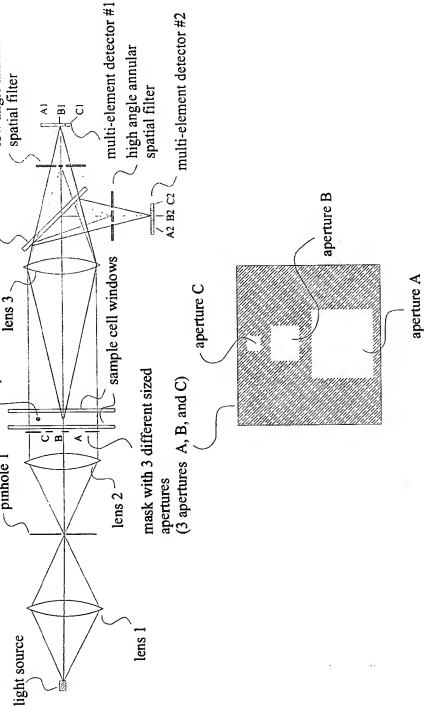
light source
lens 1
pinhole 1
lens 2
mask with 3 different sized apertures (3 apertures A, B, and C)
particle
lens 3
sample cell windows
beam splitter
low angle annular spatial filter
multi-element detector #1
high angle annular spatial filter
multi-element detector #2
A1
B1
C1
A2 B2 C2
A
B
C
aperture C
aperture B
aperture A

Figure 42

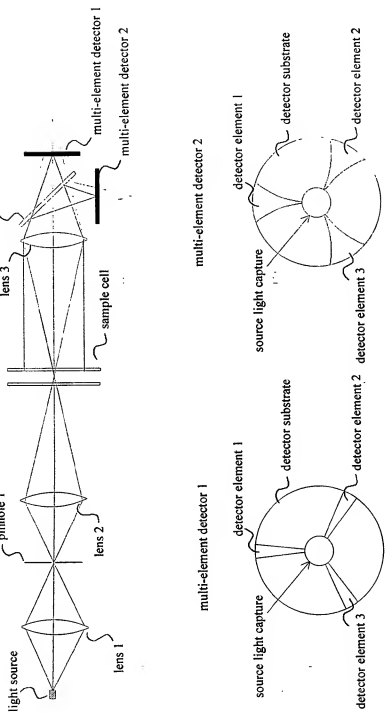
light source
lens 1
pinhole 1
lens 2
sample cell
lens 3
beam splitter
multi-element detector 1
multi-element detector 2
multi-element detector 1
detector element 1
source light capture
detector substrate
detector element 2
detector element 3
multi-element detector 2
detector element 1
source light capture
detector substrate
detector element 2
detector element 3

Figure 43

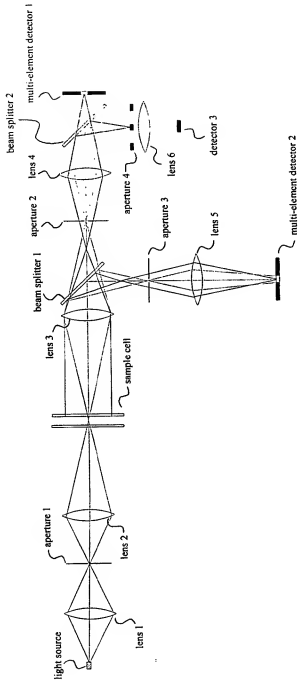
multi-element detector 1
beam splitter 2
lens 4
aperture 2
beam splitter 1
lens 3
sample cell
aperture 1
lens 2
lens 1
light source
aperture 4
lens 6
detector 3
aperture 3
lens 5
multi-element detector 2

Figure 44

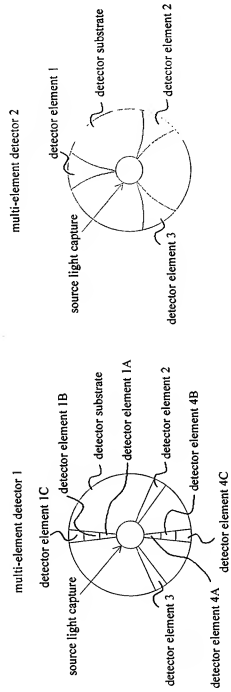
multi-element detector 2
detector element 1
detector substrate
detector element 2
source light capture
detector element 3
multi-element detector 1
detector element 1C
detector element 1B
detector substrate
detector element 1A
source light capture
detector element 2
detector element 4B
detector element 3
detector element 4A
detector element 4C

Figure 45

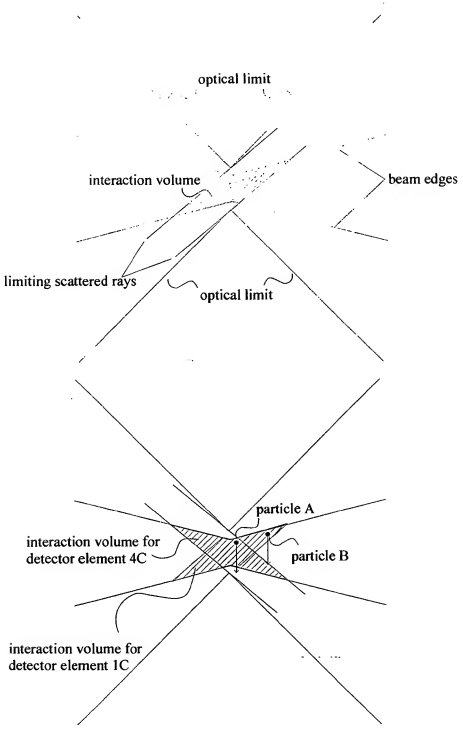
optical limit
interaction volume
beam edges
limiting scattered rays
optical limit
particle A
interaction volume for
detector element 4C
particle B
interaction volume for
detector element 1C

Figure 46

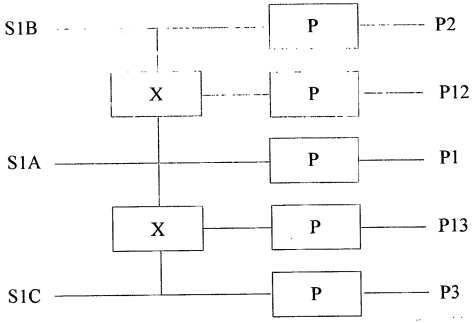

Figure 47

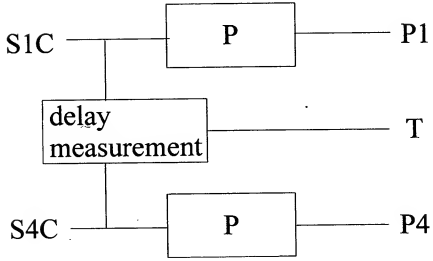

Figure 48

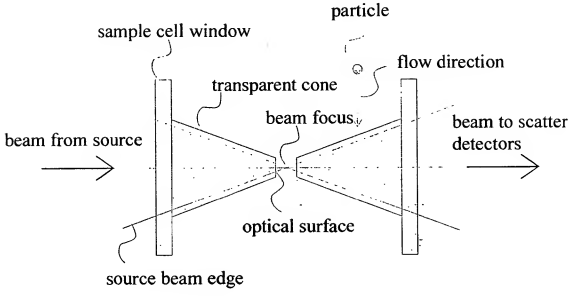
particle
sample cell window
flow direction
transparent cone
beam focus
beam to scatter detectors
beam from source
optical surface
source beam edge

Figure 49

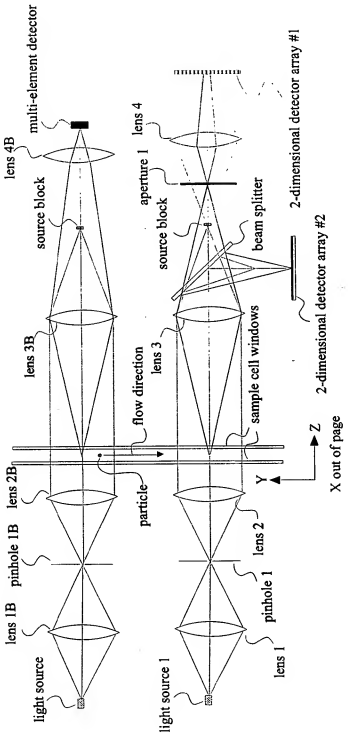
multi-element detector
lens 4B
source block
lens 3B
lens 2B
pinhole 1B
lens 1B
light source
aperture 1
lens 4
source block
beam splitter
2-dimensional detector array #1
2-dimensional detector array #2
flow direction
lens 3
sample cell windows
particle
lens 2
pinhole 1
lens 1
light source 1
Z
Y
X out of page

Figure 49B

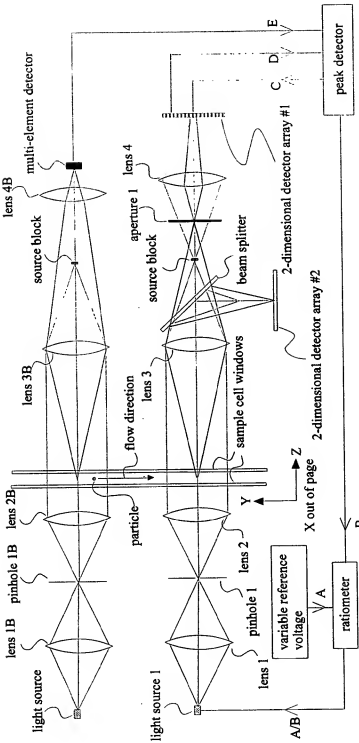
light source
lens 1B
pinhole 1B
lens 2B
lens 3B
lens 4B
multi-element detector
source block
flow direction
particle
light source 1
lens 1
pinhole 1
lens 2
variable reference voltage
A
A/B
ratiometer
B
peak detector
E
D
C
lens 4
aperture 1
source block
beam splitter
2-dimensional detector array #1
2-dimensional detector array #2
lens 3
sample cell windows
Z
Y
X out of page

Figure 50

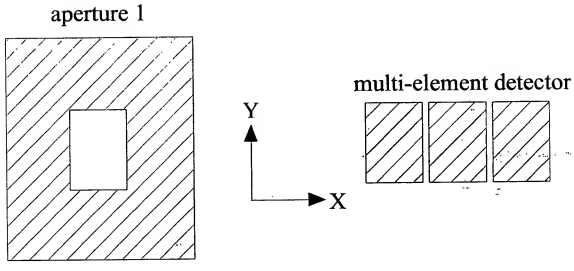

Figure 51

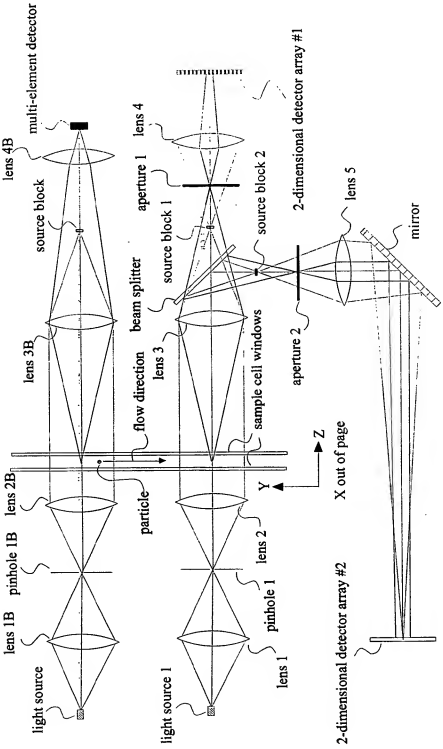
multi-element detector
lens 4B
source block
lens 3B
lens 2B
pinhole 1B
lens 1B
light source
beam splitter
flow direction
particle
lens 3
sample cell windows
lens 2
pinhole 1
lens 1
light source 1
aperture 1
lens 4
source block 1
2-dimensional detector array #1
source block 2
aperture 2
lens 5
mirror
Z
Y
X out of page
2-dimensional detector array #2

Figure 52

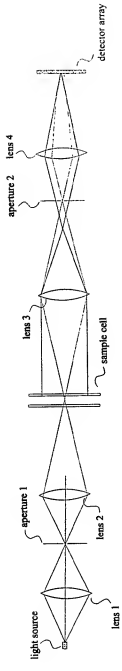
detector array
lens 4
aperture 2
lens 3
sample cell
aperture 1
lens 2
light source
lens 1

Figure 53

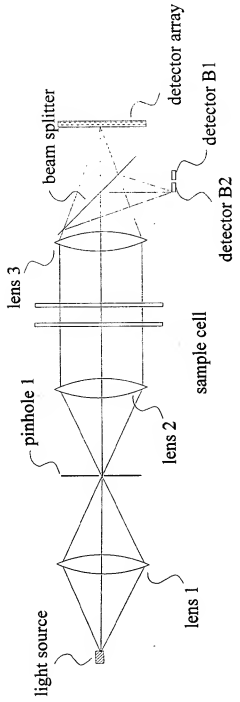
detector array
detector B1
beam splitter
detector B2
lens 3
sample cell
pinhole 1
lens 2
lens 1
light source

Figure 54

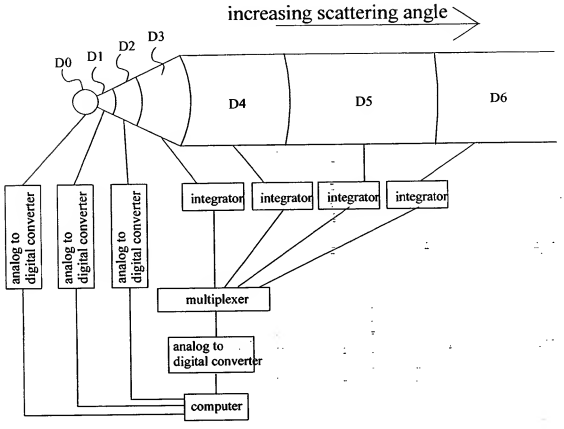
increasing scattering angle
D0
D1
D2
D3
D4
D5
D6
integrator
integrator
integrator
integrator
analog to digital converter
analog to digital converter
analog to digital converter
multiplexer
analog to digital converter
computer

Figure 55

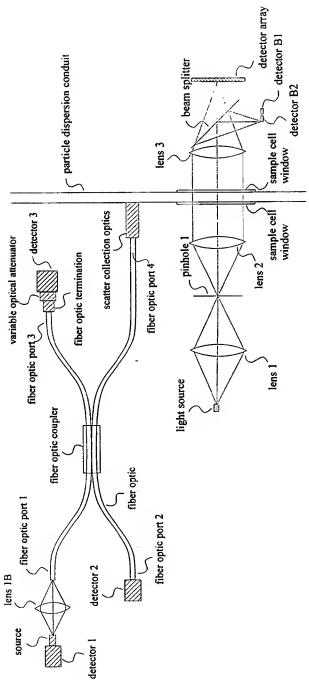
source
lens 1B
detector 1
fiber optic port 1
detector 2
fiber optic port 2
fiber optic coupler
fiber optic
fiber optic port 3
detector 3
variable optical attenuator
fiber optic termination
scatter collection optics
fiber optic port 4
particle dispersion conduit
light source
lens 1
pinhole 1
lens 2
sample cell window
sample cell window
lens 3
beam splitter
detector array
detector B1
detector B2

Figure 56

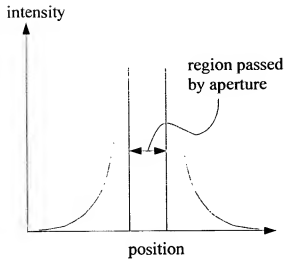

Figure 57

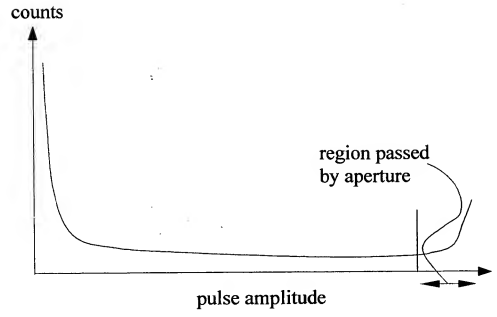

Figure 58A

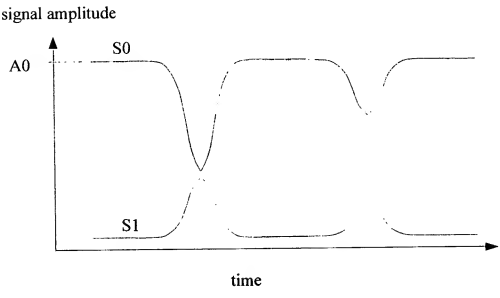

Figure 58B

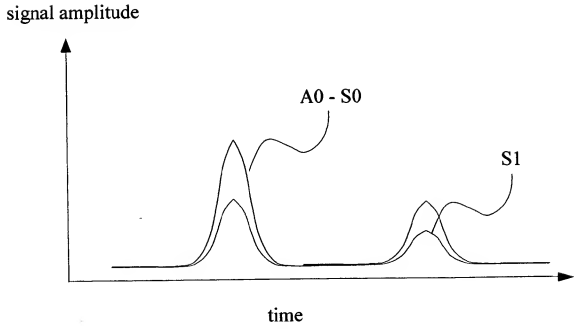

Figure 59

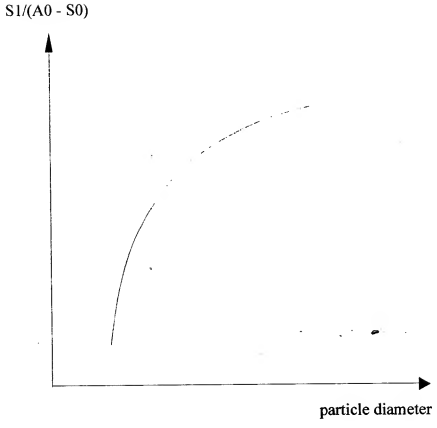

Figure 60

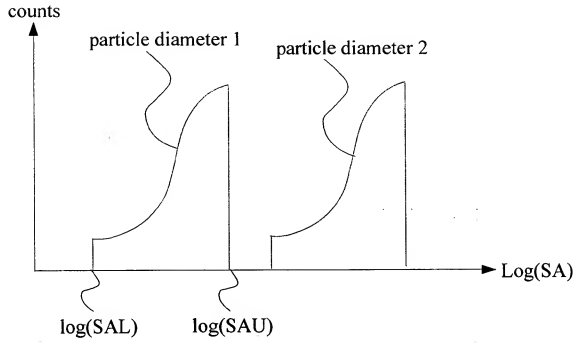
counts
particle diameter 1
particle diameter 2
Log(SA)
log(SAL)
log(SAU)

Figure 61

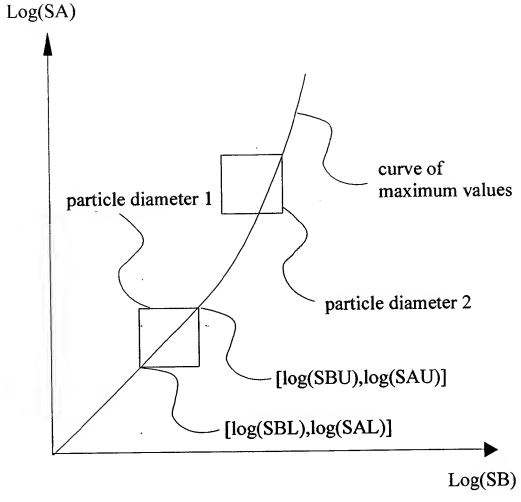
Log(SA)
curve of
maximum values
particle diameter 1
particle diameter 2
[log(SBU),log(SAU)]
[log(SBL),log(SAL)]
Log(SB)

Figure 62

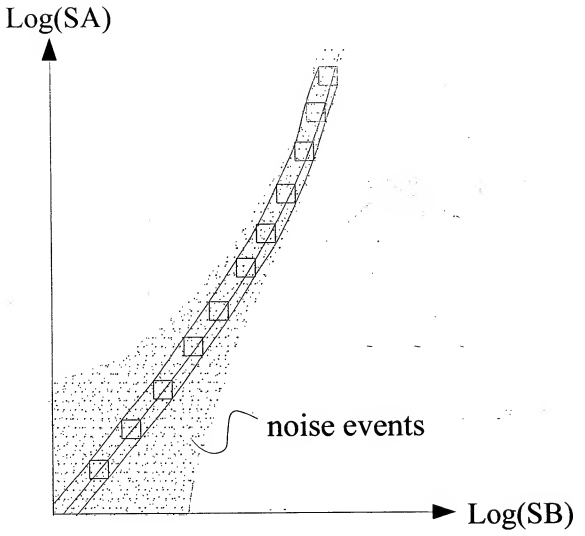

Figure 63

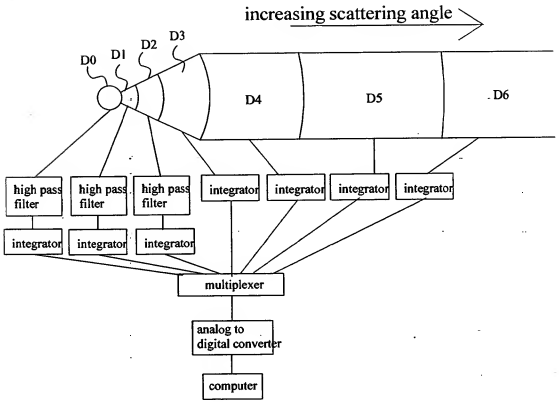
increasing scattering angle
D0
D1
D2
D3
D4
D5
D6
high pass filter
high pass filter
high pass filter
integrator
integrator
integrator
integrator
integrator
integrator
integrator
multiplexer
analog to digital converter
computer

Figure 64

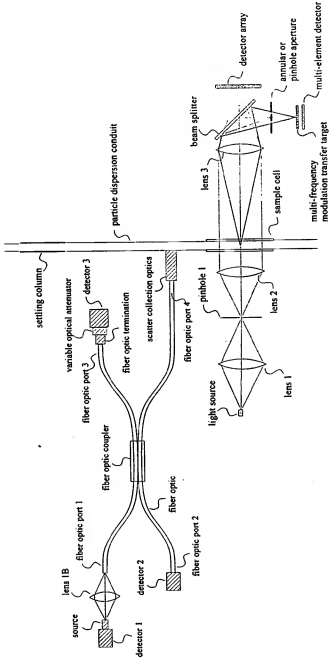
detector array
annular or pinhole aperture
multi-element detector
beam splitter
particle dispersion conduit
lens 3
sample cell
multi-frequency modulation transfer target
settling column
variable optical attenuator
detector 3
fiber optic port 3
fiber optic termination
scatter collection optics
fiber optic port 4
pinhole 1
lens 2
light source
lens 1
fiber optic coupler
fiber optic
fiber optic port 1
lens 1B
detector 2
fiber optic port 2
source
detector 1

Figure 65

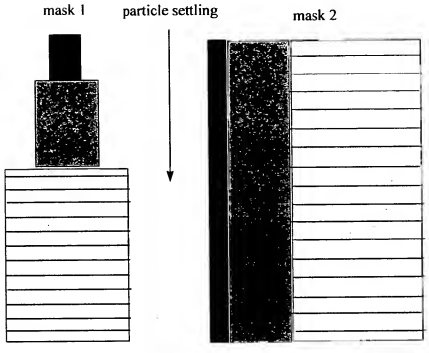

Figure 66

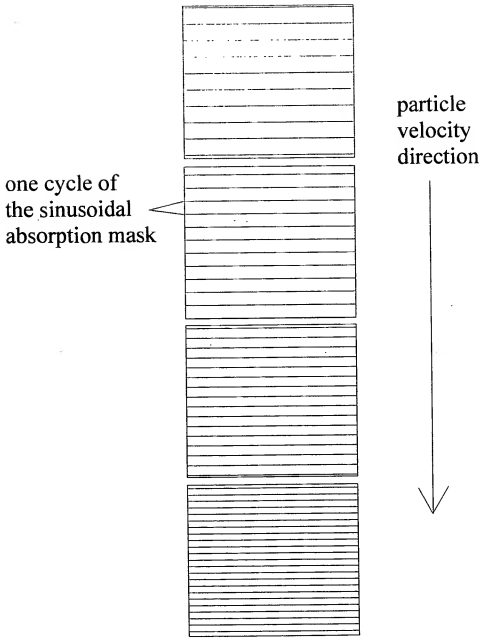
one cycle of
the sinusoidal
absorption mask
particle
velocity
direction